





ORIGINAL ARTICLE OPEN ACCESS

Smoothing of the Higher-Order Stokes Phenomenon

 Chris J. Howls¹  | John R. King²  | Gergő Nemes³  | Adri B. Olde Daalhuis⁴ 

¹School of Mathematical Sciences, University of Southampton, Highfield, Southampton, UK | ²School of Mathematical Sciences, University of Nottingham, Nottingham, UK | ³Department of Physics, Tokyo Metropolitan University, Hachioji-shi, Tokyo, Japan | ⁴School of Mathematics and Maxwell Institute for Mathematical Sciences, University of Edinburgh, Edinburgh, UK

Correspondence: Adri B. Olde Daalhuis (A.OldeDaalhuis@ed.ac.uk)

Received: 10 October 2024 | **Revised:** 20 December 2024 | **Accepted:** 26 December 2024

Funding: This research was supported by Japan Society for the Promotion of Science (JSPS), Engineering and Physical Sciences Research Council (EPSRC), and National Institute of Standards and Technology (Grant Nos. 22H01146, EP/R014604/1, and 60NANB23D131).

ABSTRACT

For over a century, the Stokes phenomenon had been perceived as a discontinuous change in the asymptotic representation of a function. In 1989, Berry demonstrated it is possible to smooth this discontinuity in broad classes of problems with the prefactor for the exponentially small contribution switching on/off taking a universal error function form. Following pioneering work of Berk, Nevins, and Roberts and the Japanese school of formally exact asymptotics, the concept of the higher-order Stokes phenomenon was introduced, whereby the ability for the exponentially small terms to cause a Stokes phenomenon may change, depending on the values of parameters in the problem, corresponding to the associated Borel-plane singularities transitioning between Riemann sheets. Until now, the higher-order Stokes phenomenon has also been treated as a discontinuous event. In this paper, we show how the higher-order Stokes phenomenon is also smooth and occurs universally with a prefactor that takes the form of a new special function, based on a Gaussian convolution of an error function. We provide a rigorous derivation of the result, with examples spanning the gamma function, a second-order nonlinear ODE, and the telegraph equation, giving rise to a ghost-like smooth contribution present in the vicinity of a Stokes line, but which rapidly tends to zero on either side. We also include a rigorous derivation of the effect of the smoothed higher-order Stokes phenomenon on the individual terms in the asymptotic series, where the additional contributions appear prefactored by an error function.

1 | Introduction

The Stokes phenomenon [7] is the apparent discontinuous appearance of additional exponentially small contributions in asymptotic representations of functions as either an asymptotic independent variable z , $z \rightarrow \infty$, or some other set of bounded system parameters $\mathbf{a} = \{a_1, a_2, \dots\}$, $a_j \in \mathbb{C}$, vary smoothly across codimension 1 sets known as Stokes lines or, in higher dimensions, Stokes sets. Such exponentially small terms may be locally neglected numerically, but can grow in size elsewhere to determine the global properties of the function.

In 1989, Berry [1] showed that under general assumptions as to the form of the late terms in an asymptotic series, the switching on of exponentially small terms in the Stokes phenomenon actually occurs smoothly across the Stokes sets, with a universal error function prefactor. This result has subsequently been rigorously justified in a wide variety of contexts [8–13].

Historically, detailed studies of the Stokes phenomenon had often focused on systems involving only two different asymptotic contributions. Consequently, it was not until 1982 when Berk et al. [2] studied a third-order ordinary differential equation that it was noticed that, when there are three or more distinct asymptotic

This is an open access article under the terms of the [Creative Commons Attribution](https://creativecommons.org/licenses/by/4.0/) License, which permits use, distribution and reproduction in any medium, provided the original work is properly cited.

© 2025 The Author(s). *Studies in Applied Mathematics* published by Wiley Periodicals LLC.

contributions to a function, two new analytical features can occur as the parameters z or \mathbf{a} vary.

The first new analytical feature is that so-called “new Stokes lines” [4] may sprout from points at which the traditional Stokes lines cross. The number of asymptotic contributions to the function may change across “new Stokes lines” but, unlike their traditional counterparts which may sprout from turning points (or caustics) in the finite plane where the arguments of the exponential prefactors coalesce and simultaneously the individual terms in the asymptotic contributions diverge, the new Stokes lines emerge from crossing points at which these terms are regular.

The second analytical feature is that, in order for monodromy to be maintained, the activity of some of the Stokes lines themselves is switched off or on as the parameters z or \mathbf{a} vary.

Howls et al. [5] termed such change in the activity of a Stokes line as the “higher-order Stokes phenomenon” and showed that it occurs as z and/or \mathbf{a} cross a “higher-order Stokes line” in parameter space, using an approach based on the use of exact, hyperasymptotic, re-expansions that explore subsubdominant exponential terms. That approach tied the activity-switching phenomenon to the movement of singularities (that generate the asymptotic contributions) between Riemann sheets in the Borel-plane representation of the function.

Chapman and Mortimer [6] and Body et al. [14] carried out an independent, parallel, analysis of the higher-order Stokes phenomenon for specific equations using matched asymptotic expansions.

The higher-order Stokes phenomenon is linked to the presence of “virtual turning points” [3, 4, 15]. At a virtual turning point, from a Borel-plane viewpoint, the exponents of the exponential prefactors of the “coalescing” contributions become equal, but the corresponding singularities in the Borel plane do not simultaneously coincide. Rather, like aircraft at different altitudes, they pass directly above one another on different Riemann sheets [15].

More generally, as a higher-order Stokes line (or set) is crossed, although no new asymptotic contribution is switched on at the first subdominant exponential level (as it would be at an ordinary Stokes phenomenon), the Stokes multiplier prefactoring the terms that are to be switched off/on in a later Stokes phenomenon may change. If this multiplier becomes zero across a higher-order Stokes line, the activity of the later Stokes line is switched off. If this multiplier grows from zero, then the activity of the later Stokes line is switched on. More generally, this multiplier might change between two nonzero values across the higher-order Stokes line, giving rise to a change in the strength of the nearby Stokes phenomenon. As we recall below, this is manifested as a change in the exact analytical hyperasymptotic re-expansion of the asymptotic remainder terms that would generate that later Stokes phenomenon.

Until recently, the higher-order Stokes phenomenon had only been studied in discrete form, that is, before and after the event had occurred [5, 6, 16, 17]. In a recent paper, Nemes [18] investigated the higher-order Stokes phenomenon with a focus on cases

where singularities in the Borel plane are collinear and equally spaced. He demonstrated that, in this specific case, the higher-order Stokes phenomenon occurs smoothly, and the smooth transition can be described using multivariable polynomials of error functions.

In this paper, we show that the higher-order Stokes phenomenon can be observed to occur smoothly in more general settings. However, in contrast to the error function smoothing of the ordinary Stokes phenomenon, the smooth prefactor of the higher-order Stokes phenomenon that takes the form of a *new* special function, being a (semi)convolution of a Gaussian and an error function, reminiscent of a power normal distribution [19].

In parallel work, we note that Shelton et al. [20] have recently considered the effect of the higher-order Stokes phenomenon on the re-expansion of the individual terms in the asymptotic series. They have shown using formal Borel resummation of a Dingle resurgence expansion of an individual late term in an asymptotic series that the switching on of subsubdominant terms is of standard error function type.

In contrast, we consider the whole progenitor function of the asymptotic series, rather than just the individual terms. The approach we take is valid for all functions that possess a hyperasymptotic expansion in terms of hyperterminants. Our wider approach not only provides a rigorous proof of the form of the smoothing for the whole progenitor function, but, as a special case, of the corresponding smoothing for individual terms.

The paper has been split into four parts, so that the reader may focus on those that most interest them. The first part of the paper (Sections 2–4) contains details of the underpinning background and a summary of the results. The main new results governing the three types of phenomena that are encountered are summarized in Equations (4.6), (4.8), (9.9), and (9.17), with notation defined in Section 9.1. The second part (Sections 5–8) contains four examples of the effects of the smoothing of the higher-order Stokes phenomenon in diverse contexts. This includes in Section 8 a rigorous approach to the smoothing of additional contributions to the late terms in an asymptotic expansion as a higher-order Stokes phenomenon occurs. The third part (Sections 9–10) contains statements and rigorous proofs of the theorems, together with a conclusion and discussion. Theorems 9.2–9.4 rigorously underpin the new results. Three appendices (A–C) contain the derivation of new integral representations for the underpinning second hyperterminant function, analytical and computational properties of the subsequent new special function governing the higher-order smoothing, and a discussion of the circumstances leading to the example in Section 7.

2 | Borel-Plane Background

The basis for the analysis of this paper is the iterative hyperasymptotic re-expansion of the exact remainder terms of the asymptotic expansions of a function $w(z; \mathbf{a})$ as $z \rightarrow \infty$. The function might have, for example, a (multiple) integral representation [21–25], or may satisfy an ODE [26–31], a difference equation [32, 33], a differential-difference equation [34], or a PDE [5, 14, 15], but can also represent eigenvalues [35, 36]. The sole requirement is the

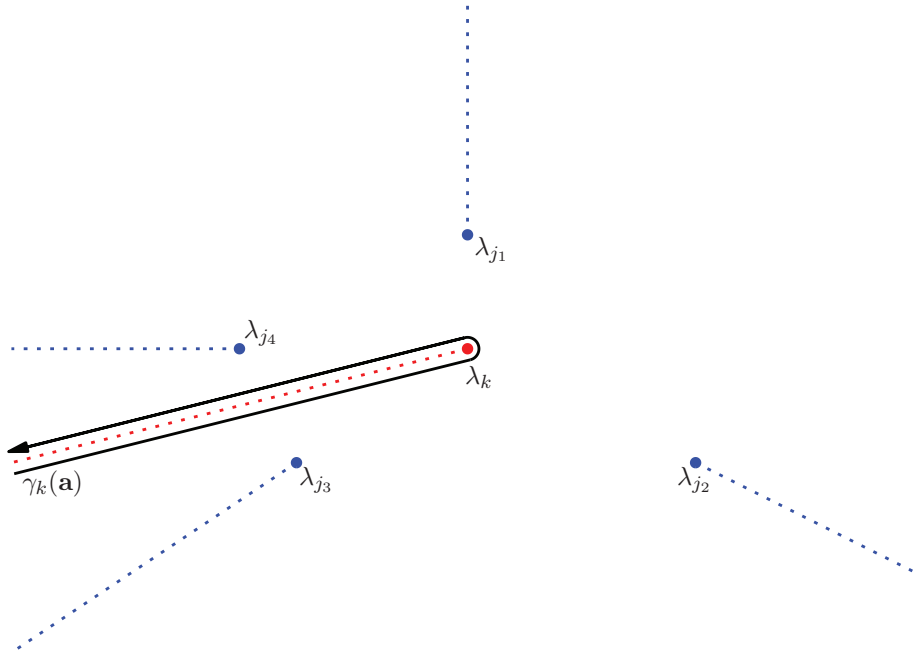


FIGURE 1 | Sketch of the Borel t -plane with singularities $\lambda_k, \lambda_j, j \neq k$ and the associated integration contour $\gamma_k(\mathbf{a})$.

existence of a Borel transform representation for $w(z; \mathbf{a})$ of the form

$$w_k(z; \mathbf{a}) = \frac{1}{2\pi i} \int_{\gamma_k(\mathbf{a})} e^{zt} B_k(t; \mathbf{a}) dt. \quad (2.1)$$

Here, the function $B_k(t; \mathbf{a})$, known as the Borel transform of $w_k(z; \mathbf{a})$, has just (for the purposes only of simplifying the explanation) algebraic branch points and/or poles, say at $t = \lambda_j(\mathbf{a})$, in the finite complex t -plane, also referred to as the Borel plane. As seen below, the explicit closed form of $B_k(t; \mathbf{a})$ is not actually required, only a (finite) number of terms in its expansion around relevant singularities.

The contour $\gamma_k(\mathbf{a})$ runs from ∞ in the Borel plane along the left-hand side of a branch cut emanating from one of these branch points at $t = \lambda_k(\mathbf{a})$, encircles this branch point once in the positive sense, and back to ∞ along the right-hand side of the cut. The cut orientation is initially chosen such that it encounters no other singularities $\lambda_j(\mathbf{a}), j = 1, 2, 3, \dots, j \neq k$, of $B_k(t; \mathbf{a})$ (see Figure 1). $B_k(t; \mathbf{a})$ is exponentially bounded at infinity in the direction of $\gamma_k(\mathbf{a})$, so that the integral converges for all sufficiently large values of z . In practice, this means that, if $\lambda_k(\mathbf{a})$ is an algebraic singularity, $B_k(t; \mathbf{a})$ may have a convergent expansion of the form

$$B_k(t; \mathbf{a}) = \sum_{r=0}^{\infty} T_r^{(k)}(\mathbf{a}) \Gamma(\mu_k - r + 1) (t - \lambda_k(\mathbf{a}))^{r - \mu_k - 1}, \quad \mu_k \notin \mathbb{Z}, \quad (2.2)$$

with a finite radius of convergence to the nearest singularity $\lambda_j(\mathbf{a}), j \neq k$ on the same Riemann sheet in t . Analogous expansions can be written down if $\lambda_k(\mathbf{a})$ is actually a logarithmic singularity [25, 37] or is of a combined power-log form.

Substitution of the convergent series (2.2) into (2.1), followed by integration over the chosen contour $\gamma_k(\mathbf{a})$, produces the divergent

asymptotic series

$$w_k(z; \mathbf{a}) \sim e^{\lambda_k(\mathbf{a})z} z^{\mu_k} \sum_{r=0}^{\infty} \frac{T_r^{(k)}(\mathbf{a})}{z^r}, \quad (2.3)$$

as $z \rightarrow \infty$.

Each of the other branch points $\lambda_j(\mathbf{a})$ give rise to functions $w_j(z; \mathbf{a})$ defined in an analogous way to (2.1) in terms of loop contours around the radial cuts between $\lambda_j(\mathbf{a})$ and infinity (see Figure 1).

When two or more of these singularities coalesce, that is, for values of $\mathbf{a} = \mathbf{a}^*$ at which $\lambda_l(\mathbf{a}^*) = \lambda_m(\mathbf{a}^*), l, m = 1, 2, 3, \dots$, then a caustic will occur and the local form of the asymptotic expansion must change to avoid individually singular terms. We avoid values of \mathbf{a} for which this occurs.

The advantage of using the Borel approach is that it is possible to provide exact representations of the remainder of a truncated convergent series (2.2) in terms of contributions from the adjacent singularities $\lambda_j(\mathbf{a}), j \neq k$ on the same Riemann sheet of the complex Borel t -plane.

To see this, we now extract the exponential and algebraic prefactors of the large- z asymptotic expansions and write each of the $w_j(z; \mathbf{a})$ as

$$w_j(z; \mathbf{a}) = e^{\lambda_j(\mathbf{a})z} z^{\mu_j} T^{(j)}(z; \mathbf{a}), \quad j = 1, 2, 3, \dots \quad (2.4)$$

Then, assuming that all the singularities in the Borel plane are of algebraic type, a calculation similar to that in [22, 28, 38] provides a representation for the remainder term in the

asymptotic expansion (2.3) of $w_k(z; \mathbf{a})$ as follows:

$$T^{(k)}(z; \mathbf{a}) = \sum_{r=0}^{N_0-1} \frac{T_r^{(k)}(\mathbf{a})}{z^r} + \frac{1}{2\pi i} \sum_{j \neq k} \frac{K_{kj}(\mathbf{a})}{z^{N_0-1}} \int_0^{[\pi-\theta_{jk}]} \frac{e^{\lambda_{jk}(\mathbf{a})t} t^{N_0+\mu_{jk}-1}}{z-t} T^{(j)}(t; \mathbf{a}) dt, \quad (2.5)$$

where

$$\lambda_{jk}(\mathbf{a}) = \lambda_j(\mathbf{a}) - \lambda_k(\mathbf{a}), \quad \theta_{jk} = \arg \lambda_{jk}(\mathbf{a}), \quad \mu_{jk} = \mu_j - \mu_k, \quad (2.6)$$

with the notation $\int_0^{[\eta]} = \int_0^{\infty e^{i\eta}}$. Taking N_0 large enough guarantees that $\text{Re}(N_0 + \mu_{jk}) > 0$ for all $j \neq k$. Note that the μ_{jk} may, or may not be, an integer or real.

The $\lambda_{jk}(\mathbf{a})$ correspond to the (negative) singularants of Dingle [39]. The $K_{kj}(\mathbf{a})$ are Stokes “constants”. If the singularities $\lambda_k(\mathbf{a})$ and $\lambda_j(\mathbf{a})$ are not located on the same Riemann sheet, then $K_{kj}(\mathbf{a}) = 0$. When $K_{kj}(\mathbf{a}) \neq 0$, then $\lambda_k(\mathbf{a})$ and $\lambda_j(\mathbf{a})$ are said to be adjacent singularities.

More generally, and more accurately, these “constants” are termed Stokes “multipliers”, since in the present context, they may change in value as a function of \mathbf{a} .

The exact representation for the remainder term on the right-hand side of (2.5) is implicit, and depends on self-similar contributions $T^{(j)}(t; \mathbf{a})$ arising from adjacent singularities in the Borel plane.

The right-hand side of (2.5) automatically encodes the Stokes phenomenon in the following way. As the parameters \mathbf{a} are varied, the cut and associated contour $\gamma_k(\mathbf{a})$ may rotate and the singularities $\lambda_k(\mathbf{a}), \lambda_j(\mathbf{a})$ may move around the Borel plane. When the quantity $\lambda_{jk}(\mathbf{a})z$ is real and negative (through the values of z and/or \mathbf{a}), the branch cut from $\lambda_k(\mathbf{a})$ and the associated contour $\gamma_k(\mathbf{a})$ encounters the singularity $\lambda_j(\mathbf{a})$. The remainder integral in (2.5) then encounters a pole in the denominator. As the contour sweeps through this pole, it automatically generates the connection formula associated with the Stokes phenomenon:

$$T^{(k)}(z; \mathbf{a})^+ = T^{(k)}(z; \mathbf{a})^- + K_{kj}(\mathbf{a}) e^{\lambda_{jk}(\mathbf{a})z} z^{\mu_{jk}} T^{(j)}(z; \mathbf{a}), \quad (2.7)$$

where $+$ and $-$ superscripts denote the functions $T^{(k)}(z; \mathbf{a})$ on either side of the Stokes line.

The Stokes phenomenon in the previous paragraph has been regarded as occurring due to changes in the system parameters \mathbf{a} . It could also have occurred due to changes in the independent variable z , and so z (or perhaps its argument) could be regarded as part of the system parameters.

Using the Borel-plane approach, it is therefore possible to write down an exact, but implicit, remainder term for the asymptotic expansion, which incorporates the analytic implications of the Stokes phenomenon, without the need to resum divergent series. Hence, this approach allows for both nondivergent analytical

generality and, as we see in Section 9, a mechanism for rigorous proof of the main results of this paper.

3 | The Role of Hyperterminants in Encoding the Stokes and Higher-Order Stokes Phenomena

Due to their importance in what follows, we recall now the detailed role that hyperterminants play in encoding analytically the Stokes and higher-order Stokes phenomena.

Let us assume that we may compute at least a finite number of terms in each of the divergent series expansions of $T^{(l)}(z; \mathbf{a}), l = k, k_1, k_2, \dots$. We may then make explicit progress to obtain better than exponentially accurate results for a given function $T^{(k)}(z; \mathbf{a})$ through re-expanding the implicit remainder term by substituting analogous exact remainder terms for $T^{(j)}(t; \mathbf{a})$ in terms of its adjacent contributions from $T^{(l)}(t; \mathbf{a}), l \neq j$ into the right-hand side of (2.5). The result, after two iterations, is a hyperasymptotic expansion of the form

$$T^{(k)}(z; \mathbf{a}) = \sum_{r=0}^{N_0-1} \frac{T_r^{(k)}(\mathbf{a})}{z^r} + \frac{1}{z^{N_0-1}} \left[\sum_{k_1 \neq k} \frac{K_{k_1 k}(\mathbf{a})}{2\pi i} \left\{ \sum_{s=0}^{N_1^{(k_1)}-1} T_s^{(k_1)}(\mathbf{a}) F^{(1)}\left(z; \begin{matrix} N_0 - s + \mu_{k_1 k} \\ \lambda_{k_1 k} \end{matrix}\right) + \sum_{k_2 \neq k_1} \frac{K_{k_2 k_1}(\mathbf{a})}{2\pi i} \left\{ \sum_{s=0}^{N_2^{(k_2)}-1} T_s^{(k_2)}(\mathbf{a}) \times F^{(2)}\left(z; \begin{matrix} N_0 - N_1^{(k_1)} + \mu_{k_1 k} + 1, N_1^{(k_1)} - s + \mu_{k_2 k_1} \\ \lambda_{k_1 k}, \lambda_{k_2 k_1} \end{matrix}\right) \right\} + R_2^{(k)}(z; \mathbf{a}) \right\} \right]. \quad (3.1)$$

Each successive re-expansion contains terms of the local expansion about each of the $\lambda_k, \lambda_{k_1}, \lambda_{k_2}$, and so forth, multiplied by a “hyperterminant” function $F^{(n)}, n = 1, 2, 3, \dots$ [40–42]. The more iterations, with suitable truncations $N_j^{(k_j)}$ chosen, the greater the overall accuracy that may be obtained.

Note that everything here is still finite and exact. The remainder term $R_2^{(k)}(z; \mathbf{a})$ may be expressed exactly in terms of an integral (involving self-similar contributions from the singularities $k_3 \neq k_2$ adjacent to those in the set k_2). In what follows, it does not contribute and so we do not need to state what it is explicitly.

The first hyperterminant takes the form:

$$F^{(1)}\left(z; \begin{matrix} a \\ \sigma_0 \end{matrix}\right) = \int_0^{[\pi-\arg \sigma_0]} \frac{e^{\sigma_0 \tau} \tau^{a-1}}{z-\tau} d\tau, \quad (3.2)$$

where $\text{Re}(a) > 0, |\arg(\sigma_0 z)| < \pi$. The parameter σ_0 represents the distance between singularities in the Borel plane, for example,

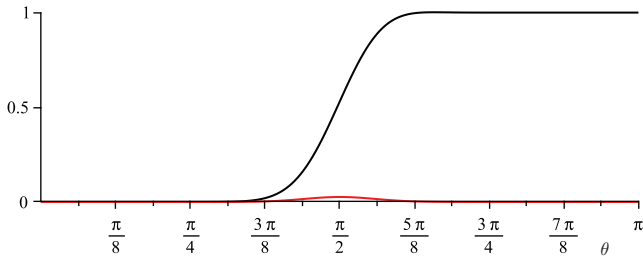


FIGURE 2 | The smoothing of the ordinary Stokes phenomenon according to (3.6). The black curve represents $\left| \frac{e^{-\sigma_0 z}}{2\pi i z^{N_0}} F^{(1)}\left(z; \frac{N_0+1}{\sigma_0}\right) \right|$, while the red curve shows $\left| \frac{e^{-\sigma_0 z}}{2\pi i z^{N_0}} F^{(1)}\left(z; \frac{N_0+1}{\sigma_0}\right) - \frac{1}{2} \operatorname{erfc}\left(\alpha_0(z) \sqrt{\frac{1}{2} N_0}\right) \right|$, a measure of the error of the approximation, for $\sigma_0 = i\sqrt{2}$, $N_0 = 30.3$, and $z = 20e^{i\theta}$.

λ_{jk} , and so forth. It is the simplest function that incorporates a Stokes phenomenon and which is compatible with a Borel transform representation. To see this, we first expand the denominator $(z - \tau)^{-1}$ in (3.2) in a truncated geometric series and this gives us

$$F^{(1)}\left(z; \frac{a}{\sigma_0}\right) = \sum_{n=0}^{N-1} \frac{(e^{\pi i/\sigma_0})^{a+n} \Gamma(a+n)}{z^{n+1}} + z^{-N} F^{(1)}\left(z; \frac{a+N}{\sigma_0}\right). \quad (3.3)$$

The right-hand side can be seen as an asymptotic expansion as $z \rightarrow \infty$. The terms in the series are typical for a divergent asymptotic expansion that possesses a Borel transform [28]. As $n \rightarrow +\infty$, the coefficients grow like a factorial divided by a power: $\Gamma(a+n)/(\sigma_0 z)^n$ (see Section 8).

If we take a as fixed, then the minimum term in this series expansion occurs at $n \approx |\sigma_0 z|$. This is known as the optimal number of terms. From Stirling's approximation, we obtain that the smallest term is of size

$$\left| \frac{(e^{\pi i/\sigma_0})^{a+n} \Gamma(a+n)}{z^{n+1}} \right| \sim \frac{\sqrt{2\pi}}{(-\sigma_0)^{i\operatorname{Im}(a+1)}} e^{-|\sigma_0 z|} |z|^{\operatorname{Re}(a)-\frac{3}{2}}, \quad (3.4)$$

as $z \rightarrow \infty$. Truncating the series at $n \approx |\sigma_0 z|$ thus leads to exponential accuracy (within a sector between two Stokes lines) [39]. Taking increasing numbers of subsequent terms will lead to a worsening approximation.

So far we have restricted z to the principal branch $|\arg(\sigma_0 z)| < \pi$. As these parameters change, the pole in the hyperterminant (3.2) moves relative to the contour of integration. At $\arg(\sigma_0 z) = \pi$, the Stokes phenomenon occurs and the pole snags on the integration contour, thereafter giving birth to an additional exponentially small residue contribution $2\pi i e^{\sigma_0 z} z^{a-1}$. This gives rise to a connection formula

$$F^{(1)}\left(ze^{-2\pi i}; \frac{a}{\sigma_0}\right) = F^{(1)}\left(z; \frac{a}{\sigma_0}\right) - 2\pi i e^{\sigma_0 z} z^{a-1}. \quad (3.5)$$

Note that on the Stokes curve this residue term is comparable in size with the smallest term in (3.4). Thus taking $N \approx |\sigma_0 z|$ in (3.3), the remainder is expected to be of the same size as $2\pi i e^{\sigma_0 z} z^{a-1}$.

Berry [1] first showed formally that the optimal remainder will definitely switch on this exponentially small term in a smooth and universal manner. For the sake of completeness, and to contrast with the main result of this paper, we provide a rigorous general justification in Theorem 9.1 (see Section 9.2). A simplified version of that result gives

$$z^{-N} F^{(1)}\left(z; \frac{a+N}{\sigma_0}\right) = \pi i e^{\sigma_0 z} z^{a-1} \left(\operatorname{erfc}\left(\alpha_0(z) \sqrt{\frac{1}{2} N_0}\right) + \mathcal{O}(z^{-1/2}) \right) \quad (3.6)$$

as $z \rightarrow \infty$, in which $\frac{1}{2} \alpha_0^2(z) = 1 + \frac{\sigma_0 z}{N_0} + \ln\left(e^{-\pi i \frac{\sigma_0 z}{N_0}}\right)$, with $N_0 = N + a - 1$ (see Figure 2).

For the class of divergent series possessing a hyperasymptotic expansion of the form (3.1), the error function smoothing in (3.6) is the local, smooth, and universal description of the Stokes phenomenon.

Of course, in exponentially improved asymptotics, if we were to naively truncate the original divergent series after an optimal number of terms and re-expand the remainder in terms of the first hyperterminants, this re-expansion will itself in general be divergent due to the presence of distant Borel-plane singularities k_2 on the mutual Riemann sheet. This divergent series will also incorporate its own Stokes phenomenon.

In order to control that re-expansion, we use the template (3.1) with the second re-expansion in terms of contributions from the k_2 set of Borel-plane singularities on the same Riemann sheet.

The second hyperterminants $F^{(2)}$ in (3.1) take the form

$$F^{(2)}\left(z; \frac{N_0+1}{\sigma_0}, \frac{N_1+1}{\sigma_1}\right) = \int_0^{[\pi-\arg\sigma_0]} \int_0^{[\pi-\arg\sigma_1]} \frac{e^{\sigma_0 \tau_0 + \sigma_1 \tau_1} \tau_0^{N_0} \tau_1^{N_1}}{(z-\tau_0)(\tau_0-\tau_1)} d\tau_1 d\tau_0, \quad (3.7)$$

where $\operatorname{Re}(N_0) > -1$ and $\operatorname{Re}(N_1) > -1$. Again the principal branch is $|\arg(\sigma_0 z)| < \pi$, and normally we will also assume that $\arg\sigma_1 - \arg\sigma_0 \in [0, 2\pi)$.

These integrals each contain poles when $z = \tau_0$, $\tau_0 = \tau_1$. Just as for $F^{(1)}$ (3.2), as the parameters z and $\arg\sigma_0$ and $\arg\sigma_1$ change, these poles may snag on the contours of integration of $F^{(2)}$. They too may thus give rise to the birth or death of additional exponentially small contributions, so generating “higher-order” Stokes phenomena.

Note that these higher-order contributions are also exponentially small, but as we see, may interfere with the terms that are switched on by the first hyperterminants $F^{(1)}$. As such they can affect the strength of the Stokes multiplier of the ordinary Stokes phenomenon, and in some cases, exactly cancel it out.

More generally, the hyperterminants (3.2), (3.7) are the first of a family of hyperterminants $F^{(n)}$, each of n integrations, but

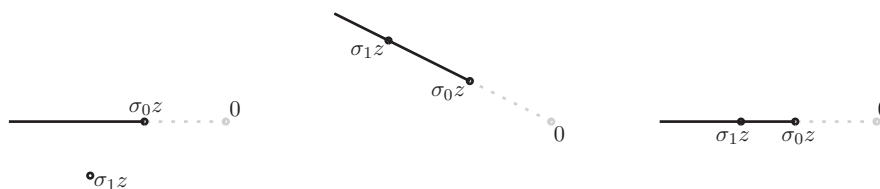


FIGURE 3 | The three cases giving rise to higher-order Stokes phenomena in (3.7). On the left diagram, the case $\arg(\sigma_0 z) = \pi$ generates a pole in (3.7) that leads to a (higher-order) Stokes phenomenon with connection formula (4.1). In the middle diagram, where $\arg \sigma_0 = \arg \sigma_1$, a pole occurs in a $F^{(2)}$ hyperterminant and leads to a (higher-order) Stokes phenomenon with connection formula (4.2). In the right-hand diagram, where $\arg(\sigma_0 z) = \arg(\sigma_1 z) = \pi$ two poles simultaneously occur in a $F^{(2)}$ hyperterminant, leading to a combined (higher-order) Stokes phenomenon with the uniform approximation (4.6).

with similar, repeated integrands, to these two. Each of these hyperterminants can possess a higher-order Stokes phenomenon. However, to answer the main questions of this paper will only need to discuss the first two such hyperterminants.

We have now arrived at the main purpose of the paper. While the birth of these exponentially small additional contributions might seem discontinuous at first glance, it is actually continuous, much like the ordinary Stokes phenomenon. In what follows, we establish that this is indeed the case and determine the (novel) form of this smoothed switching on or off of these doubly exponentially small contributions.

The next section provides a summary of these results.

4 | Summary of Main Results

The higher-order Stokes phenomenon is conveniently captured and explained by the second hyperterminant function defined in (3.7). An analysis of the two poles in integral representation (3.7) indicates that the second hyperterminant function can have two types of higher-order Stokes phenomena, one when $\arg(\sigma_0 z) = \pi$, and one when $\arg \sigma_0 = \arg \sigma_1$. There is also a degenerate case where $\arg(\sigma_0 z) = \arg(\sigma_1 z) = \pi$ leading to two simultaneous poles in the integrands of $F^{(2)}$, which generates a double higher-order Stokes phenomenon. These scenarios are illustrated in Figure 3.

The corresponding connection formulas (cf. 3.5) for the first two cases are, for $\arg(\sigma_0 z) = \pi$,

$$F^{(2)}\left(z e^{-2\pi i}, \begin{matrix} N_0 + 1, N_1 + 1 \\ \sigma_0, \sigma_1 \end{matrix}\right) = F^{(2)}\left(z; \begin{matrix} N_0 + 1, N_1 + 1 \\ \sigma_0, \sigma_1 \end{matrix}\right) - 2\pi i e^{\sigma_0 z} z^{N_0} F^{(1)}\left(z; \begin{matrix} N_1 + 1 \\ \sigma_1 \end{matrix}\right), \tag{4.1}$$

and for $\arg \sigma_0 = \arg \sigma_1$,

$$F^{(2)}\left(z; \begin{matrix} N_0 + 1, N_1 + 1 \\ \sigma_0, \sigma_1 e^{-2\pi i} \end{matrix}\right) = F^{(2)}\left(z; \begin{matrix} N_0 + 1, N_1 + 1 \\ \sigma_0, \sigma_1 \end{matrix}\right) - 2\pi i F^{(1)}\left(z; \begin{matrix} N_0 + N_1 + 1 \\ \sigma_0 + \sigma_1 \end{matrix}\right). \tag{4.2}$$

Both these connection formulas involve the generation of $F^{(1)}$ hyperterminants, as opposed to the functions $T^{(j)}(z; \mathbf{a})$ (2.7), or

exponentially small terms associated with an ordinary Stokes phenomenon (3.5), hence the “higher-order” nomenclature.

Note that it is possible for both connections to occur simultaneously. In such situations, the order in which the individual connections occur has to be chosen. The choice has no overall consequence for the final result, just in the definition of the second hyperterminant. We consider this degenerate case below.

In addition to connection formulas (4.1) and (4.2), there is one more simple identity that will be useful below:

$$F^{(2)}\left(z; \begin{matrix} N_0 + 1, N_1 + 1 \\ \sigma_0, \sigma_1 \end{matrix}\right) + F^{(2)}\left(z; \begin{matrix} N_1 + 1, N_0 + 1 \\ \sigma_1, \sigma_0 \end{matrix}\right) = F^{(1)}\left(z; \begin{matrix} N_0 + 1 \\ \sigma_0 \end{matrix}\right) F^{(1)}\left(z; \begin{matrix} N_1 + 1 \\ \sigma_1 \end{matrix}\right), \tag{4.3}$$

which may be derived from (3.7) using partial fractions [42].

So far these are discrete results, bridging between either side of a higher-order Stokes phenomenon. We now present a list of the main results, demonstrating that the transition between these states is smooth and illustrating the forms these cases take.

4.1 | The Smoothing When $\arg(\sigma_0 z) = \pi$

In Section 9.3, we will address the $\arg(\sigma_0 z) = \pi$ (higher-order) Stokes phenomenon, assuming $\arg \sigma_0 \neq \arg \sigma_1$ (left-hand diagram of Figure 3).

Identity (4.3) will prove to be quite useful in this case. A simplified version of the main result in this case (9.9) is

$$F^{(2)}\left(z; \begin{matrix} N_0 + 1, N_1 + 1 \\ \sigma_0, \sigma_1 \end{matrix}\right) \sim \pi i e^{\sigma_0 z} z^{N_0} \operatorname{erfc}\left(\alpha_0(z) \sqrt{\frac{1}{2} N_0}\right) F^{(1)}\left(z; \begin{matrix} N_1 + 1 \\ \sigma_1 \end{matrix}\right). \tag{4.4}$$

A computation of both sides is illustrated in Figure 4, thereby confirming numerically the smooth switching on of the term

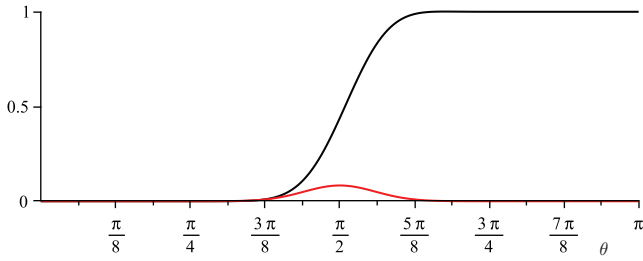


FIGURE 4 | An example of the smoothing when $\arg(\sigma_0 z) = \pi$, based on (4.4). The black curve depicts $\left| \frac{e^{-\sigma_0 z}}{2\pi i z^{N_0}} \frac{F^{(2)}(z; N_0+1, N_1+1)}{F^{(1)}(z; N_1+1)} \right|$, and the red curve shows $\left| \frac{e^{-\sigma_0 z}}{2\pi i z^{N_0}} \frac{F^{(2)}(z; N_0+1, N_1+1)}{F^{(1)}(z; N_1+1)} - \frac{1}{2} \operatorname{erfc} \left(\alpha_0(z) \sqrt{\frac{1}{2} N_0} \right) \right|$, a measure of the error of the approximation, for indicative values $\sigma_0 = i\sqrt{2}$, $N_0 = 30.3$, $\sigma_1 = i - 1$, $N_1 = 29$, and $z = 20e^{i\theta}$.

$2\pi i e^{\sigma_0 z} z^{N_0} F^{(1)}(z; N_1+1)$ in (4.1) again via a complementary error function (cf. (3.6)).

This approximation breaks down when $\frac{\sigma_0 N_1}{\sigma_1 N_0}$ approaches the positive real axis.

4.2 | The Smoothing Across $\arg \sigma_0 = \arg \sigma_1$ When $\arg(\sigma_0 z) \neq \pi$

In Section 9.4, we discuss the $\arg \sigma_0 \approx \arg \sigma_1$ (higher-order) Stokes phenomenon, assuming that $\arg(\sigma_0 z) \neq \pi$. A simplified version of the main result (9.17) is

$$F^{(2)}\left(z; \begin{matrix} N_0+1, & N_1+1 \\ \sigma_0, & \sigma_1 \end{matrix}\right) \sim -\pi i \operatorname{erfc}\left(\gamma\left(\frac{\sigma_1}{\sigma_0}\right)\sqrt{\frac{1}{2}N_1}\right)F^{(1)}\left(z; \begin{matrix} N_0+N_1+1 \\ \sigma_0+\sigma_1 \end{matrix}\right), \quad (4.5)$$

with $\gamma\left(\frac{\sigma_1}{\sigma_0}\right)$ defined in (9.13). This demonstrates how the term $2\pi i F^{(1)}\left(z; \begin{matrix} N_0+N_1+1 \\ \sigma_0+\sigma_1 \end{matrix}\right)$ is also switched on smoothly in (4.2), again via a complementary error function. An example of the accuracy and smoothness of this result is illustrated in Figure 5.

In fact, this is the simplest version of the higher-order Stokes phenomenon. In a typical situation, the $F^{(1)}\left(z; \begin{matrix} N_0+N_1+1 \\ \sigma_0+\sigma_1 \end{matrix}\right)$ are linked to doubly exponentially small terms. Through this process, the coefficient of this $F^{(1)}$ hyperterminant undergoes changes, potentially resulting in the hyperterminant being switched off or on [5].

Note that the smoothing for this type of higher-order Stokes phenomenon originates from the representation of $F^{(2)}$ in terms of a ${}_2F_1$ hypergeometric function, as its argument $x = 1 + \frac{\sigma_1}{\sigma_0}$ traverses its branch cut $x > 1$. Compare equations (9.10), (9.11), Theorem 9.2 and [44, eq. 15.2.3].

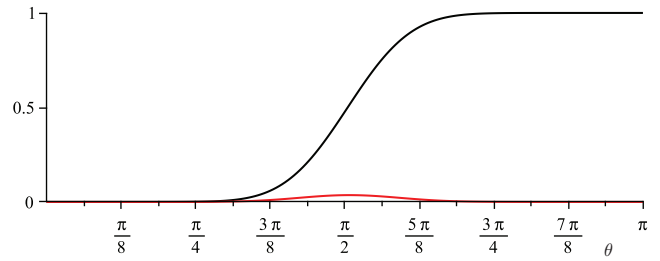


FIGURE 5 | An example of the smoothing across $\arg(\sigma_0) = \arg(\sigma_1)$, $\arg(\sigma_0 z) \neq \pi$, based on (4.5). The black curve represents $\left| \frac{F^{(2)}(z; N_0+1, N_1+1)}{2\pi i F^{(1)}(z; N_0+N_1+1)} \right|$, while the red curve shows $\left| \frac{F^{(2)}(z; N_0+1, N_1+1)}{2\pi i F^{(1)}(z; N_0+N_1+1)} + \frac{1}{2} \operatorname{erfc}\left(\gamma\left(\frac{\sigma_1}{\sigma_0}\right)\sqrt{\frac{1}{2}N_1}\right) \right|$, a measure of the error of the approximation, for indicative values $\sigma_0 = 1.5e^{i\theta}$, $N_0 = 30.3$, $\sigma_1 = i\sqrt{2}$, $N_1 = 29$, and $z = 20$.

4.3 | Uniform Approximation Covering All Three Types of Cases

To deal with the exceptional situation above where $\arg \sigma_0 = \arg \sigma_1$ and also $\arg(\sigma_0 z) = \pi$, so encompassing both poles in $F^{(2)}$ and thus both types of higher-order Stokes phenomenon simultaneously (see the right-hand, combined, case in Figure 3), it is necessary to obtain a uniform asymptotic approximation for the second hyperterminant function covering the smoothing of all the above three cases of the higher-order Stokes phenomenon. This is achieved in Section 9.5 and is given in Theorem 9.3. A simplified version is

$$F^{(2)}\left(z; \begin{matrix} N_0+1, & N_1+1 \\ \sigma_0, & \sigma_1 \end{matrix}\right) \sim -\pi^2 \operatorname{erfc}\left(d_1 \alpha_0(z) \sqrt{\frac{1}{2}N_1}; d_1 \alpha_0(\zeta_1) \sqrt{\frac{1}{2}N_1}; d_1^{-1} \sqrt{\frac{N_0}{N_1}}\right) e^{(\sigma_0+\sigma_1)z} z^{N_0+N_1} - \frac{(\sigma_0+\sigma_1)^{N_0+N_1+1} \Gamma(N_0+1) \Gamma(N_1+1)}{\sigma_0^{N_0+1} \sigma_1^{N_1} \Gamma(N_0+N_1+2)} {}_2F_1\left(\begin{matrix} 1, N_0+1 \\ N_0+N_1+2 \end{matrix}; 1 + \frac{\sigma_1}{\sigma_0}\right) \times F^{(1)}\left(z; \begin{matrix} N_0+N_1+1 \\ \sigma_0+\sigma_1 \end{matrix}\right), \quad (4.6)$$

as $z \rightarrow \infty$, with σ_0 , σ_1 , $\frac{\sigma_0 z}{N_0}$, and $\frac{\sigma_1 z}{N_1}$ and their reciprocals being bounded, and with

$$\frac{1}{2} \alpha_0^2(z) = 1 + \frac{\sigma_0 z}{N_0} + \ln\left(e^{-\pi i} \frac{\sigma_0 z}{N_0}\right), \quad d_1 = \frac{i \alpha_0(\zeta_1)}{1 - \frac{\sigma_0 N_1}{\sigma_1 N_0}}, \quad \zeta_1 = e^{\pi i} \frac{N_1}{\sigma_1}.$$

The function $\operatorname{erfc}(x; y; \lambda)$ introduced in (4.6) is a *new* special function describing the universal smoothing and is defined by

$$\operatorname{erfc}(x; y; \lambda) = \frac{2}{\sqrt{\pi}} \int_x^\infty e^{-(\tau-y)^2} \operatorname{erfc}(\lambda \tau) d\tau. \quad (4.7)$$

The function (4.7) is a generalization of the previously found complementary error function, which governs the ordinary

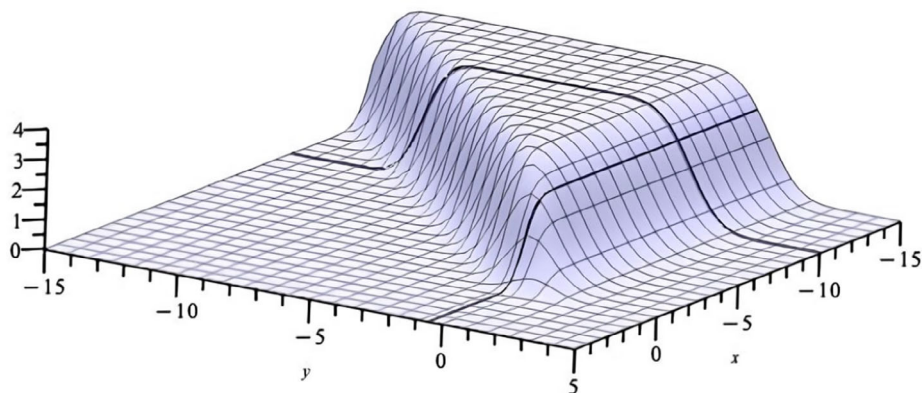


FIGURE 6 | The function $\text{erfc}(x; y; 1.2)$, and the curves $\text{erfc}(x; -0.5; 1.2)$ and $\text{erfc}(x; -10.1; 1.2)$.

Stokes phenomenon. It is effectively a Gaussian convolution of such an error function. In Appendix B, we provide a comprehensive list of properties associated with this special function, including the useful simplifications $\text{erfc}(x; y; 0) = \text{erfc}(x - y)$ and $\text{erfc}(x; 0; 1) = \frac{1}{2} \text{erfc}^2(x)$.

In the new approximant $\text{erfc}(x; y; \lambda)$, the variable x is associated with the $z \leftrightarrow \sigma_0$ higher-order Stokes phenomenon, while the variable y is linked to the $\sigma_0 \leftrightarrow \sigma_1$ higher-order Stokes phenomenon. As shown in Figure 6, for fixed y and λ , the curve $x \mapsto \text{erfc}(x; y; \lambda)$ exhibits the characteristic shape of an error function: exponentially decreasing as $x \rightarrow +\infty$, with its limit as $x \rightarrow -\infty$ being $2 \text{erfc}(\frac{\lambda y}{\sqrt{\lambda^2 + 1}})$, as seen in (B4). On the other hand, for fixed x and λ , the curve $y \mapsto \text{erfc}(x; y; \lambda)$ decreases exponentially as $y \rightarrow \pm\infty$.

4.4 | The Smoothing Across $\arg \sigma_0 = \arg \sigma_1$ when $\arg(\sigma_0 z) = \pi$

Using the uniform result (4.6), it is now possible to consider the case when $\arg \sigma_0 = \arg \sigma_1$ and also $\arg(\sigma_0 z) = \pi$ so that both of these higher-order Stokes phenomena occur simultaneously. This leads to perhaps the most interesting result of all.

We fix σ_0 and σ_1 such that $\arg \sigma_0 \approx \arg \sigma_1$, and allow z to cross the line $\arg(\sigma_0 z) = \pi$, both $\text{erfc}(x; y; \lambda)$ and the $F^{(1)}$ in (4.6) exhibit error function behavior. One function is switching on the exponentially small term $e^{(\sigma_0 + \sigma_1)z} z^{N_0 + N_1}$, while the other simultaneously is switching it off.

Despite no net discrete switching on of terms occurring away from the Stokes line, the exponentially small term remains influential on the Stokes curve itself. There is a smooth and “ghost-like” transient presence of the exponentially small term near to the Stokes line as illustrated in Figure 7. The value of the smooth multiplier of this “ghost” exactly on the Stokes curve $\arg(\sigma_0 z) = \pi$ is given by

$$2\pi \arctan \sqrt{\frac{N_0}{N_1}} + \mathcal{O}(z^{-1/2}), \quad (4.8)$$

as detailed in Corollary 9.1.

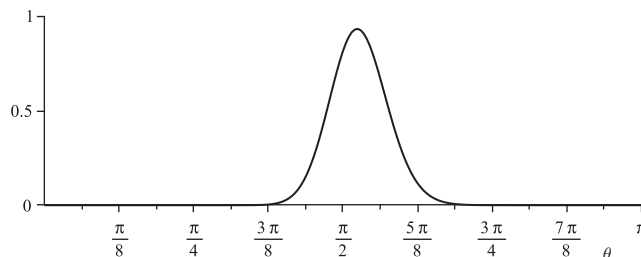


FIGURE 7 | An example of the “ghost-like” transient presence of an exponentially small term near to the Stokes line arising from the interference of terms in (4.6). The black curve shows $\left| \frac{e^{-(\sigma_0 + \sigma_1)z}}{2\pi i z^{N_0 + N_1}} F^{(2)}\left(z; \begin{matrix} N_0 + 1, N_1 + 1 \\ \sigma_0, \sigma_1 \end{matrix}; 1 \right) \right|$ for $\sigma_0 = 1.5i + 0.000001$, $N_0 = 30.3$, $\sigma_1 = i\sqrt{2}$, $N_1 = 29$, and $z = 20e^{i\theta}$. Note that the shape of this curve might suggest that it arises from parameters near to tip of the wedge in Figure 6. This is not the case. It is here arising from the combination of terms in (4.6).

In the extreme case of $\sigma_0 = \sigma_1$ and $N_0 = N_1$, the uniform approximation (4.6) simplifies to

$$\begin{aligned} & \lim_{\varepsilon \rightarrow 0^+} F^{(2)}\left(z; \begin{matrix} N + 1, N + 1 \\ \sigma e^{-\varepsilon i}, \sigma \end{matrix}; 1 \right) \\ & \sim -\pi^2 \text{erfc}\left(\alpha_0(z) \sqrt{\frac{1}{2}N}; 0; 1\right) e^{2\sigma z} z^{2N} - \pi i F^{(1)}\left(z; \frac{2N + 1}{2\sigma}\right) \\ & = -\frac{1}{2} \pi^2 \text{erfc}^2\left(\alpha_0(z) \sqrt{\frac{1}{2}N}\right) e^{2\sigma z} z^{2N} - \pi i F^{(1)}\left(z; \frac{2N + 1}{2\sigma}\right) \\ & \sim \frac{1}{2} \left(F^{(1)}\left(z; \frac{N + 1}{\sigma}\right)\right)^2 - \pi i F^{(1)}\left(z; \frac{2N + 1}{2\sigma}\right), \end{aligned}$$

in which we have used the identity $\text{erfc}(x; 0; 1) = \frac{1}{2} \text{erfc}^2(x)$, see (B3), and the normal Stokes phenomenon approximation (3.6). We remark that, in fact, the final expression is also equal to the limit on the left-hand side (see [18, eq. 4.4]).

The case where the points $0, \sigma_0$, and σ_1 align may initially seem exceptional, but it is actually rather common in practice. This occurs, among other instances, when dealing with nonlinear ODEs or when considering real-valued oscillatory solutions of PDEs. We provide examples of these cases in Sections 5–6.

It is worth noting that in our original definition (3.7), we assumed that $\arg \sigma_1 - \arg \sigma_0 \in (0, 2\pi)$, gradually approaching the case where $\arg \sigma_1 - \arg \sigma_0 = 0$ from the positive side. Had we chosen to approach it from the negative side, as per connection formula (4.2), we would have omitted the first term on the right-hand side of (4.6). This would result in the double higher-order Stokes phenomenon being a simple activation of the exponentially small term $e^{(\sigma_0 + \sigma_1)z} z^{N_0 + N_1}$. Compare with identity (5.3).

4.5 | List of Applications of the Main Results

Having summarized the main results of the paper, the next four sections contain examples of the types of smoothing of the simultaneous higher-order Stokes phenomena.

The first three examples, Sections 5–7, deal with the effect of the smoothed higher-order Stokes phenomena on the asymptotics of a progenitor function.

The first two examples in Sections 5–6 deal with the higher-order Stokes phenomena arising from a variation in the asymptotic parameter z for fixed σ_i exponent factors and in the presence of an infinite number of Borel-plane singularities. In Section 5, the associated symmetries lead to a simplification in the limit of the $F^{(2)}$ hyperterminant on the higher-order Stokes line.

In Section 7, we consider the linear telegraph PDE system with only three Borel-plane singularities. Unlike in Sections 5–6, the σ_i now move relative to one another as functions of the variables of the PDE system.

All these examples exhibit behavior that gives rise to a “ghost-like” smooth hump appearance of the higher-order Stokes phenomenon in the vicinity of the higher-order Stokes lines with a multiplier of the form (4.8) on the Stokes line. The cause of this apparition varies between examples. In some cases, it arises directly from the behavior of a single hyperterminant, in others it is the result of cancellations between hyperterminants of different orders.

In Section 8, we demonstrate the corresponding effect of the smoothing of the higher-order Stokes phenomenon on the re-expansion of the individual late terms in the asymptotic expansion, and thereby provide a rigorous derivation of the formal ideas found in Shelton et al. [20].

5 | Application: The Gamma Function and Its Reciprocal

The presence of a fixed regularly spaced collinear Borel-plane singularities is common in nonlinear ODEs, or systems involving periodic orbits. As is well demonstrated in [43], this conjunction gives rise to an infinite sequence of simultaneously occurring Stokes phenomena. Contributions from the most dominant Borel-plane singularity switch on an infinite number of subdominant contributions. The first subdominant contribution itself may simultaneously switch on an infinite number of subsubdominant contributions. Each one of these birthing subsubdominant

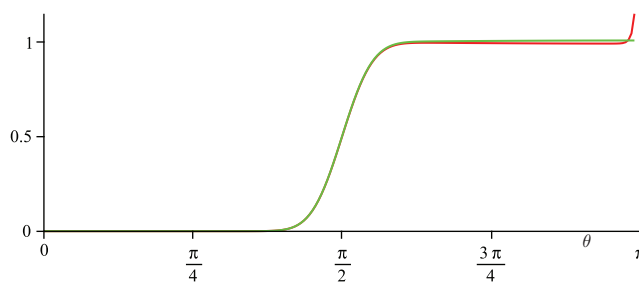


FIGURE 8 | The graphs show the remainders of the truncated expansions (5.1) $|e^{-2\pi iz} R_N^{(j)}(z)|$ with $j = 1$ (red) and $j = 2$ (green) for $N = 62$ and $z = 10e^{i\theta}$.

contributions may also simultaneously switch on sub-subsubdominant contributions, and so forth.

If the subdominant contributions are all equally spaced in the Borel plane, this may give rise to constructive interference, with the Stokes multiplier for an overall individual subdominant contribution being the sum of Stokes multipliers from all the Stokes phenomena that gave it birth.

In this section, we demonstrate the higher-order smoothing on the gamma function and its reciprocal. This is an example of the simultaneous occurrence of two higher-order Stokes phenomena when $\arg(\sigma_0 z) = \arg(\sigma_1 z) = \pi$, the right-hand case of Figure 3. In this case however, rather than just three singularities, there is an infinite collinear array of equally spaced and fixed Borel-plane singularities. Hence, this is an example of where the higher-order Stokes phenomenon is being driven by changes in the asymptotic parameter z , with fixed σ_i .

As we will illustrate below and as discussed in [18], these cases offer additional identities for the hyperterminants. Here, it transpires that the smoothing of the higher-order Stokes phenomenon can be described using the standard erfc function, exceptionally in this example due to symmetrical simplifications arising from the regular singularity spacing in a single infinite array in the Borel plane.

In our demonstration, we will study the gamma function and its reciprocal and utilize the truncated asymptotic expansions as given in [18]:

$$z^{-z} e^z \sqrt{\frac{z}{2\pi}} \Gamma(z) = \sum_{n=0}^{N-1} (-1)^n \frac{\gamma_n}{z^n} + R_N^{(1)}(z), \tag{5.1}$$

$$z^z e^{-z} \sqrt{\frac{2\pi}{z}} \frac{1}{\Gamma(z)} = \sum_{n=0}^{N-1} \frac{\gamma_n}{z^n} + R_N^{(2)}(z).$$

Here, the γ_n are known as the Stirling coefficients, with the first few values being

$$\gamma_0 = 1, \quad \gamma_1 = -\frac{1}{12}, \quad \gamma_2 = \frac{1}{288}, \quad \gamma_3 = \frac{139}{51840}, \quad \gamma_4 = -\frac{571}{2488320}.$$

The optimal number of terms has $N \approx 2\pi|z|$. Expressing $z = |z|e^{i\theta}$, the plots of $|e^{-2\pi iz} R_N^{(j)}(z)|$ are depicted in Figure 8. Note that

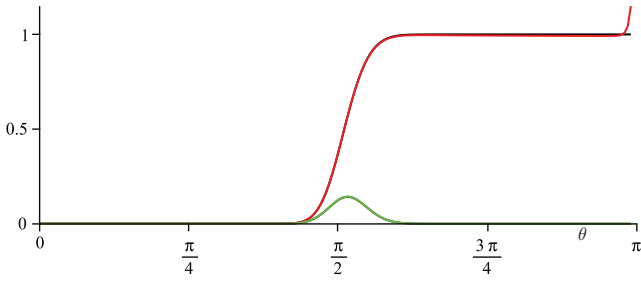


FIGURE 9 | The graphs show the remainders of the level 1 truncated expansions (5.2), $|e^{-4\pi iz} R_N^{(j)}(z)|$ with $j = 3$ (red) and $j = 4$ (green) for $N = 125$ and $z = 10e^{i\theta}$. The two black curves, depicting $\lim_{\varepsilon \rightarrow 0^+} \left| \frac{e^{-4\pi iz} z^{2-N}}{(2\pi i)^2} F^{(2)}\left(z; \frac{N}{2}, \frac{N}{2}; \frac{N}{2\pi i \pm \varepsilon}, \frac{N}{2\pi i}\right) \right|$, are covered by the red and green curves. Compare (5.3).

$\Gamma(z)$ has poles along $\theta = \pi$, causing the red curves to flip upward near $\theta = \pi$ in Figures 8 and 9.

The level 1 hyperasymptotic approximations are

$$z^{-z} e^z \sqrt{\frac{z}{2\pi}} \Gamma(z) = \sum_{n=0}^{N-1} (-1)^n \frac{\gamma_n}{z^n} + \frac{z^{1-N}}{2\pi i} \sum_{n=0}^{N/2-1} (-1)^n \gamma_n F^{(1)}\left(z; \frac{N-n}{2\pi i}\right) - \frac{z^{1-N}}{2\pi i} \sum_{n=0}^{N/2-1} (-1)^n \gamma_n F^{(1)}\left(z; \frac{N-n}{-2\pi i}\right) + R_N^{(3)}(z),$$

$$z^z e^{-z} \sqrt{\frac{2\pi}{z}} \frac{1}{\Gamma(z)} = \sum_{n=0}^{N-1} \frac{\gamma_n}{z^n} - \frac{z^{1-N}}{2\pi i} \sum_{n=0}^{N/2-1} \gamma_n F^{(1)}\left(z; \frac{N-n}{2\pi i}\right) + \frac{z^{1-N}}{2\pi i} \sum_{n=0}^{N/2-1} \gamma_n F^{(1)}\left(z; \frac{N-n}{-2\pi i}\right) + R_N^{(4)}(z). \tag{5.2}$$

When we maintain the optimal number of terms of the original expansions, $N \approx 2\pi|z|$, it may be deduced by comparing the remainder terms $R_N^{(1)}(z), R_N^{(2)}(z)$ and the $n = 0$ hyperterminants in the level 1 expansions that $F^{(1)}\left(z; \frac{N}{2\pi i}\right)$ incorporates the familiar error function smoothing, as illustrated in Figure 8.

However, when determining the optimal truncation N of the original asymptotic series to minimize the overall error after applying the level 1 hyperasymptotic approximation (see [28, Theorem 6.2]), it turns out that $N \approx 4\pi|z|$. The associated remainders in the level 1 expressions $R_N^{(j)}(z)$, for $j = 3, 4$, scaled to better reveal the smoothings, are illustrated in Figure 9.

Therefore, for $\Gamma(z)$, terms of order $e^{2\pi iz}$ (Figure 8) and $e^{4\pi iz}$ (Figure 9) are switched on as the positive imaginary axis is crossed. In fact, as the positive imaginary axis is crossed, terms of order $e^{2n\pi iz}$, where $n = 1, 2, 3, \dots$, are switched on. Resumming this transseries will reveal the poles along the negative z -axis. A similar phenomenon occurs along the negative imaginary axis. For further details, refer to [18].

For $1/\Gamma(z)$, no terms of order $e^{2n\pi iz}$, $n = 2, 3, 4, \dots$, are switched on when the positive imaginary axis is crossed (see Figure 9 for the case $n = 2$). This is reasonable because nothing notable occurs for this function near the negative z -axis.

Note that in Figure 8, the value on the Stokes line for both curves is approximately $\frac{1}{2}$, which is expected. However, in Figure 9, the red curve crosses the positive imaginary axis at $\frac{3}{8}$ and the green curve at $\frac{1}{8}$. This indicates that the higher-order Stokes phenomenon is not described merely by a single error function.

The relevant hyperterminants at level 2 are $F^{(1)}\left(z; \frac{N}{4\pi i}\right)$, which exhibits the standard error function behavior, and $F^{(2)}\left(z; \frac{N}{2\pi i}, \frac{N}{2\pi i}\right)$.

The Stokes phenomena of the general level 2 hyperterminants $F^{(2)}\left(z; \frac{N_1, N_2}{\sigma_1, \sigma_2}\right)$ are discussed in Section 9. For the special case in this section, whereby $N_1 = N_2$ and $\sigma_1 = \sigma_2$, we have the simplification

$$\lim_{\varepsilon \rightarrow 0^+} F^{(2)}\left(z; \frac{N}{2\pi i} \pm \varepsilon, \frac{N}{2\pi i}, \sigma\right) = \frac{\left(F^{(1)}\left(z; \frac{N}{2\pi i}, \sigma\right)\right)^2 \pm 2\pi i F^{(1)}\left(z; \frac{N}{2\pi i}, \sigma\right)}{2} \tag{5.3}$$

(see [18, eq. 4.4]). Using (3.6), in terms of Stokes multipliers, we can interpret the right-hand side of (5.3) on the Stokes lines (for a generic local Stokes crossing coordinate $\alpha \sim 0$) as contributing

$$\frac{\left(\frac{1}{2} \operatorname{erfc} \alpha\right)^2 \pm \frac{1}{2} \operatorname{erfc} \alpha}{2} \rightarrow \frac{\left(\frac{1}{2}\right)^2 \pm \frac{1}{2}}{2} = \frac{3}{8}, -\frac{1}{8}.$$

Note that our formula (4.8) for the general multiplier gives us the multiplier $(2\pi i)^{-2} 2\pi \arctan 1 = -\frac{1}{8}$. From (5.3) or (4.2), we obtain

$$\lim_{\varepsilon \rightarrow 0^+} \left[F^{(2)}\left(z; \frac{N}{2\pi i} + \varepsilon, \frac{N}{2\pi i}\right) - F^{(2)}\left(z; \frac{N}{2\pi i} - \varepsilon, \frac{N}{2\pi i}\right) \right] = 2\pi i F^{(1)}\left(z; \frac{N}{4\pi i}\right).$$

Hence, the green curve in Figure 9 can be seen as the difference of the red curves in Figures 9 and 8, meaning the two active Stokes phenomena of the red curves cancel each other out.

One initial interpretation of the green curve in Figure 9 suggests that there is no Stokes phenomenon occurring at a subsubdominant level. This interpretation is accurate since no doubly exponentially small terms are ultimately activated. However, the presence of the factor $\frac{1}{8}$ indicates that doubly exponentially small terms are indeed active precisely on the Stokes line itself!

6 | Application: A Second-Order Nonlinear ODE

In this example, we consider the situation in which the higher-order Stokes phenomenon is again being driven by changes in the asymptotic variable z , with fixed σ_i but where the exponents (or, equivalently, Borel-plane singularities σ_i) are not equally spaced. For the nonlinear ODE (6.1), each of these exponents $\sigma_i z$ individually generates an infinite array of subdominant exponents $n\sigma_i z$, $n \in \mathbb{Z}$ (and collectively, a multidimensional array $n\sigma_i z + m\sigma_j z + p\sigma_k z$, $i \neq j \neq k, n, m, p \in \mathbb{Z}$).

Here, the simplifications of the previous example no longer hold, yet we still observe similar ultimate results in the contribution from the smoothed higher-order Stokes phenomenon arising from $F^{(2)}$ being a “ghost-like” hump in the smoothing across the higher-order Stokes line (cf. (4.6)).

We analyze the large- z asymptotics of the second-order nonlinear ODE

$$u''(z) + (1 + \sqrt{2})u'(z) - \left(2 + \frac{3}{2}\sqrt{2}\right)u(z)u'(z) - \frac{7}{4}\sqrt{2}u^2(z) + \sqrt{2}u(z) + \frac{1}{z} = 0. \quad (6.1)$$

This equation has been chosen to yield simple yet unequally spaced exponents: $0, -z,$ and $-\sqrt{2}z$. The balance between the final two terms leads us to a formal solution of the form

$$u(z) \sim \sum_{n=0}^{\infty} \frac{a_n}{z^{n+1}}, \quad (6.2)$$

as $z \rightarrow \infty$, with $a_0 = -1/\sqrt{2}$. Subsequently, the remaining coefficients satisfy the recurrence relation

$$\begin{aligned} \sqrt{2}a_n = & (1 + \sqrt{2})na_{n-1} + \frac{7}{4}\sqrt{2} \sum_{k=0}^{n-1} a_k a_{n-1-k} - n(n-1)a_{n-2} \\ & - \left(1 + \frac{3}{4}\sqrt{2}\right)n \sum_{k=0}^{n-2} a_k a_{n-2-k} \end{aligned}$$

for $n = 1, 2, 3, \dots$

Thus far, our solution lacks any free constants. To incorporate terms representing exponentially small contributions, we introduce $u(z) = u_0(z) + u_1(z) + u_2(z) + \dots$, where $u_0(z)$ is the Borel-Laplace transform of (6.2), $u_1(z)$ is exponentially small, $u_2(z)$ is doubly exponentially small, and so forth. For $u_1(z)$, we derive the linear ODE

$$\begin{aligned} u_1''(z) + \left(1 + \sqrt{2} - \left(2 + \frac{3}{2}\sqrt{3}\right)u_0(z)\right)u_1'(z) \\ + \left(\sqrt{2} - \frac{7}{2}\sqrt{2}u_0(z) - \left(2 + \frac{3}{2}\sqrt{2}\right)u_0'(z)\right)u_1(z) = 0. \end{aligned}$$

It is easy to check that $u_1(z) \sim C_1 e^{-z} z^{-\sqrt{2}} + C_2 e^{-\sqrt{2}z} z^{-\frac{3}{2}}$. Solving the subsequent equations for $u_k(z)$, $k \geq 2$ and formally summing them, ultimately, we arrive at the transseries solution

$$u(z) \sim \sum_{k=0}^{\infty} \sum_{m=0}^{\infty} \left(C_1 e^{-z} z^{-\sqrt{2}}\right)^k \left(C_2 e^{-\sqrt{2}z} z^{-\frac{3}{2}}\right)^m \sum_{n=0}^{\infty} \frac{a_{k,m,n}}{z^n}, \quad (6.3)$$

where $a_{0,0,0} = 0$, $a_{0,0,n} = a_{n-1}$ for $n = 1, 2, 3, \dots$, and the initial recurrence relations are

$$\begin{aligned} n(\sqrt{2}-1)a_{1,0,n} = & (n + \sqrt{2})(n-1 - \sqrt{2})a_{1,0,n-1} \\ & + (2 - 2\sqrt{2}) \sum_{k=0}^{n-1} a_{0,0,n+1-k} a_{1,0,k} \\ & + \left(\left(2 + \frac{3}{2}\sqrt{2}\right)n + 3 + 2\sqrt{2}\right) \sum_{k=0}^{n-1} a_{0,0,n-k} a_{1,0,k}, \end{aligned}$$

$$\begin{aligned} n(1 - \sqrt{2})a_{0,1,n} = & \left(n + \frac{1}{2}\right)\left(n + \frac{3}{2}\right)a_{0,1,n-1} \\ & + \left(3 - \frac{3}{2}\sqrt{3}\right) \sum_{k=0}^{n-1} a_{0,0,n+1-k} a_{0,1,k} \\ & + \left(\left(2 + \frac{3}{2}\sqrt{2}\right)n + 3 + \frac{9}{4}\sqrt{2}\right) \sum_{k=0}^{n-1} a_{0,0,n-k} a_{0,1,k} \end{aligned}$$

for $n = 1, 2, 3, \dots$. Note that $a_{1,0,0}$ and $a_{0,1,0}$ are free from any constraints. Setting $a_{1,0,0} = a_{0,1,0} = 1$ without loss of generality, we allocate the freedom to C_1 and C_2 , the sole free constants in the complete transseries expansions.

To compute the first three Stokes multipliers K_{ij} , we employ the late coefficient asymptotics, as detailed in [28]. As $N_0 \rightarrow +\infty$, we have the approximation

$$\begin{aligned} a_{N_0} \sim & \frac{K_{01}}{2\pi i} \sum_{n=0}^{N_1-1} \frac{a_{1,0,n} \Gamma(N_0 + 1 - \sqrt{2} - n)}{(1)^{N_0+1-\sqrt{2}-n}} + \frac{K_{02}}{2\pi i} \sum_{n=0}^{N_2-1} \frac{a_{0,1,n} \Gamma(N_0 - \frac{1}{2} - n)}{(\sqrt{2})^{N_0 - \frac{1}{2} - n}} \\ & - \frac{K_{01}K_{12}}{(2\pi i)^2} \sum_{n=0}^{N_2-1} a_{0,1,n} F^{(2)}\left(0; \begin{matrix} N_0 - N_1 + 3 - \sqrt{2}, N_1 - \frac{3}{2} + \sqrt{2} - n \\ -1, 1 - \sqrt{2} \end{matrix}\right), \end{aligned}$$

where the optimal numbers of terms are $N_1 \approx \frac{2\sqrt{2}-2}{2\sqrt{2}-1}N_0$ and $N_2 \approx \frac{\sqrt{2}-1}{2\sqrt{2}-1}N_0$. Note that the “1” and “ $\sqrt{2}$ ” in the denominators of the approximation for a_{N_0} are the prefactors of z in the associated (small) exponents in the basis of the solution.

By setting $N_0 = 100, 102,$ and 104 (for example), we establish three equations with three unknowns, which can be solved numerically to give

$$\begin{aligned} K_{01} & \approx -199.049496506302686684534546i, \\ K_{12} & \approx 2.61181979i, \\ K_{02} & \approx 259.940707924 - 11.132449502i \\ & \approx \frac{1}{2}K_{01}K_{12} - 11.132449502i. \end{aligned}$$

All digits in these approximations are correct. Note that Stokes multipliers can be large!

When we cross the positive real z -axis, a nonlinear Stokes phenomenon occurs. In the transseries (6.3), the constants C_j are replaced by $C_j \pm K_{0j}$, depending on whether we cross the positive real axis upward or downward.

For a definite example, we will illustrate the Stokes and higher-order Stokes phenomena as we travel along the straight line $z = 40 + it$ with $t \in [-40, 40]$. In the half-plane $\text{Im}(z) < 0$, we will compute the solution $u_{0,0}(z)$, being the solution when $C_1 = C_2 = 0$. At our starting point $z_0 = 40 - 40i$, to capture the smoothing of the Stokes and higher-order Stokes phenomena, we need an approximation that is significantly more accurate than a mere optimal asymptotic approximation. To achieve this, we compute the solution at $z_1 = 40 - 80i$ via optimal truncation

of (6.2) taking approximately $|z_1|$ terms. We then numerically integrate the original nonlinear ODE (6.1) along a straight line from z_1 to z_0 . Since $|z_1| > |z_0|$, the approximation at z_1 , and hence the numerically integrated projection between z_1 and z_0 , will be more accurate than the corresponding optimal truncated approximation at z_0 . Hence, this numerically integrated result at z_0 may serve as the starting point for our subsequent numerical calculation of the Stokes and higher-order Stokes smoothings. The values of $u_{0,0}(z_0)$ and $u'_{0,0}(z_0)$ we so obtain are

$$\begin{aligned} u_{0,0}(z_0) &\approx -0.008835575253062194710342008651 \\ &\quad -0.008945607882457218431762007868i, \\ u'_{0,0}(z_0) &\approx -0.000002831892119643922083317325 \\ &\quad +0.000223551608986949913034811617i. \end{aligned}$$

In turn, these two values will serve as the starting point for numerical integration to determine the values of $u_{0,0}(z)$ along the line $z = 40 + it$, $t \in [-40, 40]$. This will allow us to compare, along that line, the level 1 hyperasymptotic approximation with the first two terms, which are of order $e^{-\sqrt{2}z}$:

$$\begin{aligned} u_{0,0}(z) &- \sum_{n=0}^{N_0-1} \frac{a_n}{z^{n+1}} \\ &- \frac{K_{01}}{2\pi i z^{N_0}} \sum_{n=0}^{N_1-1} a_{1,0,n} F^{(1)} \left(z; \begin{matrix} N_0 + 1 - \sqrt{2} - n \\ -1 \end{matrix} \right) \\ &\sim \frac{K_{02}}{2\pi i z^{N_0}} \sum_{n=0}^{N_2-1} a_{0,1,n} F^{(1)} \left(z; \begin{matrix} N_0 - \frac{1}{2} - n \\ -\sqrt{2} \end{matrix} \right) \\ &+ \frac{K_{01}K_{12}}{(2\pi i)^2 z^{N_0}} \sum_{n=0}^{N_2-1} a_{0,1,n} \\ &\quad \times F^{(2)} \left(z; \begin{matrix} N_0 - N_1 + 2 - \sqrt{2}, N_1 - \frac{3}{2} + \sqrt{2} - n \\ -1, 1 - \sqrt{2} \end{matrix} \right), \end{aligned} \tag{6.4}$$

where we take $N_0 = 56$, $N_1 = 16$, and $N_2 = 2$. Ideally for this illustration, we should have taken $N_2 = 1$, but since $a_{0,1,1} = \frac{13}{2} + \frac{31}{16}\sqrt{2} \approx 9.24$, truncating at this term is likely to lead to a relatively large error. In Figure 10, we observe that the second hyperterminant $F^{(2)}$ still exhibits the predicted simple hump.

7 | Application: The Telegraph Equation

In this example, we study the telegraph PDE system, for which a specific motivation is provided in Appendix C:

$$\begin{aligned} 2 \frac{\partial^2 v}{\partial x \partial t} &= v(x, t), \\ v(x, 0) &= e^{-x} \quad \text{Re}(x) \geq 0, \\ v(0, t) &= 1, \quad t > 0. \end{aligned}$$

Unlike the previous two examples, in the case the Borel-plane interpretation now has moving singularities, $\sigma_0(x, t)$ and $\sigma_1(x, t)$, which cross the contours of integration in both the $F^{(1)}$ and $F^{(2)}$ hyperterminants simultaneously. This gives rise to simultaneous Stokes and higher-order Stokes phenomena. Collinearity of the Borel-plane singularities is only instantaneous here, with the resulting net difference is a subdominant contribution that is only a fleetingly “ghost-like” presence, being smoothly simultaneous switching on and off according to (the spirit of) Theorem 9.3, see Figure 12. We will consider both x and t large.

The Laplace transform solution of this system for $t > 0$ is given by

$$v(x, t) = e^{-x(x+\frac{t}{2})} + \frac{1}{2\pi i} \int_{-\infty}^{(0+)} \frac{e^{pt+\frac{x}{2p}}}{p(1 \pm 2p)} dp, \quad \text{Re}(x) \geq 0, \tag{7.1}$$

where the initial (Hankel) contour of integration begins at negative infinity, circles the origin once in the positive direction, and returns to negative infinity.

We focus now on $\text{Re}(x) > 0$ and transform the relevant integral in (7.1) using $z = \sqrt{xt}/2$, $2x = \beta^2 t$, $\beta \in \mathbb{C}$, the asymptotic parameter being $z \rightarrow \infty$. The integral representation of the solution then becomes

$$v(x, t) = e^{-x-\frac{t}{2}} + \frac{1}{2\pi i} \int_{-\infty}^{(0+)} e^{-zf(p)} g(p; \beta) dp, \quad \text{Re}(z) > 0, \tag{7.2}$$

with

$$f(p) = -p - \frac{1}{p}, \quad g(p; \beta) = \frac{1}{p(1 + \beta p)}.$$

A further transformation to a variable $u = f(p)$ would render the solution of this PDE in the form of a Borel transform. The analysis could be carried out in the Borel plane, but here we carry out the analysis in the p -plane. The final results are identical.

The integral representation (7.2) above seems to suggest that the multiplier of terms of the size $e^{-x-\frac{t}{2}}$ is just 1. Remarkably, this is correct in the complex x -plane with $\text{Re}(x) > 0$, but not on $x > 0$ where, as explained below, the combination of the simultaneous Stokes and higher-order Stokes phenomena on that line give rise to a net correct multiplier of $\frac{2}{\pi} \arctan((2x/t)^{1/4})$.

The integral has two saddles at $p = \pm 1$, a pole at $p = -\frac{1}{\beta}$ and an essential singularity at $p = 0$. Deforming the contour of integration to paths of steepest descent over the saddles demonstrates that both paths run into/out of the essential singularity at $p = 0$, with an associated vanishing contribution. (An alternative analysis using the transformation $p = e^w$ can also be used to demonstrate this.)

For $x > 0$ and using [44, eqs. 10.9.19 and 10.27.6], the exact representation of the solution is given by

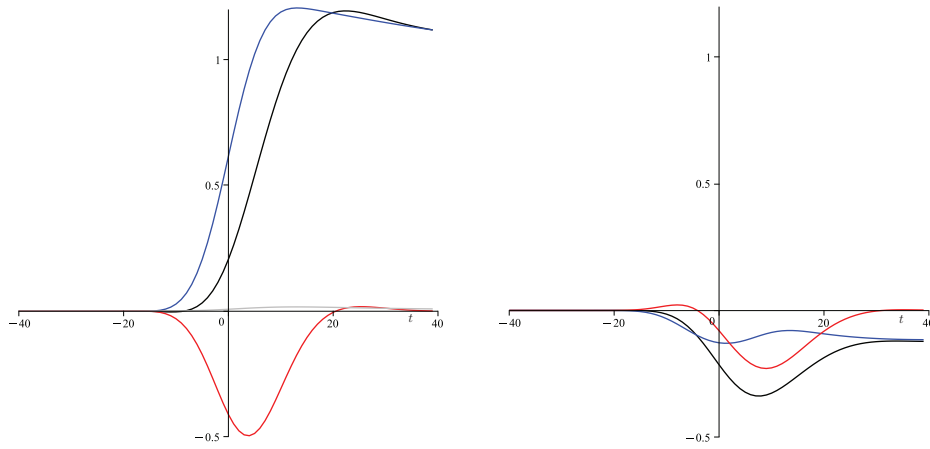


FIGURE 10 | The horizontal axis represents the imaginary part of $z = 40 + it$, with $t \in (-40, 40)$. Along the vertical axis, the real (left) and imaginary (right) parts of the three colored terms in Equation (6.4) are displayed. The gray curve (left) shows the absolute error in the approximation (6.4). All these terms have been multiplied by $e^{\sqrt{2z} z^{\frac{3}{2}} / K_{02}}$.

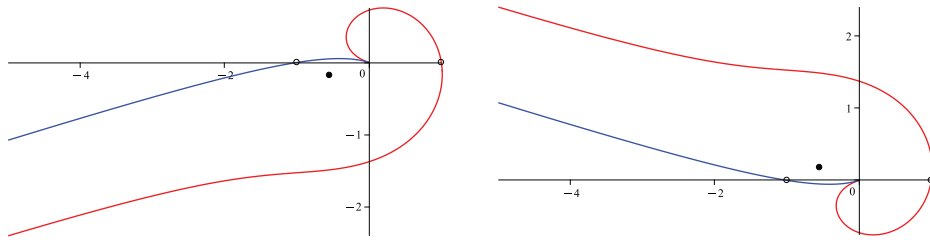


FIGURE 11 | The steepest descent paths in the cases $t = 10$, $x = 15e^{-\pi i/5}$ (left), and $x = 15e^{\pi i/5}$ (right). Note that the orientation of the blue path through the saddle point -1 changes from right-to-left in the case $\text{Im}(x) < 0$ to left-to-right in the case $\text{Im}(x) > 0$, the direction of integration along the red contour remains the same, compare with (7.2). The pole $p = -\beta^{-1}$ is located at \bullet .

$$v(x, t) = e^{-x - \frac{t}{2}} - \sum_{n=1}^{\infty} (-\beta)^{-n} I_n(2z),$$

$$I^{\pm}(z; \beta) = \frac{e^{-f_{\pm} z}}{\sqrt{z}} T^{\pm}(z; \beta), \quad T^{\pm}(z; \beta) \sim \pm \sum_{r=0}^{\infty} \frac{T_r^{\pm}(\beta)}{z^r},$$

where I_n represents the modified Bessel function of the first kind. While this is helpful, knowledge of an analytical solution is not essential, since the integrals (7.2) may be evaluated numerically along paths of steepest descent.

We start with the case $\text{Im}(\beta) < 0$ and it follows from the analysis above that both saddle point integrals contribute:

$$v(x, t) = e^{-x - \frac{t}{2}} + v_0(x, t) = e^{-(\beta + \beta^{-1})z} + I^+(z; \beta) + I^-(z; \beta),$$

$$z = \sqrt{xt/2}, \quad 2x = \beta^2 t,$$

where the terms $I^{\pm}(z; \beta)$ are the integrals along the steepest descent paths through the saddle points at $p = \pm 1$ and into/out of valleys at the essential singularity at $p = 0$, see Figure 11. The associated asymptotic expansions about the saddles $p = \pm 1$ with corresponding saddle height exponents $f_{\pm} = \mp 2$, are given by

as $z \rightarrow \infty$. The coefficients in the saddle point expansions are given by

$$T_r^+(\beta) = \frac{(-4)^{-r}}{2\sqrt{\pi}(1+\beta)} \frac{\Gamma(r + \frac{3}{2})}{r! \Gamma(\frac{3}{2} - r)} {}_2F_1\left(\frac{1}{2}, -2r; \frac{1}{1+\beta}\right),$$

$$T_r^-(\beta) = \frac{i4^{-r}}{2\sqrt{\pi}(1-\beta)} \frac{\Gamma(r + \frac{3}{2})}{r! \Gamma(\frac{3}{2} - r)} {}_2F_1\left(\frac{1}{2}, -2r; \frac{1}{1-\beta}\right).$$

Due to their arguments, these hypergeometric functions reduce to polynomials.

The level 0 asymptotic approximation is

$$v_0(x, t) = e^{2z} \sum_{r=0}^{N_0-1} \frac{T_r^+(\beta)}{z^{r+\frac{1}{2}}} + R_0(z; \beta; N_0).$$

Based on the analysis in [28], the optimal number of terms at this level is $N_0 \approx |4z|$. Moving to the level 1 hyperasymptotic approximation:

$$\begin{aligned}
 v_0(x, t) = & e^{2z} \sum_{r=0}^{N_0^+-1} \frac{T_r^+(\beta)}{z^{r+\frac{1}{2}}} + \frac{2e^{2z} z^{\frac{1}{2}-N_0^+}}{2\pi i} \sum_{r=0}^{N_0^--1} T_r^-(\beta) F^{(1)}\left(z; \begin{matrix} N_0^+ - r \\ -4 \end{matrix}\right) \\
 & - \frac{e^{2z} z^{\frac{1}{2}-N_0^+}}{2\pi i} F^{(1)}\left(z; \begin{matrix} N_0^+ + \frac{1}{2} \\ -\beta - 2 - \beta^{-1} \end{matrix}\right) \\
 & - e^{-2z} \sum_{r=0}^{N_0^--1} \frac{T_r^-(\beta)}{z^{r+\frac{1}{2}}} - \frac{e^{-2z} z^{\frac{1}{2}-N_0^-}}{2\pi i} F^{(1)}\left(z; \begin{matrix} N_0^- + \frac{1}{2} \\ -\beta + 2 - \beta^{-1} \end{matrix}\right) \\
 & + R_1(z; \beta; N_0^+, N_0^-),
 \end{aligned} \tag{7.3}$$

where the optimal numbers of terms are now

$$N_0^+ \approx |4z| + \left|(\beta - 2 + \beta^{-1})z\right| \quad \text{and} \quad N_0^- \approx \left|(\beta - 2 + \beta^{-1})z\right|. \tag{7.4}$$

In (7.3), the first two lines give the dominant expansion alongside its two re-expansions arising from its remainder terms, all sharing the common factor e^{2z} . The third line accounts for the contribution of the subdominant saddle and its re-expansion. Notably, there are two terms in (7.3) that do not involve a sum, representing the hyperasymptotic contributions of the pole at $p = -\frac{1}{\beta}$. It is important to observe that the direct pole contribution is absent, indicating the pole's inactivity when $\text{Im}(\beta) < 0$. This becomes even clearer when considering the dominant term in the level 2 re-expansion:

$$\begin{aligned}
 R_1(z; \beta; N_0^+, N_0^-) = & \frac{2e^{2z} z^{\frac{1}{2}-N_0^+}}{(2\pi i)^2} F^{(2)}\left(z; \begin{matrix} N_0^+ - N_0^- + 1, & N_0^- + \frac{1}{2} \\ -4, & -\beta + 2 - \beta^{-1} \end{matrix}\right) \\
 & + R_2(z; \beta; N_0^+, N_0^-).
 \end{aligned}$$

The terms

$$\begin{aligned}
 T(z; \beta) = & \frac{2e^{2z} z^{\frac{1}{2}-N_0^+}}{(2\pi i)^2} F^{(2)}\left(z; \begin{matrix} N_0^+ - N_0^- + 1, & N_0^- + \frac{1}{2} \\ -4, & -\beta + 2 - \beta^{-1} \end{matrix}\right) \\
 & - \frac{e^{2z} z^{\frac{1}{2}-N_0^+}}{2\pi i} F^{(1)}\left(z; \begin{matrix} N_0^+ + \frac{1}{2} \\ -\beta - 2 - \beta^{-1} \end{matrix}\right) \\
 & - \frac{e^{-2z} z^{\frac{1}{2}-N_0^-}}{2\pi i} F^{(1)}\left(z; \begin{matrix} N_0^- + \frac{1}{2} \\ -\beta + 2 - \beta^{-1} \end{matrix}\right),
 \end{aligned} \tag{7.5}$$

address the switching on/off of the pole contribution, which is of size $e^{-x-\frac{t}{2}}$, across a Stokes line.

Then in the asymptotics of the solution of the above problem terms of the order $(xt/2)^{-1/4} e^{\pm\sqrt{2xt}}$ appear, but there is also a subsubdominant term of the order $e^{-x-\frac{t}{2}}$.

When comparing the real parts of these terms relative to $e^{-x-\frac{t}{2}}$ in Figure 12, several observations become apparent. Notably, the contributions from the two $F^{(1)}$ terms exhibit considerable similarity, as evidenced by the overlap of the blue and magenta curves. Moreover, the sum of all three terms (depicted by the black curve) approaches zero asymptotically across most regions, except in proximity to $\text{Im}(\beta) = 0$. Consequently, in the two half-planes $\text{Im}(\beta) \leq 0$, the multiplier governing the subsubdominant contribution of the integral in (7.2) vanishes.

However, the subsubdominant term has a “ghost-like” nonzero presence on (and only very close to) the positive real line ($\text{Im}(\beta) = 0$) (cf. Figure 12), and there has a multiplier $\frac{-1}{\pi} \arctan \frac{2\sqrt{\beta}}{|\beta-1|}$ when $x > 0$, as indicated by substituting in the values (7.4) into (4.8). Note that when $2x > t > 0$, we have $\beta > 1$, and the expression $1 - \frac{1}{\pi} \arctan \frac{2\sqrt{\beta}}{|\beta-1|}$ simplifies to $\frac{2}{\pi} \arctan \sqrt{\beta} = \frac{2}{\pi} \arctan \left((2x/t)^{1/4}\right)$.

To exemplify the applicability of Theorem 9.3, we additionally display in Figure 12 (right) the expression

$$\begin{aligned}
 & \frac{2e^{(\beta+2+\beta^{-1})z} z^{\frac{1}{2}-N_0^+}}{(2\pi i)^2} F^{(2)}\left(z; \begin{matrix} N_0^+ - N_0^- + 1, & N_0^- + \frac{1}{2} \\ -4, & -\beta + 2 - \beta^{-1} \end{matrix}\right) \\
 \sim & \frac{(\beta+1)^{2N_0^++1}}{(4\beta)^{N_0^+-N_0^-+1} (\beta-1)^{2N_0^--1}} \frac{\Gamma(N_0^+ - N_0^- + 1) \Gamma\left(N_0^- + \frac{1}{2}\right)}{\Gamma\left(N_0^+ + \frac{3}{2}\right)} {}_2F_1\left(\begin{matrix} 1, N_0^+ - N_0^- + 1 \\ N_0^+ + \frac{3}{2} \end{matrix}; \frac{(\beta+1)^2}{4\beta}\right) \\
 & \times \frac{e^{(\beta+2+\beta^{-1})z} z^{\frac{1}{2}-N_0^+}}{2\pi^2} F^{(1)}\left(z; \begin{matrix} N_0^+ + \frac{1}{2} \\ -\beta - 2 - \beta^{-1} \end{matrix}\right) \\
 & + \frac{1}{2} \operatorname{erfc}\left(d_1 \alpha_0(z) \sqrt{\frac{N_0^- - \frac{1}{2}}{2}}; d_1 \alpha_0(\zeta_1) \sqrt{\frac{N_0^- - \frac{1}{2}}{2}}; d_1^{-1} \sqrt{\frac{N_0^+ - N_0^-}{N_0^- - \frac{1}{2}}}\right),
 \end{aligned} \tag{7.6}$$

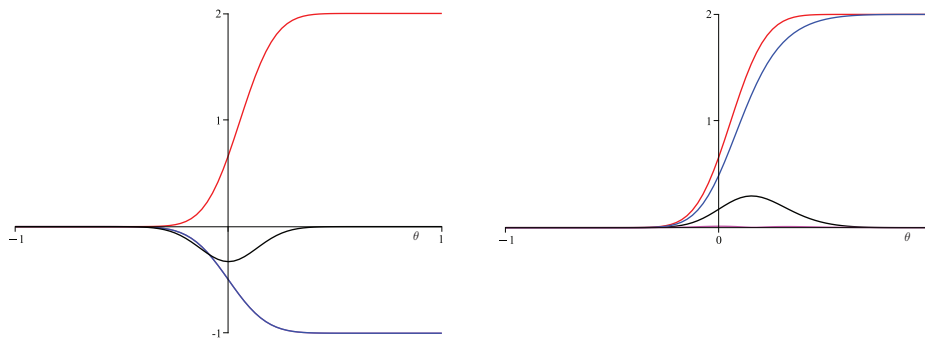


FIGURE 12 | The case $t = 10$, $x = 50e^{i\theta}$, $N_0^+ = 86$, $N_0^- = 23$. For the left figure along the vertical axis, we display the real part of the terms in the solution of the telegraph equation (7.5) divided by the extra factor $e^{-(\beta+\beta^{-1})z}$ (the pole contribution). The real parts of the magenta and blue terms in (7.5) are almost identical and so indistinguishable on the graph. The black curve is the net result $T(z; \beta)$, representing the switching on/off of the pole contribution in the vicinity of the Stokes line, and is the sum of the red, blue, and magenta contributions. It seen to vanish rapidly, but smoothly, away from the line, with only a “ghost-like” nonzero apparition on the Stokes line. For the right figure along the vertical axis, we display the real part of the terms in the approximation of the $F^{(2)}$ hyperterminant (7.6) The colors on the graphs refer to the colored terms in the respective equations. The magenta curve is the absolute value of the error in the two-term approximation (7.6).

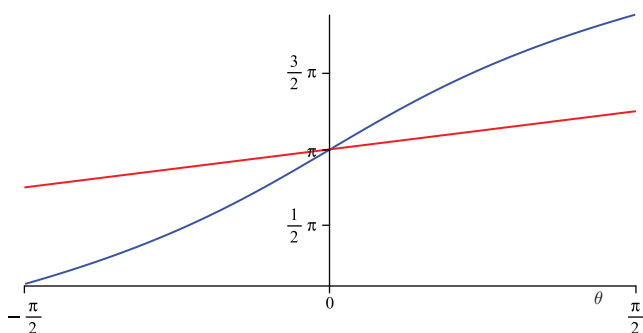


FIGURE 13 | The red curve represents $\arg(\sigma_0 z)$, while the blue curve represents $\arg(\sigma_1 z)$.

utilizing the notation defined in Section 9.1 for d_1 and α_0 . It is worth noting that in this instance, the primary contribution on the right-hand side of (7.6) arises from the $F^{(1)}$ term.

Recalling that $z = \sqrt{xt/2}$ and $\beta = \sqrt{2x/t}$, and considering the hyperterminant $F^{(2)}$ in (7.6) where $\sigma_0 = 4e^{\pi i}$ and $\sigma_1 = -\beta + 2 - \beta^{-1}$, we depict $\arg(\sigma_0 z)$ and $\arg(\sigma_1 z)$ in Figure 13. The red curve indicates that the $\arg(\sigma_0 z) = \pi$ higher-order Stokes phenomenon occurs when $\arg x = \theta = 0$. Simultaneously, the $\arg \sigma_0 = \arg \sigma_1$ higher-order Stokes phenomenon emerges as the blue curve intersects the red curve.

8 | Application: Late-Late Coefficient Smoothing

Given that there is a smoothing of the higher-order Stokes phenomenon at a functional level, it is natural to ask [20] what the corresponding effect is on individual terms in the asymptotic expansions that are being switched on at a Stokes line. Following the spirit of Berry [1], Shelton et al. [20] derived the smoothing for such terms using a formal Borel resummation of the divergent tails of the asymptotic re-expansions of the individual terms themselves, followed by an optimal truncation and a sequence of approximations for resulting integrals. The result is a smooth error function multiplier for the additional contributions to the late terms of the original asymptotic series that are switching on at the higher-order Stokes line (see (3.15), (3.23) of [20]). A Borel-hyperasymptotic approach allows for a straightforward alternative rigorous derivation of this result, without the need to resum divergent series.

To do this, we can rewrite the asymptotic series of the expansion of the original function (2.5) as

$$T^{(k)}(z; \mathbf{a}) = \sum_{r=0}^{N_0-1} \frac{T_r^{(k)}(\mathbf{a})}{z^r} + R_{N_0}(z; \mathbf{a}), \quad (8.1)$$

and combine two exact copies of this (with truncations N_0 and $N_0 + 1$) with (3.1) to derive the hyperasymptotics for individual late coefficients in that expansion:

$$\begin{aligned} T_{N_0}^{(k)}(\mathbf{a}) &= z^{N_0} (R_{N_0}(z; \mathbf{a}) - R_{N_0+1}(z; \mathbf{a})) \\ &= - \sum_{k_1 \neq k} \frac{K_{k_1 k}(\mathbf{a})}{2\pi i} \left[\sum_{s=0}^{N_1^{(k_1)}-1} T_s^{(k_1)}(\mathbf{a}) F^{(1)} \left(0; \begin{matrix} N_0 + 1 - s + \mu_{k_1 k} \\ \lambda_{k_1 k} \end{matrix} \right) \right. \\ &\quad \left. + \sum_{k_2 \neq k_1} \frac{K_{k_2 k_1}(\mathbf{a})}{2\pi i} \left\{ \sum_{s=0}^{N_2^{(k_2)}-1} T_s^{(k_2)}(\mathbf{a}) F^{(2)} \left(0; \begin{matrix} N_0 - N_1^{(k_1)} + \mu_{k_1 k} + 2, N_1^{(k_1)} - s + \mu_{k_2 k_1} \\ \lambda_{k_1 k}, \lambda_{k_2 k_1} \end{matrix} \right) \right\} \right. \\ &\quad \left. + \dots \right]. \end{aligned}$$

This observation was originally used in [28, eq. 7.4]. In addition, from [42, eq. 2.2], we know that $F^{(1)}\left(0; \begin{smallmatrix} M+1 \\ \sigma \end{smallmatrix}\right) = -e^{M\pi i} \sigma^{-M} \Gamma(M)$. By resetting $N_0 = r$, $N_1^{(k_1)} = S^{(k_1)}$, for convenience, we obtain

$$T_r^{(k)}(\mathbf{a}) \sim \sum_{k_1 \neq k} \frac{K_{k_1 k}(\mathbf{a})}{2\pi i} \left[\sum_{s=0}^{S^{(k_1)}-1} T_s^{(k_1)}(\mathbf{a}) \frac{\Gamma(r-s+\mu_{k_1 k})}{\lambda_{k k_1}^{r-s+\mu_{k_1 k}}} - \sum_{k_2 \neq k_1} \frac{K_{k_2 k_1}(\mathbf{a})}{2\pi i} \sum_{s=0}^{\infty} T_s^{(k_2)}(\mathbf{a}) \times F^{(2)}\left(0; \begin{smallmatrix} r-S^{(k_1)}+\mu_{k_1 k}+2, S^{(k_1)}-s+\mu_{k_2 k_1} \\ \lambda_{k_1 k}, \lambda_{k_2 k_1} \end{smallmatrix}\right) \right]. \quad (8.2)$$

With suitable truncations, this form provides an exponentially improved large- r expansion for the late coefficients $T_r^{(k)}$. Note that z does not appear in this result, so preventing an $\arg(\sigma_0 z) \approx \pi$ higher-order Stokes phenomenon, though one may occur when $\arg \sigma_0 \approx \arg \sigma_1$ (cf. (4.2)). From [42, eq. 3.2], we have

$$F^{(2)}\left(0; \begin{smallmatrix} N_0+2, N_1+1 \\ \sigma_0, \sigma_1 \end{smallmatrix}\right) = \frac{e^{(N_0+N_1+1)\pi i} \Gamma(N_0+1)\Gamma(N_1+1)}{\sigma_0^{N_0+1} \sigma_1^{N_1}} \frac{\Gamma(N_0+1)\Gamma(N_1+1)}{N_0+N_1+1} {}_2F_1\left(\begin{smallmatrix} 1, N_0+1 \\ N_0+N_1+2 \end{smallmatrix}; 1+\frac{\sigma_1}{\sigma_0}\right),$$

and, hence, from Theorem 9.2:

$$F^{(2)}\left(0; \begin{smallmatrix} N_0+2, N_1+1 \\ \sigma_0, \sigma_1 \end{smallmatrix}\right) \sim \frac{e^{(N_0+N_1+1)\pi i} \Gamma(N_0+N_1+1)}{(\sigma_0+\sigma_1)^{N_0+N_1+1}} \pi i \operatorname{erfc}\left(\gamma\left(\frac{\sigma_1}{\sigma_0}\right) \sqrt{\frac{1}{2}N_1}\right),$$

where $\gamma\left(\frac{\sigma_1}{\sigma_0}\right)$ is defined in (9.13). Consequently, we have

$$F^{(2)}\left(0; \begin{smallmatrix} r-S^{(k_1)}+\mu_{k_1 k}+2, S^{(k_1)}+\mu_{k_2 k_1} \\ \lambda_{k_1 k}, \lambda_{k_2 k_1} \end{smallmatrix}\right) \sim \frac{\Gamma(r+\mu_{k_2 k})}{\lambda_{k k_2}^{r+\mu_{k_2 k}}} \pi i \operatorname{erfc}\left(\gamma\left(\frac{\lambda_{k_2 k_1}}{\lambda_{k_1 k}}\right) \sqrt{\frac{S^{(k_1)}+\mu_{k_2 k_1}-1}{2}}\right),$$

as $r \rightarrow +\infty$.

Note that $\Gamma(r+\mu_{k_2 k})/\lambda_{k k_2}^{r+\mu_{k_2 k}}$ is the exponentially subdominant contribution to the $T_r^{(k)}$, that is, here switched on smoothly. This term depends on the larger (in modulus) singulant $\lambda_{k_2 k}$ and so is contributing in (8.2) at an exponentially small level. In absolute terms, this contribution is at a scale that is doubly exponentially smaller relative to the original asymptotic expansion (8.1).

Thus we see that, when $\arg \sigma_0 \approx \arg \sigma_1$ for the nearest Borel-plane singularity $k^* \neq k_1$ in the singularity set k_2 (relative to the original Borel singularity around which the initial expansion was made),

at the leading order of the doubly exponentially small level, we have

$$T_r^{(k)}(\mathbf{a}) \sim \sum_{k_1 \neq k} \frac{K_{k_1 k}(\mathbf{a})}{2\pi i} \sum_{s=0}^{S^{(k_1)}-1} T_s^{(k_1)}(\mathbf{a}) \frac{\Gamma(r-s+\mu_{k_1 k})}{\lambda_{k k_1}^{r-s+\mu_{k_1 k}}} - \frac{K_{k^* k_1}(\mathbf{a})}{2} \operatorname{erfc}\left(\gamma\left(\frac{\lambda_{k^* k_1}}{\lambda_{k_1 k}}\right) \sqrt{\frac{S^{(k^*)}+\mu_{k^* k_1}-1}{2}}\right) \times \frac{\Gamma(r+\mu_{k^* k})}{\lambda_{k^* k}^{r+\mu_{k^* k}}} T_0^{(k^*)}(\mathbf{a}), \quad (8.3)$$

where the sums over k_1 are truncated at $S^{(k_1)} - 1$ to include only terms that are larger in magnitude than the term containing the error function. This is a rigorous derivation of [20, Section 3.4].

For a numerical illustration of this result, we can derive the asymptotic approximation for the late coefficients of the telegraph equation expansion $T_r^+(\beta)$, of Section 7

$$T_r^+(\beta) \sim \frac{2}{2\pi i} \sum_{s=0}^{S-1} T_s^-(\beta) \frac{\Gamma(r-s)}{4^{r-s}} - \frac{2}{(2\pi i)^2} F^{(2)}\left(0; \begin{smallmatrix} r-S+2, S+\frac{1}{2} \\ -4, -\beta+2-\beta^{-1} \end{smallmatrix}\right) + \frac{\Gamma\left(r+\frac{1}{2}\right)}{2\pi i(\beta+2+\beta^{-1})^{r+\frac{1}{2}}}$$

as $r \rightarrow +\infty$, with the optimal $S \approx \left|\frac{\beta-2+\beta^{-1}}{\beta+2+\beta^{-1}}\right|r$. The last term in the approximation is only a single term because it is a contribution from the simple pole at $p = -\frac{1}{\beta}$ in (7.2), rather than from a saddle point.

The purpose of the $F^{(2)}$ hyperterminant, and consequently, the higher-order Stokes phenomenon, is to provide a smooth interpretation of the naive asymptotic approximation

$$T_r^+(\beta) \sim \frac{2}{2\pi i} \sum_{s=0}^{S-1} T_s^-(\beta) \frac{\Gamma(r-s)}{4^{r-s}} \pm \frac{\Gamma\left(r+\frac{1}{2}\right)}{2\pi i(\beta+2+\beta^{-1})^{r+\frac{1}{2}}},$$

as $r \rightarrow +\infty$. The upper or lower sign in the final term is chosen depending on whether β is in the upper or lower half-plane. This term is absent if $\arg \beta = 0$. We illustrate this smoothing by depicting the quantity

$$Q = \frac{T_r^+(\beta) - \frac{2}{2\pi i} \sum_{s=0}^{S-1} T_s^-(\beta) \frac{\Gamma(r-s)}{4^{r-s}}}{\frac{\Gamma\left(r+\frac{1}{2}\right)}{2\pi i(\beta+2+\beta^{-1})^{r+\frac{1}{2}}}} \quad (8.4)$$

in Figure 14. The difference between Q and the predicted error function smoothing in (8.3) is also shown there (in red) on the same scale, which confirms the validity of the result.

9 | Rigorous Proofs of the Higher-Order Stokes Smoothings

In this section, we provide the rigorous proofs for the main results outlined in Sections 3 and 4.

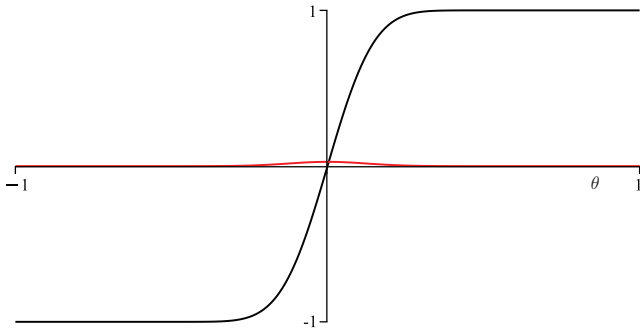


FIGURE 14 | With Q defined in (8.4), $r = 100$, $S = 27$, and $\beta = \sqrt{10}e^{i\theta}$: the black curve represents $\text{Re}(Q)$, while the red curve depicts $\left|Q + \text{erfc}\left(\gamma\left(\frac{\beta-2+\beta^{-1}}{4}\right)\sqrt{\frac{S-\frac{1}{2}}{2}}\right) - 1\right|$. This illustrates the smooth nature of the effect of the higher-order Stokes phenomenon on the late terms as per (8.3).

9.1 | Notation

Let $\sigma_2 = \sigma_0 + \sigma_1$, $N_2 = N_0 + N_1$, and $\frac{\sigma_1}{\sigma_0} = \frac{N_1}{N_0}e^{i\nu}$, $\nu \in \mathbb{C}$. For $j = 0, 1, 2$, we introduce the following notation:

$$\zeta_j = e^{\pi i} \frac{N_j}{\sigma_j}, \quad ia_j(z) = ia_j = 1 + \frac{\sigma_j z}{N_j}. \quad (9.1)$$

In addition, we define $\alpha_j = \alpha_j(z)$ by

$$\frac{1}{2}\alpha_j^2 = ia_j + \ln(1 - ia_j) = 1 + \frac{\sigma_j z}{N_j} + \ln\left(e^{-\pi i} \frac{\sigma_j z}{N_j}\right), \quad (9.2)$$

with the branches specified by

$$(-1)^j a_j \sim \alpha_j - \frac{1}{3}i\alpha_j^2 \quad (9.3)$$

as $|\alpha_j| \rightarrow 0$. Each α_j is a univalent analytic function of z in the sector $|\arg(e^{-\pi i} \sigma_j z N_j^{-1})| < 2\pi$ (see, e.g., [46, Section 5]). Finally, we set

$$g_j(z) = \frac{1}{a_j(z)} - \frac{1}{\alpha_j(z)}, \quad d_1 = \frac{i\alpha_0(\zeta_1)}{1 - \frac{\zeta_1}{\zeta_0}}, \quad d_2(z) = \frac{i - \frac{z\alpha'_0(z)}{\zeta_1\alpha'_0(\zeta_1)}ie^{N_1 r(z)}}{1 - \frac{z}{\zeta_1}}, \quad (9.4)$$

and $r(z) = \frac{1}{2}\alpha_1^2(z) - \frac{1}{2}d_1^2(\alpha_0(z) - \alpha_0(\zeta_1))^2$. We observe that $\alpha_j(z)\alpha'_j(z) = \frac{ia_j(z)}{z} = \frac{1}{z} - \frac{1}{\zeta_j}$. Consequently, $\alpha'_j(z) \sim \frac{i}{z}$ when $a_j(z) \sim \alpha_j(z)$. Furthermore, we note that $d_1^2 = \frac{-2(1-\nu+\ln\nu)}{(1-\nu)^2}$, where $\nu = \frac{\sigma_0 N_1}{\sigma_1 N_0}$. The integral representation $d_1^2 = 2\int_0^{+\infty} \frac{ds}{(s+\nu)(s+1)^2}$, combined with an argument analogous to the proof of [47, Corollary 6.6], shows that $|\arg(d_1^2)| \leq |\arg\nu|$ for $\arg\nu \in (-\pi, \pi)$. This property will be used in Section 9.5.

9.2 | The Ordinary Stokes Phenomenon

The first hyperterminant is essentially an incomplete gamma function, given by: $F^{(1)}\left(z; \frac{N}{\sigma}\right) = \Gamma(N)e^{\sigma z + N\pi i} z^{N-1} \Gamma(1-N, \sigma z)$.

Its uniform asymptotic expansion is well-known (see [45]): we include its derivation, as it is particularly relevant because it involves a uniform asymptotic approximation of integrals in the case of a saddle point near a pole. This situation will reappear in the proof of Theorem 9.2. Moreover, the notation introduced here will be essential for the proof of Theorem 9.3.

The following describes the switching on of $2\pi i e^{\sigma_0 z} z^{N_0}$ as we cross the line $\arg(\sigma_0 z) = \pi$. For comparison, see Equation (3.5). We use the notation from Section 9.1.

Theorem 9.1. *Assuming that σ_0 and its reciprocal are bounded, we have*

$$\begin{aligned} \frac{e^{-\sigma_0 z}}{z^{N_0}} F^{(1)}\left(z; \frac{N_0+1}{\sigma_0}\right) &= \pi i \operatorname{erfc}\left(\alpha_0(z)\sqrt{\frac{1}{2}N_0}\right) \\ &+ i\sqrt{\frac{2\pi}{N_0}} g_0(z) e^{-\frac{1}{2}\alpha_0^2(z)N_0} + \mathcal{O}\left(e^{-\frac{1}{2}\alpha_0^2(z)N_0} N_0^{-3/2}\right), \end{aligned} \quad (9.5)$$

as $\text{Re}(N_0) \rightarrow +\infty$, uniformly with respect to $|\arg(e^{-\pi i} \sigma_0 z N_0^{-1})| \leq 2\pi - \delta (< 2\pi)$.

Proof. Let us temporarily assume that both N_0 and $e^{-\pi i} \sigma_0 z$ are positive. We employ the method described in [48, Section 21.1]. By substituting $\tau = e^{\pi i} t N_0 / \sigma_0$ into the integral representation of the first hyperterminant, we arrive at

$$\begin{aligned} F^{(1)}\left(z; \frac{N_0+1}{\sigma_0}\right) &= \int_0^{[\pi - \arg \sigma_0]} \frac{e^{\sigma_0 \tau} \tau^{N_0}}{z - \tau} d\tau \\ &= \left(\frac{e^{\pi i} N_0}{\sigma_0}\right)^{N_0} \int_0^{+\infty} \frac{e^{-N_0 t} t^{N_0}}{1 - ia_0 - t} dt \\ &= \left(\frac{e^{\pi i} N_0}{e\sigma_0}\right)^{N_0} \int_{-\infty}^{+\infty} \frac{e^{-N_0 \frac{1}{2} s^2} f(s)}{-ia_0 - s} ds \\ &= f(-ia_0) \left(\frac{e^{\pi i} N_0}{e\sigma_0}\right)^{N_0} \int_{-\infty}^{+\infty} \frac{e^{-N_0 \frac{1}{2} s^2}}{-ia_0 - s} ds \\ &\quad - \left(\frac{e^{\pi i} N_0}{e\sigma_0}\right)^{N_0} \int_{-\infty}^{+\infty} e^{-N_0 \frac{1}{2} s^2} g(s) ds, \end{aligned}$$

where we have used the transformations

$$\begin{aligned} \frac{1}{2}s^2 &= t - 1 - \ln t, & \frac{dt}{ds} &= \frac{st}{t-1}, \\ f(s) &= \frac{s + ia_0}{t - 1 + ia_0} \frac{dt}{ds}, & g(s) &= \frac{f(s) - f(-ia_0)}{s + ia_0} \end{aligned}$$

in the integrals with respect to t and s , the paths pass above the poles located at $t = 1 - ia_0$ and $s = ia_0$, respectively. Note that

$$f(-ia_0) = 1, \quad g(0) = \frac{1}{ia_0} - \frac{1}{ia_0}, \quad \frac{e^{-\sigma_0 z}}{z^{N_0}} \left(\frac{e^{\pi i} N_0}{e\sigma_0}\right)^{N_0} = e^{-\frac{1}{2}\alpha_0^2 N_0},$$

and that

$$\int_{-\infty}^{+\infty} \frac{e^{-N_0 \frac{1}{2} s^2}}{-ia_0 - s} ds = \pi i e^{\frac{1}{2}\alpha_0^2 N_0} \operatorname{erfc}\left(\alpha_0 \sqrt{\frac{1}{2}N_0}\right).$$

Hence,

$$\begin{aligned} \frac{e^{-\sigma_0 z}}{z^{N_0}} F^{(1)}\left(z; \begin{matrix} N_0 + 1 \\ \sigma_0 \end{matrix}\right) &= \pi i \operatorname{erfc}\left(\alpha_0 \sqrt{\frac{1}{2} N_0}\right) \\ &+ \sqrt{\frac{2\pi}{N_0}} e^{-\frac{1}{2} \alpha_0^2 N_0} (ig_0(z) - N_0^{-1} r_0(z)), \end{aligned} \quad (9.6)$$

with

$$r_0(z) = \sqrt{\frac{N_0}{2\pi}} \int_{-\infty}^{+\infty} e^{-N_0 \frac{1}{2} s^2} \frac{d}{ds} \left(\frac{g(s) - g(0)}{s} \right) ds.$$

Now, $g(s)$ is analytic and bounded on the real line, and it is analytic with respect to z in the sector where $|\arg(e^{-\pi i} \sigma_0 z N_0^{-1})| < 2\pi$. Consequently, (9.6) holds when $\operatorname{Re}(N_0) > 0$ and $|\arg(e^{-\pi i} \sigma_0 z N_0^{-1})| < 2\pi$. Furthermore, $r_0(z) = \mathcal{O}(1)$ as $\operatorname{Re}(N_0) \rightarrow +\infty$. \square

For a simple approximation applicable away from the Stokes line, we combine the first displayed expression from the proof above with Stirling's approximation. This yields

$$\begin{aligned} \frac{e^{-\sigma_0 z}}{z^{N_0}} F^{(1)}\left(z; \begin{matrix} N_0 + 1 \\ \sigma_0 \end{matrix}\right) &= \frac{e^{-\sigma_0 z}}{z^{N_0}} \left(\frac{e^{\pi i} N_0}{\sigma_0} \right)^{N_0} \int_0^{+\infty} \frac{e^{-N_0 t} t^{N_0}}{1 - ia_0 - t} dt \\ &\sim \frac{e^{-\sigma_0 z}}{z^{N_0}} \left(\frac{e^{\pi i} N_0}{\sigma_0} \right)^{N_0} \int_0^{+\infty} \frac{e^{-N_0 t} t^{N_0}}{-ia_0} dt \\ &\sim -\sqrt{\frac{2\pi}{N_0}} \frac{e^{-\frac{1}{2} \alpha_0^2(z) N_0}}{1 + \frac{\sigma_0 z}{N_0}}, \end{aligned} \quad (9.7)$$

as $\operatorname{Re}(N_0) \rightarrow +\infty$, provided that $|\arg(\sigma_0 z N_0^{-1})| \leq \pi - \delta (< \pi)$.

Similarly, by utilizing the first integral representation in Section 9.4, we obtain

$$\frac{e^{-(\sigma_0 + \sigma_1)z}}{z^{N_0 + N_1}} F^{(2)}\left(z; \begin{matrix} N_0 + 1, N_1 + 1 \\ \sigma_0, \sigma_1 \end{matrix}\right) \sim \frac{2\pi}{\sqrt{N_0 N_1}} \frac{e^{-\frac{1}{2} \alpha_0^2(z) N_0 - \frac{1}{2} \alpha_1^2(z) N_1}}{\left(1 + \frac{\sigma_0 z}{N_0}\right) \left(1 - \frac{\sigma_1 N_0}{\sigma_0 N_1}\right)}, \quad (9.8)$$

as $\operatorname{Re}(N_0), \operatorname{Re}(N_1) \rightarrow +\infty$, provided that $|\arg(\sigma_0 z N_0^{-1})| \leq \pi - \delta (< \pi)$ and $|\arg(e^{-\pi i} \frac{\sigma_1 N_0}{\sigma_0 N_1})| \leq \pi - \delta (< \pi)$. Thus, (9.8) holds away from the potential Stokes phenomena associated with this second hyperterminant.

9.3 | The Higher-Order Stokes Phenomena Arising from $F^{(2)}$ When $\arg(\sigma_0 z) \approx \pi$

When $\arg(\sigma_0 z) \approx \pi$ and $\frac{\sigma_0 N_1}{\sigma_1 N_0}$ is bounded away from the positive real axis, we can combine (4.3) with (9.5) to obtain

$$\begin{aligned} &F^{(2)}\left(z; \begin{matrix} N_0 + 1, N_1 + 1 \\ \sigma_0, \sigma_1 \end{matrix}\right) \\ &\sim \pi i e^{\sigma_0 z} z^{N_0} \operatorname{erfc}\left(\alpha_0 \sqrt{\frac{1}{2} N_0}\right) F^{(1)}\left(z; \begin{matrix} N_1 + 1 \\ \sigma_1 \end{matrix}\right) \end{aligned}$$

$$\begin{aligned} &+ i \sqrt{\frac{2\pi}{N_0}} g_0(z) e^{-\frac{1}{2} \alpha_0^2(z) N_0} e^{\sigma_0 z} z^{N_0} F^{(1)}\left(z; \begin{matrix} N_1 + 1 \\ \sigma_1 \end{matrix}\right) \\ &- F^{(2)}\left(z; \begin{matrix} N_1 + 1, N_0 + 1 \\ \sigma_1, \sigma_0 \end{matrix}\right), \end{aligned} \quad (9.9)$$

as $\operatorname{Re}(N_0) \rightarrow +\infty$, uniformly with respect to $|\arg(e^{-\pi i} \sigma_0 z N_0^{-1})| \leq 2\pi - \delta (< 2\pi)$. This formula represents the switching on of the term $2\pi i e^{\sigma_0 z} z^{N_0} F^{(1)}\left(z; \begin{matrix} N_1 + 1 \\ \sigma_1 \end{matrix}\right)$; compare with (4.1). To derive an approximation in terms of $F^{(1)}\left(z; \begin{matrix} N_1 + 1 \\ \sigma_1 \end{matrix}\right)$, we use (9.7) and (9.8) for the final term in (9.9), resulting in

$$\begin{aligned} &F^{(2)}\left(z; \begin{matrix} N_0 + 1, N_1 + 1 \\ \sigma_0, \sigma_1 \end{matrix}\right) \\ &\sim \pi i e^{\sigma_0 z} z^{N_0} \operatorname{erfc}\left(\alpha_0 \sqrt{\frac{1}{2} N_0}\right) F^{(1)}\left(z; \begin{matrix} N_1 + 1 \\ \sigma_1 \end{matrix}\right) \\ &+ \sqrt{\frac{2\pi}{N_0}} e^{\sigma_0 z - \frac{1}{2} \alpha_0^2(z) N_0} z^{N_0} \left(ig_0(z) + \left(1 - \frac{\sigma_0 N_1}{\sigma_1 N_0}\right)^{-1} \right) \\ &\times F^{(1)}\left(z; \begin{matrix} N_1 + 1 \\ \sigma_1 \end{matrix}\right), \end{aligned}$$

as $\operatorname{Re}(N_0), \operatorname{Re}(N_1) \rightarrow +\infty$, provided that $|\arg(e^{-\pi i} \sigma_0 z N_0^{-1})| \leq 2\pi - \delta (< 2\pi)$, $|\arg(\sigma_1 z N_1^{-1})| \leq \pi - \delta (< \pi)$, and $|\arg(e^{-\pi i} \frac{\sigma_0 N_1}{\sigma_1 N_0})| \leq \pi - \delta (< \pi)$. This approximation breaks down when $\frac{\sigma_0 N_1}{\sigma_1 N_0}$ approaches the positive real axis.

9.4 | The Higher-Order Stokes Phenomenon for $F^{(2)}$ When $\arg \sigma_0 \approx \arg \sigma_1$

In this subsection, we consider the case where $\arg \sigma_0 \approx \arg \sigma_1$ and $\sigma_0 z$ is bounded away from the negative real axis. We present the integral representation (A2) as follows:

$$\begin{aligned} &F^{(2)}\left(z; \begin{matrix} N_0 + 1, N_1 + 1 \\ \sigma_0, \sigma_1 \end{matrix}\right) \\ &= -F^{(1)}\left(z; \begin{matrix} N_0 + N_1 + 1 \\ \sigma_0 + \sigma_1 \end{matrix}\right) \frac{(\sigma_0 + \sigma_1)^{N_0 + N_1 + 1}}{\sigma_0^{N_0 + 1} \sigma_1^{N_1}} I\left(\frac{\sigma_1}{\sigma_0}\right) \\ &- \frac{\Gamma(N_1 + 1)}{(e^{-\pi i} \sigma_1)^{N_1}} e^{(\sigma_0 + \sigma_1)z} z^{N_0 + N_1} \int_z^\infty \frac{e^{-(\sigma_0 + \sigma_1)t}}{t^{N_0 + N_1 + 1}} F^{(1)}\left(t; \begin{matrix} N_0 + 1 \\ \sigma_0 \end{matrix}\right) dt, \end{aligned} \quad (9.10)$$

where the integral $I(\beta)$ has a pole near a saddle point, resulting in an error function behavior, as follows.

Theorem 9.2. Assume that both β and its reciprocal are bounded, and that $|\arg \beta| < \pi$. Define

$$I(\beta) = \frac{\Gamma(N_0 + 1) \Gamma(N_1 + 1)}{\Gamma(N_0 + N_1 + 2)} {}_2F_1\left(\begin{matrix} 1, N_0 + 1 \\ N_0 + N_1 + 2 \end{matrix}; 1 + \beta\right). \quad (9.11)$$

Let $s^* = \frac{N_1}{N_0}$, and assume that both s^* and its reciprocal are bounded. Then, we have

$$I(\beta) \sim \frac{\beta^{N_1}}{(1+\beta)^{N_0+N_1+1}} \pi i \operatorname{erfc} \left(\gamma(\beta) \sqrt{\frac{1}{2} N_1} \right) + g(0, \beta) \frac{N_0^{N_0} N_1^{N_1}}{(N_0 + N_1)^{N_0+N_1}} \sqrt{\frac{2\pi}{N_1}}, \quad (9.12)$$

as $\operatorname{Re}(N_1) \rightarrow +\infty$. Here,

$$\frac{1}{2} \gamma^2(\beta) = \left(1 + \frac{1}{s^*} \right) \ln \left(\frac{1+s^*}{1+\beta} \right) - \ln \left(\frac{s^*}{\beta} \right), \quad (9.13)$$

with the branch specified by $\gamma(s^* e^{i\nu}) \sim \nu / \sqrt{1+s^*}$ as $\nu \rightarrow 0$. Furthermore,

$$g(0, \beta) = \frac{(1+s^*)^{-1/2}}{1 - \frac{\beta}{s^*}} - \frac{i}{(1+\beta)\gamma(\beta)}. \quad (9.14)$$

Observe that $\gamma(\beta)$ is a univalent analytic function of β within the sector $|\arg \beta| < \pi$. In addition, the condition that both s^* and its reciprocal are bounded implies that the validity of the asymptotics (9.12) necessitates that both $\operatorname{Re}(N_1)$ and $\operatorname{Re}(N_0)$ be large.

Proof. Initially, we assume that $\arg \beta \in (0, \pi)$. We follow the method outlined in [48, Section 21.1]. By making a simple change of integration variables in the standard integral representation of the hypergeometric function [44, eq. 15.6.1], we can write

$$I(\beta) = \int_0^{+\infty} \frac{e^{-N_1 h(s)}}{(s-\beta)(1+s)} ds,$$

with

$$h(s) = \left(1 + \frac{N_0}{N_1} \right) \ln(1+s) - \ln s, \quad h'(s) = \frac{\frac{N_0}{N_1} s - 1}{s(1+s)}.$$

Thus, there is a saddle point at $s^* = \frac{N_1}{N_0}$. Using the substitution

$$\frac{1}{2} x^2 = h(s) - h(s^*), \quad \frac{ds}{dx} = \frac{xs(1+s)}{\frac{N_0}{N_1} s - 1},$$

we obtain the canonical integral representation

$$I(\beta) = \frac{N_0^{N_0} N_1^{N_1}}{(N_0 + N_1)^{N_0+N_1}} \int_{-\infty}^{+\infty} \frac{e^{-N_1 \frac{1}{2} x^2} f(x)}{x - i\gamma} dx, \quad (9.15)$$

with

$$f(x) = \frac{x - i\gamma}{(s - \beta)(s + 1)} \frac{ds}{dx},$$

and

$$\frac{1}{2} \gamma^2 = h(s^*) - h(\beta) = \left(1 + \frac{1}{s^*} \right) \ln \left(\frac{1+s^*}{1+\beta} \right) - \ln \left(\frac{s^*}{\beta} \right).$$

It is straightforward to show that $f(i\gamma) = (1+\beta)^{-1}$. We introduce the function

$$g(x, \beta) = \frac{f(x) - f(i\gamma)}{x - i\gamma}, \quad g(0, \beta) = \frac{(1+s^*)^{-1/2}}{1 - \frac{\beta}{s^*}} - \frac{i}{\gamma(1+\beta)},$$

and use $\frac{f(x)}{x - i\gamma} = \frac{1}{(1+\beta)(x - i\gamma)} + g(x, \beta)$ in (9.15) to obtain

$$I(\beta) = \frac{\beta^{N_1}}{(1+\beta)^{N_0+N_1+1}} \pi i \operatorname{erfc} \left(\gamma \sqrt{\frac{1}{2} N_1} \right) + \frac{N_0^{N_0} N_1^{N_1}}{(N_0 + N_1)^{N_0+N_1}} \int_{-\infty}^{+\infty} e^{-N_1 \frac{1}{2} x^2} g(x, \beta) dx. \quad (9.16)$$

Note that $\lim_{|\gamma| \rightarrow 0} g(0, \beta) = \frac{1-s^*}{3(1+s^*)^{3/2}}$. Thus, $g(x, \beta)$ is analytic and bounded on the real x -line, and it is analytic with respect to β in the sector where $|\arg \beta| < \pi$. Consequently, (9.16) holds when $\operatorname{Re}(N_1) > 0$ and $|\arg \beta| < \pi$. Furthermore,

$$\int_{-\infty}^{+\infty} e^{-N_1 \frac{1}{2} x^2} g(x, \beta) dx \sim g(0, \beta) \sqrt{\frac{2\pi}{N_1}},$$

as $\operatorname{Re}(N_1) \rightarrow +\infty$. □

We still need to derive an approximation for the final integral in (9.10). We consider the case where $\operatorname{Re}(N_0), \operatorname{Re}(N_1) \rightarrow +\infty$ and $|\arg(\sigma_0 z N_0^{-1})| \leq \pi - \delta (< \pi)$. Then,

$$\begin{aligned} & \int_z^\infty e^{-(\sigma_0 + \sigma_1)t} t^{-N_0 - N_1 - 1} F^{(1)} \left(t; \begin{matrix} N_0 + 1 \\ \sigma_0 \end{matrix} \right) dt \\ & \sim - \frac{\sqrt{2\pi} N_0^{N_0 - \frac{1}{2}} e^{-N_0}}{(e^{-\pi i} \sigma_0)^{N_0}} \int_z^\infty \frac{e^{-(\sigma_0 + \sigma_1)t} t^{-N_0 - N_1 - 1}}{1 + \frac{\sigma_0 t}{N_0}} dt \\ & \sim - \frac{\sqrt{2\pi} N_0^{N_0 - \frac{1}{2}} e^{-N_0}}{(e^{-\pi i} \sigma_0)^{N_0}} \int_z^\infty \frac{e^{-(\sigma_0 + \sigma_1)t} t^{-N_0 - N_1 - 1}}{1 + \frac{\sigma_0 z}{N_0}} dt \\ & = \frac{\sqrt{2\pi} N_0^{N_0 - \frac{1}{2}} e^{-N_0}}{(e^{-\pi i} \sigma_0)^{N_0}} \frac{(e^{-\pi i} (\sigma_0 + \sigma_1))^{N_0 + N_1} e^{-(\sigma_0 + \sigma_1)z}}{z^{N_0 + N_1} \Gamma(N_0 + N_1 + 1) \left(1 + \frac{\sigma_0 z}{N_0} \right)} \\ & \quad \times F^{(1)} \left(z; \begin{matrix} N_0 + N_1 + 1 \\ \sigma_0 + \sigma_1 \end{matrix} \right) \\ & \sim \frac{(e^{-\pi i} (\sigma_0 + \sigma_1))^{N_0 + N_1} \Gamma(N_0)}{(e^{-\pi i} \sigma_0)^{N_0} \Gamma(N_0 + N_1 + 1) \left(1 + \frac{\sigma_0 z}{N_0} \right)} \frac{e^{-(\sigma_0 + \sigma_1)z}}{z^{N_0 + N_1}} \\ & \quad \times F^{(1)} \left(z; \begin{matrix} N_0 + N_1 + 1 \\ \sigma_0 + \sigma_1 \end{matrix} \right). \end{aligned}$$

In the first step, we used (9.7); in the second step, we considered the main contribution coming from $t = z$; in the third step,

we identified the integral first in terms of incomplete gamma functions and then in terms of the first hyperterminant; and, finally, we used Stirling's formula for $\Gamma(N_0)$. This approximation breaks down when $\frac{\sigma_0 z}{N_0}$ approaches the negative real axis.

Theorem 9.3. Let $\sigma_0, \sigma_1, \frac{\sigma_0 z}{N_0}, \frac{\sigma_1 z}{N_1}$ and their reciprocals be bounded. In addition, we impose the constraints $|\arg N_j| \leq \frac{\pi}{2} - \delta$ ($< \frac{\pi}{2}$) for $j = 0, 1$, $|\arg(\frac{\sigma_0 N_1}{\sigma_1 N_0})| \leq \pi - 2\epsilon - 2\delta$, and $|\arg(e^{-\frac{\pi}{2}i} \sigma_j z)| \leq \pi - \delta$ ($< \pi$) for $j = 0, 1, 2$. Then,

$$\begin{aligned} & \frac{e^{-(\sigma_0+\sigma_1)z}}{z^{N_0+N_1}} F^{(2)}\left(z; \begin{matrix} N_0+1, N_1+1 \\ \sigma_0, \sigma_1 \end{matrix}\right) = \\ & - \frac{\sigma_2^{N_2+1}}{\sigma_0^{N_0+1} \sigma_1^{N_1}} \frac{\Gamma(N_0+1)\Gamma(N_1+1)}{\Gamma(N_2+2)} {}_2F_1\left(\begin{matrix} 1, N_0+1 \\ N_2+2 \end{matrix}; 1 + \frac{\sigma_1}{\sigma_0}\right) \frac{e^{-(\sigma_0+\sigma_1)z}}{z^{N_0+N_1}} F^{(1)}\left(z; \begin{matrix} N_0+N_1+1 \\ \sigma_0+\sigma_1 \end{matrix}\right) \\ & - \pi^2 \operatorname{erfc}\left(d_1 \alpha_0(z) \sqrt{\frac{1}{2}N_1}; d_1 \alpha_0(\zeta_1) \sqrt{\frac{1}{2}N_1}; d_1^{-1} \sqrt{\frac{N_0}{N_1}}\right) + R^{(1)}(z), \end{aligned}$$

Combining the results above with Stirling's formula, we obtain the following approximation:

$$\begin{aligned} & \frac{F^{(2)}\left(z; \begin{matrix} N_0+1, N_1+1 \\ \sigma_0, \sigma_1 \end{matrix}\right)}{F^{(1)}\left(z; \begin{matrix} N_0+N_1+1 \\ \sigma_0+\sigma_1 \end{matrix}\right)} \sim -\pi i \operatorname{erfc}\left(\gamma\left(\frac{\sigma_1}{\sigma_0}\right) \sqrt{\frac{1}{2}N_1}\right) \\ & - \sqrt{\frac{2\pi}{N_0}} \frac{\left(\frac{\sigma_0+\sigma_1}{N_0+N_1}\right)^{N_0+N_1}}{\left(\frac{\sigma_0}{N_0}\right)^{N_0} \left(\frac{\sigma_1}{N_1}\right)^{N_1}} \\ & \times \left(g\left(0, \frac{\sigma_1}{\sigma_0}\right) \left(1 + \frac{\sigma_1}{\sigma_0}\right) \sqrt{\frac{N_0}{N_1}} + \frac{\sqrt{N_1/(N_0+N_1)}}{1 + \frac{\sigma_0 z}{N_0}}\right), \end{aligned} \tag{9.17}$$

which signifies the switching on of $-2\pi i F^{(1)}\left(z; \begin{matrix} N_0+N_1+1 \\ \sigma_0+\sigma_1 \end{matrix}\right)$. Compare with (4.2). In the case where $N_0 = N_1 = N$ and $\sigma_0 = \sigma_1 = \sigma$, the first term on the right-hand side simplifies to $-\pi i$.

In Figure 5, we illustrate the switching on of $-2\pi i F^{(1)}\left(z; \begin{matrix} N_0+N_1+1 \\ \sigma_0+\sigma_1 \end{matrix}\right)$ as $\theta = \arg\left(\frac{\sigma_1}{\sigma_0}\right)$ transitions from positive to negative values.

9.5 | The Full Uniform Higher-Order Stokes Phenomenon

In this subsection, the main result is Theorem 9.3, which gives an approximation allowing both $\arg(\sigma_0 z) \approx \pi$ and $\arg \sigma_0 \approx \arg \sigma_1$. This theorem is expressed in terms of the new special function $\operatorname{erfc}(x; y; \lambda)$. Results for the extreme collinear case, $\frac{\sigma_1}{\sigma_0} = \frac{N_1}{N_0}$, are presented in Theorem 9.4 and Corollary 9.1. Lemma 9.1 is a preliminary version of Theorem 9.3; however, providing a proof for this lemma is convenient, allowing us then to deduce Theorem 9.3. We use the notation from Section 9.1.

where $R^{(1)}(z) = \mathcal{O}\left(|\operatorname{Erfc}|N_1^{-1/2}\right)$ as $\operatorname{Re}(N_1) \rightarrow +\infty$. An additional term in the approximation is

$$\begin{aligned} R^{(1)}(z) = & -d_2(z) \pi \sqrt{\frac{2\pi}{N_1}} e^{-\frac{1}{2}\alpha_1^2(z)N_1} \operatorname{erfc}\left(\alpha_0(z) \sqrt{\frac{1}{2}N_0}\right) \\ & + \left(\frac{d_2(z)\alpha_0'(\zeta_2)}{\sigma_2} \sqrt{2\pi} \frac{N_0 N_2}{N_1} + i g_0(\zeta_2) \sqrt{\frac{2\pi N_1}{N_0 N_2}}\right) \\ & \times e^{\frac{1}{2}\alpha_2^2(z)N_2 - \frac{1}{2}\alpha_0^2(z)N_0 - \frac{1}{2}\alpha_1^2(z)N_1} \frac{e^{-(\sigma_0+\sigma_1)z}}{z^{N_0+N_1}} \\ & \times F^{(1)}\left(z; \begin{matrix} N_0+N_1+1 \\ \sigma_0+\sigma_1 \end{matrix}\right) \\ & + \frac{2\pi i}{\sigma_2} \sqrt{\frac{N_1}{N_0}} \frac{g_0(z) - g_0(\zeta_2)}{z - \zeta_2} e^{-\frac{1}{2}\alpha_0^2(z)N_0 - \frac{1}{2}\alpha_1^2(z)N_1} \\ & + \mathcal{O}\left(|\operatorname{Erfc}|N_1^{-1}\right), \end{aligned}$$

where

$$\begin{aligned} |\operatorname{Erfc}| = & \left| \operatorname{erfc}\left(d_1 \alpha_0(z) \sqrt{\frac{1}{2}N_1}; d_1 \alpha_0(\zeta_1) \sqrt{\frac{1}{2}N_1}; d_1^{-1} \sqrt{\frac{N_0}{N_1}}\right) \right| \\ & + \left| \operatorname{erfc}\left(\alpha_2(z) \sqrt{\frac{1}{2}N_2}\right) \right| + \frac{1}{\sqrt{N_2}} \left| e^{-\frac{1}{2}\alpha_0^2(z)N_0 - \frac{1}{2}\alpha_1^2(z)N_1} \right|. \end{aligned} \tag{9.18}$$

In most applications, ϵ will be very small. From the final remarks in Section 9.1, it follows that under the constraints $|\arg N_j| \leq \frac{\pi}{2} - \delta$ ($< \frac{\pi}{2}$) for $j = 0, 1$ and $|\arg(\frac{\sigma_0 N_1}{\sigma_1 N_0})| \leq \pi - 2\epsilon - 2\delta$, we obtain $|\arg(d_1^{-1} \sqrt{\frac{N_0}{N_1}})| \leq \frac{\pi}{2} - \delta$ ($< \frac{\pi}{2}$). This is essential because the function $\operatorname{erfc}(x; y; \lambda)$ has branch cuts along segments of the imaginary axis in the λ -plane (cf. Appendix B).

A numerical example is given in Figure 15.

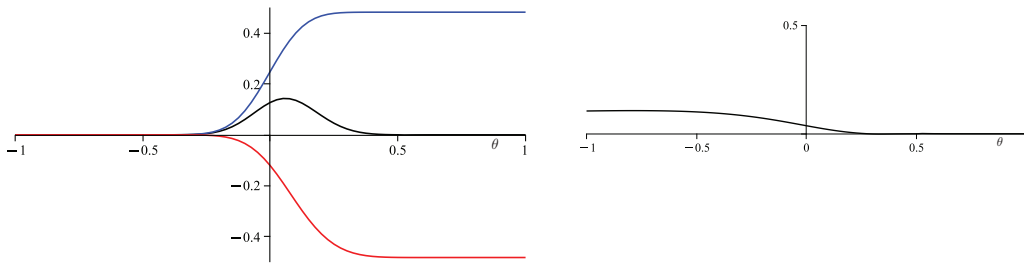


FIGURE 15 | The case $z = 41e^{(\pi-0.5+\theta)i}$, $\sigma_0 = 1.1e^{0.5i}$, $\sigma_1 = 0.9e^{0.51i}$, $N_0 = 44.4$, and $N_1 = 37.7$. This results in $\nu = 0.01 + 0.037i$. In the left figure, the vertical axis displays the real part of the respectively colored terms in the approximation from Theorem 9.3, normalized by a factor of $(2\pi)^{-2}$. In the right figure, the vertical axis shows the absolute error $|R^{(1)}(z)|$ for this approximation, divided by $|\text{Erfc}|N_1^{-1/2}$. This demonstrates that the implied constant is uniformly bounded.

If $\frac{\sigma_1}{\sigma_0} = \frac{N_1}{N_0}$, we can apply Lemma 9.2 to simplify the results of Theorem 9.3, as follows.

Theorem 9.4. Let $\sigma_0, \sigma_1, \frac{\sigma_0 z}{N_0}$ and their reciprocals be bounded. In addition, we impose the constraints $|\arg N_j| \leq \frac{\pi}{2} - \delta (< \frac{\pi}{2})$ for $j = 0, 1$ and $|\arg(e^{-\frac{\pi}{2}i}\sigma_j z)| \leq \pi - \delta (< \pi)$ for $j = 0, 1, 2$. In the extreme collinear case where $\frac{\sigma_1}{\sigma_0} = \frac{N_1}{N_0}$, we have

$$\begin{aligned} & \frac{e^{-(\sigma_0+\sigma_1)z}}{z^{N_0+N_1}} F^{(2)}\left(z; \begin{matrix} N_0+1, N_1+1 \\ \sigma_0, \sigma_1 \end{matrix}\right) \\ &= \pi^2 \operatorname{erfc}\left(\alpha_0(z)\sqrt{\frac{1}{2}N_2}\right) \\ & \quad - \pi^2 \operatorname{erfc}\left(\alpha_0(z)\sqrt{\frac{1}{2}N_1}; 0; \sqrt{\frac{N_0}{N_1}}\right) + R^{(1)}(z), \end{aligned}$$

where $R^{(1)}(z) = \mathcal{O}(|\text{Erfc}|N_1^{-1/2})$ as $\operatorname{Re}(N_1) \rightarrow +\infty$. An additional term in the approximation is

$$\begin{aligned} R^{(1)}(z) &= \left(\frac{1}{3}i - g_0(z)\right)\pi\sqrt{\frac{2\pi N_0}{N_1 N_2}} \operatorname{erfc}\left(\alpha_0(z)\sqrt{\frac{1}{2}N_2}\right) \\ & \quad - g_0(z)\pi\sqrt{\frac{2\pi}{N_1}} e^{-\frac{1}{2}\alpha_0^2(z)N_1} \operatorname{erfc}\left(\alpha_0(z)\sqrt{\frac{1}{2}N_0}\right) \\ & \quad + \left(\frac{2\pi i}{\sigma_2}\sqrt{\frac{N_1}{N_0}}\frac{g_0(z) - \frac{1}{3}i}{z - \zeta_2} + \pi g_0(z)\sqrt{\frac{2\pi}{N_2}}\right) e^{-\frac{1}{2}\alpha_0^2(z)N_2} \\ & \quad + \mathcal{O}(|\text{Erfc}|N_1^{-1}), \end{aligned}$$

where

$$\begin{aligned} |\text{Erfc}| &= \left| \operatorname{erfc}\left(\alpha_0(z)\sqrt{\frac{1}{2}N_1}; 0; \sqrt{\frac{N_0}{N_1}}\right) \right| \\ & \quad + \left| \operatorname{erfc}\left(\alpha_0(z)\sqrt{\frac{1}{2}N_2}\right) \right| + \frac{1}{\sqrt{N_2}} \left| e^{-\frac{1}{2}\alpha_0^2(z)N_2} \right|. \end{aligned}$$

At the center where the double Stokes phenomenon occurs, specifically when $e^{-\pi i}z = \frac{N_0}{\sigma_0} = \frac{N_1}{\sigma_1}$, we find $\alpha_0(z) = 0$. The following corollary results from the preceding theorem and the final identity in (B3).

Corollary 9.1. Let σ_0, σ_1 and their reciprocals be bounded. In addition, we impose the constraints $|\arg N_j| \leq \frac{\pi}{2} - \delta (< \frac{\pi}{2})$ for $j = 0, 1$ and $|\arg(e^{-\frac{\pi}{2}i}\sigma_2 z)| \leq \pi - \delta (< \pi)$. Then, when $e^{-\pi i}z = \frac{N_0}{\sigma_0} = \frac{N_1}{\sigma_1}$, we have

$$\begin{aligned} & \frac{e^{-(\sigma_0+\sigma_1)z}}{z^{N_0+N_1}} F^{(2)}\left(z; \begin{matrix} N_0+1, N_1+1 \\ \sigma_0, \sigma_1 \end{matrix}\right) = \\ & \quad 2\pi \arctan\sqrt{\frac{N_0}{N_1}} - \frac{\pi i}{3}\sqrt{\frac{2\pi}{N_1}} \left(1 - \frac{1}{\sqrt{1 + \frac{N_0}{N_1}}}\right) + \mathcal{O}(N_1^{-1}), \end{aligned}$$

as $\operatorname{Re}(N_1) \rightarrow +\infty$.

For the proofs of the above results, we will rely on the following two lemmas.

Lemma 9.1. Let $\sigma_0, \sigma_1, \frac{\sigma_0 z}{N_0}, \frac{\sigma_1 z}{N_1}$ and their reciprocals be bounded. In addition, we impose the constraints $|\arg N_j| \leq \frac{\pi}{2} - \delta (< \frac{\pi}{2})$ for $j = 0, 1$, $|\arg(\frac{\sigma_0 N_1}{\sigma_1 N_0})| \leq \pi - 2\varepsilon - 2\delta$ and $|\arg(e^{-\frac{\pi}{2}i}\sigma_j z)| \leq \pi - \delta (< \pi)$ for $j = 0, 1, 2$. Then

$$\begin{aligned} & \frac{e^{-(\sigma_0+\sigma_1)z}}{z^{N_0+N_1}} F^{(2)}\left(z; \begin{matrix} N_0+1, N_1+1 \\ \sigma_0, \sigma_1 \end{matrix}\right) = \\ & \quad - \frac{\sigma_2^{N_2+1}}{\sigma_0^{N_0+1}\sigma_1^{N_1}} \frac{\Gamma(N_0+1)\Gamma(N_1+1)}{\Gamma(N_2+2)} {}_2F_1\left(\begin{matrix} 1, N_0+1 \\ N_2+2 \end{matrix}; 1 + \frac{\sigma_1}{\sigma_0}\right) \frac{e^{-(\sigma_0+\sigma_1)z}}{z^{N_0+N_1}} F^{(1)}\left(z; \begin{matrix} N_0+N_1+1 \\ \sigma_0+\sigma_1 \end{matrix}\right) \\ & \quad - \frac{\pi^{\frac{3}{2}}\Gamma(N_1)e^{N_1}}{\sqrt{2}N_1^{N_1-\frac{1}{2}}} \operatorname{erfc}\left(d_1\alpha_0(z)\sqrt{\frac{1}{2}N_1}; d_1\alpha_0(\zeta_1)\sqrt{\frac{1}{2}N_1}; d_1^{-1}\sqrt{\frac{N_0}{N_1}}\right) + R^{(1)}(z), \end{aligned}$$

where $R^{(1)}(z) = \mathcal{O}(|\mathbf{Erfc}|N_1^{-1/2})$ as $\text{Re}(N_1) \rightarrow +\infty$. The quantity $|\mathbf{Erfc}|$ is defined in (9.18). An additional term in the approximation is

$$\begin{aligned} R^{(1)}(z) &= d_2(z)\alpha_0'(\zeta_2) \frac{\sigma_2^{N_2-1} \sqrt{2\pi} N_0^{N_0+\frac{1}{2}} e^{-N_0} \Gamma(N_1)}{\sigma_0^{N_0} \sigma_1^{N_1} \Gamma(N_2)} \\ &\quad \times \frac{e^{-(\sigma_0+\sigma_1)z}}{z^{N_0+N_1}} F^{(1)}\left(z; \begin{matrix} N_0+N_1+1 \\ \sigma_0+\sigma_1 \end{matrix}\right) \\ &\quad - d_2(z) \frac{\pi \Gamma(N_1)}{(e^{-\pi i} \sigma_1)^{N_1}} \frac{e^{-\sigma_1 z}}{z^{N_1}} \operatorname{erfc}\left(\alpha_0(z) \sqrt{\frac{1}{2} N_0}\right) \\ &\quad + ig_0(\zeta_2) \frac{\sigma_2^{N_2}}{\sigma_0^{N_0} \sigma_1^{N_1}} \frac{\Gamma(N_0)\Gamma(N_1+1)}{\Gamma(N_2+1)} \\ &\quad \times \frac{e^{-(\sigma_0+\sigma_1)z}}{z^{N_0+N_1}} F^{(1)}\left(z; \begin{matrix} N_0+N_1+1 \\ \sigma_0+\sigma_1 \end{matrix}\right) \\ &\quad - \frac{i\sqrt{2\pi}\Gamma(N_1+1)N_0^{N_0-\frac{1}{2}} e^{-N_0}}{\sigma_2(e^{-\pi i} \sigma_0)^{N_0} (e^{-\pi i} \sigma_1)^{N_1}} \frac{g_0(z) - g_0(\zeta_2)}{z - \zeta_2} \frac{e^{-(\sigma_0+\sigma_1)z}}{z^{N_0+N_1}} \\ &\quad + \mathcal{O}(|\mathbf{Erfc}|N_1^{-1}). \end{aligned}$$

Lemma 9.2. Let σ_0, σ_1 and their reciprocals be bounded. Assume that $\frac{\sigma_1}{\sigma_0} = \frac{N_1}{N_0} e^{i\nu}$ with $\nu = \mathcal{O}(N_1^{-1})$ as $\text{Re}(N_1) \rightarrow +\infty$. In addition, assume that $|\arg(\frac{\sigma_1}{\sigma_0})| < \pi$. Then, we have

$$\begin{aligned} &\frac{(\sigma_0 + \sigma_1)^{N_0+N_1+1}}{\sigma_0^{N_0+1} \sigma_1^{N_1}} \frac{\Gamma(N_0+1)\Gamma(N_1+1)}{\Gamma(N_0+N_1+2)} {}_2F_1\left(\begin{matrix} 1, N_0+1 \\ N_0+N_1+2 \end{matrix}; 1 + \frac{\sigma_1}{\sigma_0}\right) \\ &= \pi i - i\sqrt{\frac{2\pi N_0 N_1}{N_0+N_1}} \nu + \frac{N_0 - N_1}{3} \sqrt{\frac{2\pi}{N_0 N_1 (N_0+N_1)}} + \mathcal{O}(N_1^{-1}), \end{aligned}$$

as $\text{Re}(N_1) \rightarrow +\infty$.

Proof of Lemma 9.2. With the notation from (9.11), we have

$$\begin{aligned} &\frac{(\sigma_0 + \sigma_1)^{N_0+N_1+1}}{\sigma_0^{N_0+1} \sigma_1^{N_1}} \frac{\Gamma(N_0+1)\Gamma(N_1+1)}{\Gamma(N_0+N_1+2)} {}_2F_1\left(\begin{matrix} 1, N_0+1 \\ N_0+N_1+2 \end{matrix}; 1 + \frac{\sigma_1}{\sigma_0}\right) \\ &= \frac{\left(1 + \frac{\sigma_1}{\sigma_0}\right)^{N_0+N_1+1}}{\left(\frac{\sigma_1}{\sigma_0}\right)^{N_1}} I\left(\frac{\sigma_1}{\sigma_0}\right). \end{aligned}$$

Using (9.13) and (9.14), we find

$$\gamma \sim \sqrt{\frac{N_0}{N_0+N_1}} \left(\nu + \frac{N_0 - N_1}{N_0+N_1} \frac{i\nu^2}{6} \right),$$

$$g\left(0, \frac{\sigma_1}{\sigma_0}\right) \sim \frac{1}{3} \sqrt{\frac{N_0}{N_0+N_1}} \frac{N_0 - N_1}{N_0+N_1}.$$

We combine this with (9.12) and use two terms from the Maclaurin series for $\operatorname{erfc}(x)$. \square

Proof of Theorem 9.3. This theorem is a consequence of Lemma 9.1. Note that all the terms on the right-hand side of Lemma 9.1 are of the order $\mathcal{O}(|\mathbf{Erfc}|)$. Therefore, any manipulation of these terms by a factor $1 + \mathcal{O}(N_1^{-1})$ is permissible. We also use the approximation $\Gamma(N_j) e^{N_j} N_j^{-N_j+1} = \sqrt{2\pi N_j} (1 + \mathcal{O}(N_1^{-1}))$. \square

Proof of Lemma 9.1. Recall the integral representation (A2):

$$\begin{aligned} F^{(2)}\left(z; \begin{matrix} N_0+1, N_1+1 \\ \sigma_0, \sigma_1 \end{matrix}\right) &= \\ &= \frac{(\sigma_0 + \sigma_1)^{N_0+N_1+1}}{\sigma_0^{N_0+1} \sigma_1^{N_1}} \frac{\Gamma(N_0+1)\Gamma(N_1+1)}{\Gamma(N_0+N_1+2)} \\ &\quad \times {}_2F_1\left(\begin{matrix} 1, N_0+1 \\ N_0+N_1+2 \end{matrix}; 1 + \frac{\sigma_1}{\sigma_0}\right) F^{(1)}\left(z; \begin{matrix} N_0+N_1+1 \\ \sigma_0+\sigma_1 \end{matrix}\right) \\ &\quad - \frac{\Gamma(N_1+1)}{(e^{-\pi i} \sigma_1)^{N_1}} \frac{e^{(\sigma_0+\sigma_1)z}}{z^{N_0+N_1}} \int_z^\infty \frac{e^{-(\sigma_0+\sigma_1)t}}{t^{N_0+N_1+1}} F^{(1)}\left(t; \begin{matrix} N_0+1 \\ \sigma_0 \end{matrix}\right) dt. \end{aligned}$$

We use the representation (9.6) in the last integral to rewrite it as follows:

$$\begin{aligned} &= \frac{\Gamma(N_1+1)}{(e^{-\pi i} \sigma_1)^{N_1}} \int_z^\infty \frac{e^{-(\sigma_0+\sigma_1)t}}{t^{N_0+N_1+1}} F^{(1)}\left(t; \begin{matrix} N_0+1 \\ \sigma_0 \end{matrix}\right) dt \\ &= w_1(z) + w_2(z) + r_1(z), \end{aligned}$$

with

$$\begin{aligned} w_1(z) &= -\frac{\pi i \Gamma(N_1+1)}{(e^{-\pi i} \sigma_1)^{N_1}} \int_z^\infty e^{-\sigma_1 t} t^{-N_1-1} \operatorname{erfc}\left(\alpha_0(t) \sqrt{\frac{1}{2} N_0}\right) dt, \\ w_2(z) &= -i\sqrt{\frac{2\pi}{N_0}} \frac{\Gamma(N_1+1) N_0^{N_0} e^{-N_0}}{(e^{-\pi i} \sigma_0)^{N_0} (e^{-\pi i} \sigma_1)^{N_1}} \int_z^\infty e^{-\sigma_2 t} t^{-N_2-1} g_0(t) dt, \\ r_1(z) &= \frac{\sqrt{2\pi}}{N_0^{3/2}} \frac{\Gamma(N_1+1) N_0^{N_0} e^{-N_0}}{(e^{-\pi i} \sigma_0)^{N_0} (e^{-\pi i} \sigma_1)^{N_1}} \int_z^\infty e^{-\sigma_2 t} t^{-N_2-1} r_0(t) dt. \end{aligned} \tag{9.19}$$

In deriving (9.6), we applied the conditions $\text{Re}(N_0) > 0$ and $|\arg(e^{-\pi i} \sigma_0 z N_0^{-1})| < 2\pi$. These conditions are satisfied when $\text{Re}(N_0) > 0$ and $|\arg(e^{-\pi i} \sigma_0 z)| < \frac{3\pi}{2}$. In the subsequent analysis detailed below, we require the integration paths in (9.19) to be progressive (cf. [49, Section 6.11.3]). Our constraints include $|\arg N_j| \leq \frac{\pi}{2} - \delta (< \frac{\pi}{2})$ for $j = 0, 1$, $|\arg(\frac{\sigma_0 N_1}{\sigma_1 N_0})| \leq \pi - 2\epsilon - 2\delta$ and $|\arg(e^{-\frac{\pi}{2} i} \sigma_j z)| \leq \pi - \delta (< \pi)$, $j = 0, 1, 2$.

We can express the integral representation for $w_1(z)$ as follows:

$$w_1(z) = -\frac{\pi \Gamma(N_1+1) e^{N_1}}{N_1^{N_1}} \int_z^\infty e^{-\frac{1}{2} \alpha_1^2(t) N_1} \operatorname{erfc}\left(\alpha_0(t) \sqrt{\frac{1}{2} N_0}\right) \frac{i}{t} dt. \tag{9.20}$$

Hereafter, we employ the substitution $\tau = \alpha_0(t)$. Observe that

$$\alpha_j(t) \alpha_j'(t) = \frac{1}{t} + \frac{\sigma_j}{N_j}, \tag{9.21}$$

and take $t^* = \zeta_1 = e^{\pi i} N_1 / \sigma_1$, the saddle point of the exponential in (9.20), and $\tau^* = \alpha_0(t^*) \sim \nu$, as $\nu \rightarrow 0$. Therefore,

$f(\tau) = \frac{1}{2}\alpha_1^2(\tau)$ has a saddle point at $\tau = \tau^*$. From (9.21), it follows that $\tau = (\frac{1}{t} + \frac{\sigma_0}{N_0})t'(\tau)$ and $f'(\tau) = (\frac{1}{t} + \frac{\sigma_1}{N_1})t'(\tau)$, hence $f'(\tau) - \tau = (\frac{\sigma_1}{N_1} - \frac{\sigma_0}{N_0})t'(\tau)$. Differentiating this result gives us $f''(\tau) - 1 = (\frac{\sigma_1}{N_1} - \frac{\sigma_0}{N_0})t''(\tau)$ and $f^{(n)}(\tau) = (\frac{\sigma_1}{N_1} - \frac{\sigma_0}{N_0})t^{(n)}(\tau)$ for $n \geq 3$. We have

$$f(\tau^*) = f'(\tau^*) = 0, \quad f''(\tau^*) = \left(\frac{i\tau^*}{1 - e^{-i\nu}}\right)^2 = d_1^2,$$

where d_1 is defined below. Hence, for the function

$$r(t) = \frac{1}{2}\alpha_1^2(t) - \frac{1}{2}d_1^2(\alpha_0(t) - \tau^*)^2 = f(\tau) - \frac{1}{2}f''(\tau^*)(\tau - \tau^*)^2,$$

we find that

$$r(t^*) = \frac{dr(t^*)}{d\tau} = \frac{d^2r(t^*)}{d\tau^2} = 0, \quad \frac{d^n r(t)}{d\tau^n} = \left(\frac{\sigma_1}{N_1} - \frac{\sigma_0}{N_0}\right)t^{(n)}(\tau), \quad n \geq 3.$$

Consequently, $e^{N_1 r(t)}$ remains bounded in a large neighborhood of $t = t^*$.

For the integral in (9.20), we apply the Bleistein ansatz (see, e.g., [50, Section 2])

$$h_0(\tau) = \frac{i}{t} = d_1 \alpha_0'(t) e^{N_1 r(t)} + d_2(z) \alpha_1(t) \alpha_1'(t) + (t - z) \alpha_1(t) \alpha_1'(t) h_1(t),$$

where

$$d_1 = \frac{i}{t^* \alpha_0'(t^*)} = \frac{i \alpha_0(t^*)}{1 - e^{-i\nu}} \sim 1, \quad d_2(z) = \frac{i \left(1 - \frac{\alpha_0(t^*)}{1 - e^{-i\nu}} \frac{1 + \frac{\sigma_0 z}{\alpha_0(z)}}{\alpha_0(z)} e^{N_1 r(z)}\right)}{1 + \frac{\sigma_1 z}{N_1}}.$$

The ~ 1 is specific to the critical case $\nu \rightarrow 0$. We derive the expression

$$\begin{aligned} w_1(z) = & -\frac{\pi\Gamma(N_1 + 1)e^{N_1}}{N_1^{N_1}} d_1 \int_{\alpha_0(z)}^{\infty} e^{-\frac{1}{2}d_1^2(\tau - \tau^*)^2 N_1} \operatorname{erfc}\left(\tau \sqrt{\frac{1}{2}N_0}\right) d\tau \\ & - \frac{\pi\Gamma(N_1 + 1)e^{N_1}}{N_1^{N_1}} d_2(z) \int_z^{\infty} \alpha_1(t) \alpha_1'(t) e^{-\frac{1}{2}\alpha_1^2(t)N_1} \operatorname{erfc}\left(\alpha_0(t) \sqrt{\frac{1}{2}N_0}\right) dt \\ & - R_1(z), \end{aligned} \quad (9.22)$$

where

$$\begin{aligned} R_1(z) = & \frac{\pi\Gamma(N_1 + 1)e^{N_1}}{N_1^{N_1}} d_2(z) \int_z^{\infty} \alpha_1(t) \alpha_1'(t) e^{-\frac{1}{2}\alpha_1^2(t)N_1} \\ & \times \operatorname{erfc}\left(\alpha_0(t) \sqrt{\frac{1}{2}N_0}\right) (t - z) h_1(t) dt. \end{aligned}$$

The first integral in (9.22) can be expressed using our new special function

$$\begin{aligned} & -\frac{\pi\Gamma(N_1 + 1)e^{N_1}}{N_1^{N_1}} d_1 \int_{\alpha_0(z)}^{\infty} e^{-\frac{1}{2}d_1^2(\tau - \tau^*)^2 N_1} \operatorname{erfc}\left(\tau \sqrt{\frac{1}{2}N_0}\right) d\tau \\ = & -\frac{\pi^{\frac{3}{2}}\Gamma(N_1 + 1)e^{N_1}}{\sqrt{2}N_1^{N_1 + \frac{1}{2}}} \operatorname{erfc}\left(d_1 \alpha_0(z) \sqrt{\frac{1}{2}N_1}; d_1 \tau^* \sqrt{\frac{1}{2}N_1}; d_1^{-1} \sqrt{\frac{N_0}{N_1}}\right). \end{aligned} \quad (9.23)$$

For the second integral in (9.22), we apply integration by parts and derive

$$\begin{aligned} & -\frac{\pi\Gamma(N_1 + 1)e^{N_1}}{N_1^{N_1}} d_2(z) \int_z^{\infty} \alpha_1(t) \alpha_1'(t) e^{-\frac{1}{2}\alpha_1^2(t)N_1} \operatorname{erfc}\left(\alpha_0(t) \sqrt{\frac{1}{2}N_0}\right) dt \\ = & -d_2(z) \frac{\pi\Gamma(N_1)}{(e^{-\pi i \sigma_1})^{N_1}} \frac{e^{-\sigma_1 z}}{z^{N_1}} \operatorname{erfc}\left(\alpha_0(z) \sqrt{\frac{1}{2}N_0}\right) \\ & + \frac{\sqrt{2\pi N_0}\Gamma(N_1 + 1)e^{N_1}}{N_1^{N_1 + 1}} d_2(z) \int_z^{\infty} e^{-\frac{1}{2}\alpha_0^2(t)N_0 - \frac{1}{2}\alpha_1^2(t)N_1} \alpha_0'(t) dt. \end{aligned}$$

The final integral has a saddle point at $t = \zeta_2$ and an endpoint at $t = z$. Again, we apply the Bleistein method using

$$\begin{aligned} \alpha_0'(t) = & e_1 + e_2 \left(\alpha_0(t) \alpha_0'(t) + \frac{N_1}{N_0} \alpha_1(t) \alpha_1'(t)\right) \\ & + (t - z) \left(\alpha_0(t) \alpha_0'(t) + \frac{N_1}{N_0} \alpha_1(t) \alpha_1'(t)\right) \tilde{h}_1(t), \end{aligned}$$

where

$$e_1 = \alpha_0'(\zeta_2) = \frac{\frac{1}{\zeta_2} + \frac{\sigma_0}{N_0}}{\alpha_0(\zeta_2)}, \quad e_2 = \frac{N_0}{N_0 + N_1} \frac{\alpha_0'(z) - \alpha_0'(\zeta_2)}{\frac{1}{z} - \frac{1}{\zeta_2}},$$

yielding the approximation

$$\begin{aligned} & \frac{\sqrt{2\pi N_0}\Gamma(N_1 + 1)e^{N_1}}{N_1^{N_1 + 1}} d_2(z) \int_z^{\infty} e^{-\frac{1}{2}\alpha_0^2(t)N_0 - \frac{1}{2}\alpha_1^2(t)N_1} \alpha_0'(t) dt \\ \sim & -d_2(z) e_1 \frac{\sqrt{2\pi N_0}^{N_0 + \frac{1}{2}} e^{-N_0}\Gamma(N_1) (e^{-\pi i \sigma_2})^{N_2 - 1} e^{-(\sigma_0 + \sigma_1)z}}{(e^{-\pi i \sigma_0})^{N_0} (e^{-\pi i \sigma_1})^{N_1} \Gamma(N_2)} \frac{e^{-(\sigma_0 + \sigma_1)z}}{z^{N_0 + N_1 - 1}} \\ & \times F^{(1)}\left(z; \begin{matrix} N_0 + N_1 \\ \sigma_0 + \sigma_1 \end{matrix}\right) + d_2(z) e_2 \frac{\sqrt{2\pi N_0}^{N_0 - \frac{1}{2}} e^{-N_0}\Gamma(N_1) e^{-(\sigma_0 + \sigma_1)z}}{(e^{-\pi i \sigma_0})^{N_0} (e^{-\pi i \sigma_1})^{N_1} z^{N_0 + N_1}} \\ = & d_2(z) e_1 \frac{\sqrt{2\pi N_0}^{N_0 + \frac{1}{2}} e^{-N_0}\Gamma(N_1) \sigma_2^{N_2 - 1} e^{-(\sigma_0 + \sigma_1)z}}{\sigma_0^{N_0} \sigma_1^{N_1} \Gamma(N_2)} \frac{e^{-(\sigma_0 + \sigma_1)z}}{z^{N_0 + N_1}} \\ & \times F^{(1)}\left(z; \begin{matrix} N_0 + N_1 + 1 \\ \sigma_0 + \sigma_1 \end{matrix}\right) + d_2(z) e_2 \frac{\sqrt{2\pi N_0}^{N_0 + \frac{1}{2}} e^{-N_0}\Gamma(N_1) e^{-(\sigma_0 + \sigma_1)z}}{\sigma_2 (e^{-\pi i \sigma_0})^{N_0} (e^{-\pi i \sigma_1})^{N_1} z^{N_0 + N_1}} \\ & + d_2(z) e_2 \frac{\sqrt{2\pi N_0}^{N_0 - \frac{1}{2}} e^{-N_0}\Gamma(N_1) e^{-(\sigma_0 + \sigma_1)z}}{(e^{-\pi i \sigma_0})^{N_0} (e^{-\pi i \sigma_1})^{N_1} z^{N_0 + N_1}}. \end{aligned}$$

In the final step, we employ (3.3) with $N = 1$. Consequently, the last term can be incorporated into $\mathcal{O}(|\mathbf{Erfc}|N_1^{-1})$, and similarly for the penultimate terms, since $e_1 = \alpha_0'(\zeta_2) = \mathcal{O}(N_1^{-1})$.

For $w_2(z)$, we utilize

$$\begin{aligned} & \int_1^{\infty} e^{-\sigma_2 z t} t^{-N_2 - 1} (g_0(z t) - g_0(\zeta_2)) dt \\ = & \int_1^{\infty} e^{-\sigma_2 z t} t^{-N_2} \left(z - \frac{\zeta_2}{t}\right) \frac{g_0(z t) - g_0(\zeta_2)}{z t - \zeta_2} dt \\ = & \frac{e^{-\sigma_2 z} g_0(z) - g_0(\zeta_2)}{\sigma_2 z - \zeta_2} + \frac{1}{\sigma_2} \int_1^{\infty} e^{-\sigma_2 z t} t^{-N_2} \frac{d}{dt} \left(\frac{g_0(z t) - g_0(\zeta_2)}{z t - \zeta_2}\right) dt. \end{aligned}$$

Thus, we derive the asymptotic approximation

$$w_2(z) \sim i \frac{\sigma_2^{N_2}}{\sigma_0^{N_0} \sigma_1^{N_1}} \frac{\Gamma(N_0)\Gamma(N_1+1)}{\Gamma(N_2+1)} \times \frac{e^{-(\sigma_0+\sigma_1)z}}{z^{N_0+N_1}} F^{(1)}\left(z; \begin{matrix} N_0+N_1+1 \\ \sigma_0+\sigma_1 \end{matrix}\right) g_0(\zeta_2) - \frac{i\sqrt{2\pi}\Gamma(N_1+1)N_0^{N_0-\frac{1}{2}}e^{-N_0}}{\sigma_2(e^{-\pi i}\sigma_0)^{N_0}(e^{-\pi i}\sigma_1)^{N_1}} \frac{g_0(z) - g_0(\zeta_2)}{z - \zeta_2} \frac{e^{-(\sigma_0+\sigma_1)z}}{z^{N_0+N_1}}.$$

From this result and Theorem 9.1 with all occurrences of $*_0$ replaced by $*_2$, we conclude that both terms in the approximation for $w_2(z)$ are $\mathcal{O}(|\mathbf{Erfc}|)$, and the remainder in this approximation is $\mathcal{O}(N_1^{-1})$ smaller in magnitude.

Lastly, comparing the representation of $w_2(z)$ in (9.19) with $r_1(z)$, we observe an additional factor of N_0^{-1} . Based on the observation from the previous paragraph, it follows that $r_1(z) = \mathcal{O}(|\mathbf{Erfc}|N_1^{-1})$. \square

10 | Conclusion and Discussion

We have rigorously proved that the higher-order Stokes phenomenon arising from the second-order hyperterminants $F^{(2)}$ may be smoothed using a universal prefactor that is based on the Gaussian convolution of an error function (4.7). As such this approach is expected to be valid for all functions possessing a Borel transform representation with algebraic singularities in the associated Borel plane. We have provided a variety of examples of the occurrence of the smoothing, which demonstrate that it may give rise to “ghost-like” contributions on and in the immediate vicinity of a higher-order Stokes line but which rapidly and smoothly vanish elsewhere.

Moreover, when a Stokes line and a higher-order Stokes line coincide, the value of the Stokes multiplier on the Stokes line is no longer given by the value of $\frac{1}{2}$ associated with an ordinary Stokes phenomenon, but the contribution of the higher-order Stokes phenomenon may amend this to the value given by the formula (4.8), involving an arctangent function. It would be interesting to examine if this formula can be derived using a median summation approach [51, 52].

Given that uniform approximations of hyperterminants $F^{(1)}$ give rise to the error function smoothing (3.6) of the ordinary Stokes phenomenon, and in turn that the uniform approximation of hyperterminants $F^{(2)}$ gives rise to the Gaussian convolution of an error function smoothing (4.7) of the first higher-order Stokes phenomena, this is likely to be the start of a hierarchy of such convolution smoothing functions. Each such function would arise from uniform approximations of the increasingly higher-order hyperterminants $F^{(n)}$, $n \geq 2$. Obviously this could be investigated, but is likely to have a decreasing analytical benefit for the rapidly increasing amount of work required (whether rigorous or formal).

Finally, it is well known that the smoothed Stokes phenomenon is associated with many physical processes, (for example particle

creation [53, 54]). The example in Section 7 above shows, that an additional smoothed ghost-like contribution may occur along, and in the immediate vicinity of, a (higher-order) Stokes line in real space. The role that a smoothed higher-order Stokes phenomenon might therefore play in physical systems merits further investigation.

Acknowledgments

The authors wish to thank the Isaac Newton Institute for Mathematical Sciences for their support during the program “Applicable Resurgent Asymptotics: Towards a Universal Theory,” funded by EPSRC Grant No. EP/R014604/1. JRK gratefully acknowledges a Royal Society Leverhulme Trust Research Fellowship. GN’s research was partially supported by the JSPS KAKENHI Grant No. 22H01146. AOD’s research was supported by the Measurement Science and Engineering (MSE) Research Grant No. 60NANB23D131 from the National Institute of Standards and Technology.

Data Availability Statement

Data sharing not applicable to this article as no data sets were generated or analyzed during the current study.

References

1. M. V. Berry, “Uniform Asymptotic Smoothing of Stokes’s Discontinuities,” *Proceedings of the Royal Society of London Series A, Mathematical and Physical Sciences* 422 (1989): 7–21.
2. H. L. Berk, W. M. Nevins, and K. V. Roberts, “New Stokes’ Line in WKB Theory,” *Journal of Mathematical and Physical Sciences* 23 (1982): 988–1002.
3. T. Aoki, T. Kawai, and Y. Takei, “New Turning Points in the Exact WKB Analysis for Higher-Order Ordinary Differential Equations,” in *Analyse Algébrique Des Perturbations Singulières, I (Marseille-Luminy, 1991)*, Vol. 47 of Travaux en Cours, Hermann, Paris, 1994, xiii, xv, 69–84.
4. T. Aoki, T. Kawai, and Y. Takei, “On the Exact Steepest Descent Method: A New Method for the Description of Stokes Curves,” *Journal of Mathematical and Physical Sciences* 42 (2001): 3691–3713.
5. C. J. Howls, P. J. Langman, and A. B. Olde Daalhuis, “On the Higher-Order Stokes Phenomenon,” *Proceedings of the Royal Society of London Series A Mathematical, Physical and Engineering Sciences* 460 (2004): 2285–2303.
6. S. J. Chapman and D. B. Mortimer, “Exponential Asymptotics and Stokes Lines in a Partial Differential Equation,” *Proceedings of the Royal Society of London Series A Mathematical, Physical and Engineering Sciences* 461 (2005): 2385–2421.
7. G. G. Stokes, “On the Discontinuity of Arbitrary Constants Which Appear in Divergent Developments,” *Transactions of the Cambridge Philosophical Society* 10 (1857): 105–128.
8. M. V. Berry, “Infinitely Many Stokes Smoothings in the Gamma Function,” *Proceedings of the Royal Society of London Series A, Mathematical and Physical Sciences* 434 (1991): 465–472.
9. W. G. C. Boyd, “Stieltjes Transforms and the Stokes Phenomenon,” *Proceedings of the Royal Society of London Series A, Mathematical and Physical Sciences* 429 (1990): 227–246.
10. A. B. Olde Daalhuis, S. J. Chapman, J. R. King, J. R. Ockendon, and R. H. Tew, “Stokes Phenomenon and Matched Asymptotic Expansions,” *SIAM Journal on Applied Mathematics* 55 (1995): 1469–1483.
11. F. W. J. Olver, “Uniform, Exponentially Improved, Asymptotic Expansions for the Confluent Hypergeometric Function and Other Integral Transforms,” *SIAM Journal on Mathematical Analysis* 22 (1991): 1475–1489.

12. F. W. J. Olver, "Uniform, Exponentially Improved, Asymptotic Expansions for the Generalized Exponential Integral," *SIAM Journal on Mathematical Analysis* 22 (1991): 1460–1474.
13. R. Paris, "Smoothing of the Stokes Phenomenon Using Mellin–Barnes Integrals," *Journal of Computational and Applied Mathematics* 41 (1992): 117–133.
14. G. L. Body, J. R. King, and R. H. Tew, "Exponential Asymptotics of a Fifth-Order Partial Differential Equation," *European Journal of Applied Mathematics* 16 (2005): 647–681.
15. S. J. Chapman, C. J. Howls, J. R. King, and A. B. Olde Daalhuis, "Why is a Shock Not a Caustic? The Higher-Order Stokes Phenomenon and Smoothed Shock Formation," *Nonlinearity* 20 (2007): 2425–2452.
16. C. J. Howls and A. B. Olde Daalhuis, "Exponentially Accurate Solution Tracking for Nonlinear ODEs, The Higher Order Stokes Phenomenon and Double Transseries Resummation," *Nonlinearity* 25 (2012): 1559–1584.
17. A. B. Olde Daalhuis, "On Higher-Order Stokes Phenomena of an Inhomogeneous Linear Ordinary Differential Equation," *Journal of Computational and Applied Mathematics* 169 (2004): 235–246.
18. G. Nemes, "Dingle's Final Main Rule, Berry's Transition, and Howls' Conjecture," *Journal of Physics A: Mathematical and Theoretical* 55 (2022): 494001.
19. R. Gonçalves, "The Power Normal Distribution," *Journal of Physics: Conference Series* 1334 (2019): 012014.
20. J. Shelton, S. Crew, and P. H. Trinh, "Exponential Asymptotics and Higher-Order Stokes Phenomenon in Singularly Perturbed ODEs," *SIAM Journal on Applied Mathematics*, preprint, arxiv, 2023, <https://doi.org/10.48550/arXiv:2303.07866>.
21. T. Bennett, C. J. Howls, G. Nemes, and A. B. Olde Daalhuis, "Globally Exact Asymptotics for Integrals With Arbitrary Order Saddles," *SIAM Journal on Mathematical Analysis* 50 (2018): 2144–2177.
22. M. V. Berry and C. J. Howls, "Hyperasymptotics for Integrals With Saddles," *Proceedings of the Royal Society of London Series A, Mathematical and Physical Sciences* 434 (1991): 657–675.
23. E. Delabaere and C. J. Howls, "Global Asymptotics for Multiple Integrals with Boundaries," *Duke Mathematical Journal* 112 (2002): 199–264.
24. C. J. Howls, "Hyperasymptotics for Integrals With Finite Endpoints," *Proceedings of the Royal Society of London, Series A, Mathematical and Physical Sciences* 439 (1992): 373–396.
25. C. J. Howls, "Hyperasymptotics for Multidimensional Integrals, Exact Remainder Terms and the Global Connection Problem," *Proceedings of Royal Society of London Series A, Mathematical, Physical and Engineering Sciences* 453 (1997): 2271–2294.
26. C. J. Howls and A. B. Olde Daalhuis, "Hyperasymptotic Solutions of Inhomogeneous Linear Differential Equations With a Singularity of Rank One," *Proceedings of Royal Society of London Series A, Mathematical, Physical and Engineering Sciences* 459 (2003): 2599–2612.
27. A. B. Olde Daalhuis, "Hyperasymptotic Solutions of Second-Order Linear Differential Equations. II," *Methods and Applications of Analysis* 2 (1995): 198–211.
28. A. B. Olde Daalhuis, "Hyperasymptotic Solutions of Higher Order Linear Differential Equations With a Singularity of Rank One," *Proceedings of Royal Society of London Series A, Mathematical, Physical and Engineering Sciences* 454 (1998): 1–29.
29. A. B. Olde Daalhuis and F. W. J. Olver, "Hyperasymptotic Solutions of Second-Order Linear Differential Equations. I," *Methods and Applications of Analysis* 2 (1995): 173–197.
30. A. B. Olde Daalhuis and F. W. J. Olver, "On the Calculation of Stokes Multipliers for Linear Differential Equations of the Second Order," *Methods and Applications of Analysis* 2 (1995): 348–367.
31. S. Crew and P. H. Trinh, "Resurgent Aspects of Applied Exponential Asymptotics," *Studies in Applied Mathematics* 152 (2024): 974–1025.
32. A. B. Olde Daalhuis, "Inverse Factorial-Series Solutions of Difference Equations," *Proceedings of the Edinburgh Mathematical Society* 47 (2004): 421–448.
33. F. W. J. Olver, "Resurgence in Difference Equations, With an Application to Legendre Functions," in *Proceedings of Special Functions, Hong Kong, 1999* (River Edge, NJ: World Scientific Publishing, 2000), 221–235.
34. G. Deng and C. J. Lustrri, "Exponential Asymptotics of Woodpile Chain Nanoptera Using Numerical Analytic Continuation," *Studies in Applied Mathematics* 150 (2023): 520–557.
35. G. Álvarez, C. J. Howls, and H. J. Silverstone, "Anharmonic Oscillator Discontinuity Formulae up to Second-Exponentially-Small Order," *Journal of Physics A: Mathematical and General* 35 (2002): 4003–4016.
36. G. Álvarez, C. J. Howls, and H. J. Silverstone, "Dispersive Hyperasymptotics and the Anharmonic Oscillator," *Journal of Physics A: Mathematical and General* 35 (2002): 4017–4042.
37. G. Álvarez and C. Casares, "Exponentially Small Corrections in the Asymptotic Expansion of the Eigenvalues of the Cubic Anharmonic Oscillator," *Journal of Physics A: Mathematical and General* 33 (2000): 5171.
38. C. J. Howls, "An Introduction to Hyperasymptotics Using Borel-Laplace Transforms," *RIMS Kôkyûroku* 968 (1996): 31–48.
39. R. B. Dingle, *Asymptotic Expansions: Their Derivation and Interpretation* (London-New York: Academic Press [A subsidiary of Harcourt Brace Jovanovich, Publishers], 1973).
40. A. B. Olde Daalhuis, "Hyperterminants I," *Journal of Computational and Applied Mathematics* 76 (1996): 255–264.
41. A. B. Olde Daalhuis, "Hyperterminants II," *Journal of Computational and Applied Mathematics* 89 (1998): 87–95.
42. A. B. Olde Daalhuis, "Hyperasymptotics and Hyperterminants: Exceptional Cases," *Journal of Computational and Applied Mathematics* 233 (2009): 555–563.
43. I. Aniceto, G. Başar, and R. Schiappa, "A Primer on Resurgent Transseries and Their Asymptotics," *Physics Reports* 809 (2019): 1–135.
44. F. W. J. Olver, A. B. Olde Daalhuis, D. W. Lozier, et al., eds. *NIST Digital Library of Mathematical Functions*, Release 1.2.3 of December 15, 2024, <https://dlmf.nist.gov/>.
45. N. M. Temme, "Uniform Asymptotics for the Incomplete Gamma Functions Starting From Negative Values of the Parameters," *Methods and Applications of Analysis* 3 (1996): 335–344.
46. N. M. Temme, "The Asymptotic Expansion of the Incomplete Gamma Functions," *SIAM Journal on Mathematical Analysis* 10 (1979): 757–766.
47. R. L. Schilling, R. Song, and Z. Vondraček, *Bernstein Functions: Theory and Applications* (Berlin, Boston: De Gruyter, 2012).
48. N. M. Temme, *Asymptotic Methods for Integrals*, Vol. 6 of Series in Analysis (Hackensack, NJ: World Scientific Publishing, 2015).
49. F. W. J. Olver, *Asymptotics and Special Functions*, AKP Classics (Wellesley, MA: A K Peters Ltd. 1997), Reprint of the 1974 original.
50. S. F. Khwaja and A. B. Olde Daalhuis, "Computation of the Coefficients Appearing in the Uniform Asymptotic Expansions of Integrals," *Studies in Applied Mathematics* 139 (2017): 551–567.
51. E. Delabaere and F. Pham, "Resurgent Methods in Semi-Classical Asymptotics," *Annales de l'Institut Henri Poincaré Physique théorique* 71 (1999): 1–94.
52. J. Écalle, *Six Lectures on Transseries, Analysable Functions and the Constructive Proof of Dulac's Conjecture* (Dordrecht: Springer Netherlands, 1993), 75–184.
53. C. K. Dumlu and G. V. Dunne, "Stokes Phenomenon and Schwinger Vacuum Pair Production in Time-Dependent Laser Pulses," *Physical Review Letters* 104 (2010): 250402.

54. S. Hashiba and Y. Yamada, “Stokes Phenomenon and Gravitational Particle Production—How to Evaluate It in Practice,” *Journal of Cosmology and Astroparticle Physics* 2021 (2021): 022.

55. J. D. Murray, *Mathematical Biology: I. An Introduction*, 3rd ed., Vol. 17 of Interdisciplinary Applied Mathematics (New York: Springer-Verlag, 2002).

56. A. N. Stokes, “On Two Types of Moving Front in Quasilinear Diffusion,” *Mathematical Biosciences* 31 (1976): 307–315.

Appendix A: A New Integral Representation for the Second Hyperterminant Function

In this appendix, we derive the main underpinning result, a new integral representation for the second hyperterminant function. We also provide background information on the hyperterminants that may be of use to those using different machinery to study the same problem.

A detailed description of the hyperterminant functions is provided in references [21, 41, 42]. Although the ordinary differential equations governing these functions are not as widely documented, they prove valuable when employing alternative methods such as matched asymptotics to derive exponentially improved asymptotic expansions. In the following, we demonstrate how the inhomogeneous ODEs lead directly to a novel integral representation for the second hyperterminant function.

The first hyperterminant $y(z) = F^{(1)}\left(z; \begin{smallmatrix} N_0+1 \\ \sigma_0 \end{smallmatrix}\right)$ satisfies the inhomogeneous ODE

$$zy'(z) - (N_0 + \sigma_0 z)y(z) = \frac{\Gamma(N_0 + 1)}{(e^{-\pi i} \sigma_0)^{N_0}}.$$

Upon differentiating both sides with respect to z , we obtain the following homogeneous ODE:

$$zy''(z) + (1 - N_0 - \sigma_0 z)y'(z) - \sigma_0 y(z) = 0.$$

A second solution to this homogeneous equation is given by $y(z) = e^{\sigma_0 z} z^{N_0}$. For the rescaled first hyperterminant $v(z) = e^{-\sigma_0 z} z^{-N_0} F^{(1)}\left(z; \begin{smallmatrix} N_0+1 \\ \sigma_0 \end{smallmatrix}\right)$, we find

$$v'(z) = \frac{\Gamma(N_0 + 1)}{(e^{-\pi i} \sigma_0)^{N_0}} e^{-\sigma_0 z} z^{-N_0-1}, \quad v''(z) + \left(\sigma_0 + \frac{N_0 + 1}{z}\right)v'(z) = 0.$$

The second hyperterminant $y(z) = F^{(2)}\left(z; \begin{smallmatrix} N_0+1, N_1+1 \\ \sigma_0, \sigma_1 \end{smallmatrix}\right)$ is a solution of the inhomogeneous ODE

$$\begin{aligned} &zy''(z) + (1 - N_0 - N_1 - (\sigma_0 + \sigma_1)z)y'(z) - (\sigma_0 + \sigma_1)y(z) \\ &= \frac{\Gamma(N_1 + 1)}{(e^{-\pi i} \sigma_1)^{N_1}} \frac{d}{dz} F^{(1)}\left(z; \begin{smallmatrix} N_0 + 1 \\ \sigma_0 \end{smallmatrix}\right). \end{aligned} \tag{A1}$$

Solutions to the homogeneous part include $F^{(1)}\left(z; \begin{smallmatrix} N_0+N_1+1 \\ \sigma_0+\sigma_1 \end{smallmatrix}\right)$ and $e^{(\sigma_0+\sigma_1)z} z^{N_0+N_1}$. For the rescaled second hyperterminant $v(z) = e^{-(\sigma_0+\sigma_1)z} z^{-N_0-N_1} F^{(2)}\left(z; \begin{smallmatrix} N_0+1, N_1+1 \\ \sigma_0, \sigma_1 \end{smallmatrix}\right)$, we find

$$\begin{aligned} &v''(z) + \left(\sigma_0 + \sigma_1 + \frac{N_0 + N_1 + 1}{z}\right)v'(z) \\ &= \frac{\Gamma(N_1 + 1)}{(e^{-\pi i} \sigma_1)^{N_1}} e^{-(\sigma_0+\sigma_1)z} z^{-N_0-N_1-1} \frac{d}{dz} F^{(1)}\left(z; \begin{smallmatrix} N_0 + 1 \\ \sigma_0 \end{smallmatrix}\right). \end{aligned}$$

By employing the method of variation of parameters, we derive the following new representation:

$$\begin{aligned} F^{(2)}\left(z; \begin{smallmatrix} N_0 + 1, N_1 + 1 \\ \sigma_0, \sigma_1 \end{smallmatrix}\right) &= -\frac{(\sigma_0 + \sigma_1)^{N_0+N_1+1}}{\sigma_0^{N_0+1} \sigma_1^{N_1}} \frac{\Gamma(N_0 + 1)\Gamma(N_1 + 1)}{\Gamma(N_0 + N_1 + 2)} \\ &\times {}_2F_1\left(\begin{smallmatrix} 1, N_0 + 1 \\ N_0 + N_1 + 2 \end{smallmatrix}; 1 + \frac{\sigma_1}{\sigma_0}\right) F^{(1)}\left(z; \begin{smallmatrix} N_0 + N_1 + 1 \\ \sigma_0 + \sigma_1 \end{smallmatrix}\right) \\ &- \frac{\Gamma(N_1 + 1)}{(e^{-\pi i} \sigma_1)^{N_1}} e^{(\sigma_0+\sigma_1)z} z^{N_0+N_1} \int_z^\infty \frac{e^{-(\sigma_0+\sigma_1)t}}{t^{N_0+N_1+1}} F^{(1)}\left(t; \begin{smallmatrix} N_0 + 1 \\ \sigma_0 \end{smallmatrix}\right) dt. \end{aligned} \tag{A2}$$

The key points to note here are that the right-hand side of (A2) solves (A1), and when N_0, N_1 are bounded, $\text{Re}(\sigma_0) > 0$, $\text{Re}(\sigma_1) > 0$, $\text{Im}(\sigma_1 - \sigma_0) > 0$, and $\text{Re}(z)$ is large and positive, all terms in (A2) are well-defined. Furthermore,

$$\begin{aligned} F^{(2)}\left(z; \begin{smallmatrix} N_0 + 1, N_1 + 1 \\ \sigma_0, \sigma_1 \end{smallmatrix}\right) &\sim \frac{-1}{z} F^{(2)}\left(0; \begin{smallmatrix} N_0 + 2, N_1 + 1 \\ \sigma_0, \sigma_1 \end{smallmatrix}\right), \\ F^{(1)}\left(z; \begin{smallmatrix} N_0 + N_1 + 1 \\ \sigma_0 + \sigma_1 \end{smallmatrix}\right) &\sim \frac{-1}{z} F^{(1)}\left(0; \begin{smallmatrix} N_0 + N_1 + 2 \\ \sigma_0 + \sigma_1 \end{smallmatrix}\right), \end{aligned}$$

and the final term in (A2) is $\mathcal{O}(z^{-2})$. Hence, (A2) holds if

$$\begin{aligned} F^{(2)}\left(0; \begin{smallmatrix} N_0 + 2, N_1 + 1 \\ \sigma_0, \sigma_1 \end{smallmatrix}\right) &= -\frac{(\sigma_0 + \sigma_1)^{N_0+N_1+1}}{\sigma_0^{N_0+1} \sigma_1^{N_1}} \frac{\Gamma(N_0 + 1)\Gamma(N_1 + 1)}{\Gamma(N_0 + N_1 + 2)} \\ &\times {}_2F_1\left(\begin{smallmatrix} 1, N_0 + 1 \\ N_0 + N_1 + 2 \end{smallmatrix}; 1 + \frac{\sigma_1}{\sigma_0}\right) F^{(1)}\left(0; \begin{smallmatrix} N_0 + N_1 + 2 \\ \sigma_0 + \sigma_1 \end{smallmatrix}\right). \end{aligned}$$

This identity is, however, a straightforward consequence of [42, eqs. 2.2 and 3.2].

The right-hand side of (A2) contains two terms. The first term incorporates the $\sigma_0 \leftrightarrow \sigma_1$ higher-order Stokes phenomenon, while the final term includes the $z \leftrightarrow \sigma_0$ higher-order Stokes phenomenon (cf. connection formulas (4.1) and (4.2)).

We use analytic continuation to remove the constraints on the parameters in the derivation of (A2). However, when changing $\arg(\sigma_0 + \sigma_1)$, we must rotate the contour of integration to ensure $|\arg((\sigma_0 + \sigma_1)t)| < \frac{\pi}{2}$ as $t \rightarrow \infty$ along the path of integration. While this adjustment is always possible, we must avoid crossing too many branch cuts of the functions involved in Equation (A2). Therefore, we will use the constraints $|\arg(\sigma_0 z)| \leq \frac{3\pi}{2} - \delta$ ($< \frac{3\pi}{2}$) and $|\arg(1 + \frac{\sigma_1}{\sigma_0})| \leq \pi - \delta$ ($< \pi$).

Appendix B: The New Special Function and Its Evaluation

The new approximant that we encountered in Section 9.5 is given by

$$\text{erfc}(x; y; \lambda) = \frac{2}{\sqrt{\pi}} \int_x^\infty e^{-(\tau-y)^2} \text{erfc}(\lambda\tau) d\tau. \tag{B1}$$

Initially, $x, y \in \mathbb{C}$, $\lambda \geq 0$ and the path of integration is chosen such that $\arg \tau = 0$ for sufficiently large values of $|\tau|$. It is then extended to $\lambda \in \mathbb{C} \setminus \{it : t \in \mathbb{R}, |t| \geq 1\}$ through analytic continuation, achieved by appropriately deforming the integration contour. In this manner, $\text{erfc}(x; y; \lambda)$ becomes an analytic function over the domain $\mathbb{C} \times \mathbb{C} \times \mathbb{C} \setminus \{it : t \in \mathbb{R}, |t| \geq 1\}$. This function possesses the following properties that are relevant to the argument in the main text.

Integration by parts applied to (B1) yields

$$\operatorname{erfc}(x; y; \lambda) + \operatorname{erfc}(\lambda(x - y); -\lambda y; \lambda^{-1}) = \operatorname{erfc}(x - y) \operatorname{erfc}(\lambda x), \quad \lambda \neq 0. \quad (\text{B2})$$

Specific values are as follows:

$$\begin{aligned} \operatorname{erfc}(x; y; 0) &= \operatorname{erfc}(x - y), & \operatorname{erfc}(x; 0; 1) &= \frac{1}{2} \operatorname{erfc}^2(x), \\ \operatorname{erfc}(0; 0; \lambda) &= 1 - \frac{2}{\pi} \arctan(\lambda). \end{aligned} \quad (\text{B3})$$

In addition, the function satisfies the reflection formulas

$$\operatorname{erfc}(-x; y; \lambda) = \operatorname{erfc}(x; -y; \lambda) + 2 \operatorname{erfc}\left(\frac{\lambda y}{\sqrt{\lambda^2 + 1}}\right) - 2 \operatorname{erfc}(x + y), \quad (\text{B4})$$

$$\operatorname{erfc}(x; y; -\lambda) = -\operatorname{erfc}(x; y; \lambda) + 2 \operatorname{erfc}(x - y),$$

and serves as a particular solution to the linear differential equation

$$\frac{d}{dx} \left(e^{(x-y)^2} \frac{dw(x)}{dx} \right) = \frac{4\lambda}{\pi} e^{-\lambda^2 x^2}, \quad (\text{B5})$$

whose general solution is of the form

$$w(x) = A + B \operatorname{erfc}(x - y) + \operatorname{erfc}(x; y; \lambda), \quad A, B \in \mathbb{C}.$$

Furthermore, the new special function possesses the following partial derivatives:

$$\frac{\partial \operatorname{erfc}(x; y; \lambda)}{\partial x} = -\frac{2}{\sqrt{\pi}} e^{-(x-y)^2} \operatorname{erfc}(\lambda x), \quad (\text{B6})$$

$$\frac{\partial \operatorname{erfc}(x; y; \lambda)}{\partial y} = \frac{2}{\sqrt{\pi}} e^{-(x-y)^2} \operatorname{erfc}(\lambda x) - \frac{2\lambda e^{-\frac{\lambda^2 y^2}{\lambda^2 + 1}} \operatorname{erfc}\left(\frac{\lambda^2 x + x - y}{\sqrt{\lambda^2 + 1}}\right)}{\sqrt{\pi} \sqrt{\lambda^2 + 1}}, \quad (\text{B7})$$

$$\frac{\partial \operatorname{erfc}(x; y; \lambda)}{\partial \lambda} = -\frac{2e^{-\lambda^2 x^2 - (x-y)^2}}{\pi(\lambda^2 + 1)} - \frac{2ye^{-\frac{\lambda^2 y^2}{\lambda^2 + 1}} \operatorname{erfc}\left(\frac{\lambda^2 x + x - y}{\sqrt{\lambda^2 + 1}}\right)}{\sqrt{\pi}(\lambda^2 + 1)^{3/2}}.$$

We can utilize the differential equation (B5) to derive a recurrence relation for the coefficients $a_n = a_n(x, y, \lambda)$ of the Maclaurin series

$$\operatorname{erfc}(x; y; \lambda) = \operatorname{erfc}(0; y; \lambda) - \frac{2}{\sqrt{\pi}} e^{-y^2} \sum_{n=1}^{\infty} a_n x^n$$

with respect to the variable x . Substituting into (B5), we obtain

$$\begin{aligned} (n+3)(n+2)(n+1)a_{n+3} &= 4y(n+2)(n+1)a_{n+2} \\ &\quad - 2((\lambda^2 + 2)n + 2y^2 + 1)(n+1)a_{n+1} \\ &\quad + 4(\lambda^2 + 2)yna_n - 4(\lambda^2 + 1)(n-1)a_{n-1} \end{aligned}$$

for $n = 0, 1, 2, \dots$, with initial conditions

$$a_{-1} = a_0 = 0, \quad a_1 = 1, \quad a_2 = y - \frac{\lambda}{\sqrt{\pi}}.$$

Thus, it becomes necessary to establish a formula for $\operatorname{erfc}(0; y; \lambda)$. We already know from (B3) that $\operatorname{erfc}(0; 0; \lambda) = 1 - \frac{2}{\pi} \arctan(\lambda)$. This can be generalized as

$$\begin{aligned} \operatorname{erfc}(0; y; \lambda) &= 1 - \frac{2}{\pi} \arctan(\lambda) + \operatorname{erf} y - \operatorname{erf}\left(\frac{\lambda y}{\sqrt{\lambda^2 + 1}}\right) \\ &\quad - \frac{2\lambda}{\pi} \int_0^y \frac{e^{-t^2}}{\sqrt{\lambda^2 + 1}} e^{-t^2 \lambda^2} \operatorname{erf} t \, dt \end{aligned}$$

$$\begin{aligned} &= 1 - \frac{2}{\pi} \arctan(\lambda) + \operatorname{erf} y - \operatorname{erf}\left(\frac{\lambda y}{\sqrt{\lambda^2 + 1}}\right) \\ &\quad + \frac{2}{\pi} \sum_{k=0}^{\infty} \frac{\binom{-y^2}{k}}{(k+1)!} \sum_{m=0}^k \binom{k}{m} \frac{\lambda^{2m+1}}{2k-2m+1} \end{aligned}$$

using [44, eq. 7.6.1].

In the following theorem, we present an asymptotic expansion for $\operatorname{erfc}(x; y; \lambda)$, applicable when x is large and y and λ are bounded.

Theorem B.1. *Let y and λ be bounded such that $\operatorname{Re}(\lambda^2) \geq 0$ and $\lambda \neq 0$. Then,*

$$\operatorname{erfc}(x; y; \lambda) \sim e^{-\lambda^2 x^2 - (x-y)^2} \sum_{n=2}^{\infty} \frac{b_n}{x^n}, \quad (\text{B8})$$

as $x \rightarrow \infty$ in the sector $|\arg x| \leq \frac{\pi}{2} - \delta$ ($\delta < \frac{\pi}{2}$). The coefficients $b_n = b_n(y, \lambda)$ satisfy the recurrence relation

$$\begin{aligned} 4\lambda^2(\lambda^2 + 1)b_{n+2} &= 4y\lambda^2 b_{n+1} - 2((2n-1)(\lambda^2 + 1) - n)b_n \\ &\quad + 2y(n-1)b_{n-1} - (n-1)(n-2)b_{n-2} \end{aligned}$$

for $n = 1, 2, 3, \dots$, with initial conditions

$$b_{-1} = b_0 = b_1 = 0, \quad b_2 = \frac{1}{\pi\lambda(\lambda^2 + 1)}.$$

We note that employing the first partial derivative (B6) and the standard asymptotic expansion of erfc [44, eq. 7.12.1], we can derive the following alternative recursion:

$$(\lambda^2 + 1)b_{2n+1} - yb_{2n} + \left(n - \frac{1}{2}\right)b_{2n-1} = 0,$$

$$(\lambda^2 + 1)b_{2n+2} - yb_{2n+1} + nb_{2n} = \frac{(-1)^n \left(\frac{1}{2}\right)_n}{\pi\lambda^{2n+1}}$$

for $n = 1, 2, 3, \dots$. Here, $(a)_n = \Gamma(a+n)/\Gamma(a)$ denotes the Pochhammer symbol.

Proof. For every $N \geq 3$, we introduce the remainder term $R_N(x; y; \lambda)$ defined by

$$\operatorname{erfc}(x; y; \lambda) = e^{-\lambda^2 x^2 - (x-y)^2} \sum_{n=2}^N \frac{b_n}{x^n} + R_N(x; y; \lambda), \quad (\text{B9})$$

where the coefficients b_n are those specified in the theorem. By substituting (B9) into (B5), we derive a differential equation for $R_N(x; y; \lambda)$

$$\frac{\partial}{\partial x} \left(e^{(x-y)^2} \frac{\partial}{\partial x} R_N(x; y; \lambda) \right) = e^{-\lambda^2 x^2} x^{1-N} Q(x), \quad (\text{B10})$$

where

$$\begin{aligned} Q(x) &= 4\lambda^2(\lambda^2 + 1)b_{N+1} + \frac{4\lambda^2(\lambda^2 + 1)b_{N+2} - 4y\lambda^2 b_{N+1}}{x} \\ &\quad + \frac{2yNb_N - N(N-1)b_{N-1}}{x^2} - \frac{(N+1)Nb_N}{x^3}. \end{aligned}$$

This leads to the integral representation

$$R_N(x; y; \lambda) = \frac{\sqrt{\pi}}{2} \int_x^{\infty} \left(\operatorname{erfc}(x-y) - \operatorname{erfc}(t-y) \right) e^{-\lambda^2 t^2} t^{1-N} Q(t) \, dt. \quad (\text{B11})$$

Other solutions to (B10) differ from (B11) by incorporating an additional term in the form of

$$A + Be^{y^2} \operatorname{erf}(x - y), \quad A, B \in \mathbb{C}, \quad AB \neq 0,$$

but these do not diminish as $x \rightarrow +\infty$. Integrating once by parts in (B11) yields

$$R_N(x; y; \lambda) = \int_x^\infty e^{-(t-y)^2} \int_t^\infty e^{-\lambda^2 s^2} \frac{Q(s)}{s^{N-1}} ds dt.$$

Now, by substituting $t - y = \sqrt{u + (x - y)^2}$ and $s = \sqrt{v + x^2}$, we obtain

$$R_N(x; y; \lambda) = \frac{e^{-\lambda^2 x^2 - (x-y)^2}}{4(x-y)x^N} \int_0^\infty \frac{e^{-u}}{\sqrt{1 + \frac{u}{(x-y)^2}}} \times \int_{v^*(u)}^\infty e^{-\lambda^2 v} \frac{Q(\sqrt{v+x^2})}{\left(1 + \frac{v}{x^2}\right)^{N/2}} dv du,$$

with $v^*(u) = u(1 + \frac{2y}{\sqrt{u+(x-y)^2+x-y}})$. The paths of integration are chosen such that $|\arg u| \leq \delta \leq \frac{\pi}{2}$ and $\arg v = 0$ holds for all sufficiently large values of $|u|$ and $|v|$. If we assume $\operatorname{Re}(\lambda^2) \geq 0$ and $\lambda \neq 0$, then the double integral is bounded within the sector $|\arg x| \leq \frac{\pi}{2} - \delta (< \frac{\pi}{2})$ for sufficiently large $|x|$. Consequently,

$$R_N(x; y; \lambda) = e^{-\lambda^2 x^2 - (x-y)^2} \mathcal{O}(x^{-N-1})$$

as $x \rightarrow \infty$ in the sector $|\arg x| \leq \frac{\pi}{2} - \delta (< \frac{\pi}{2})$. □

Considering the case where $x \rightarrow \infty$ in the sector $|\arg(-x)| \leq \frac{\pi}{2} - \delta (< \frac{\pi}{2})$, we can combine (B8) with the reflection formula (B4). In the specific case where $x \rightarrow -\infty$, we find

$$\operatorname{erfc}(x; y; \lambda) \sim 2 \operatorname{erfc}\left(\frac{\lambda y}{\sqrt{\lambda^2 + 1}}\right)$$

provided y and λ are bounded, $\operatorname{Re}(\lambda^2) \geq 0$ and $\lambda \neq 0$.

In the theorem that follows, we provide an asymptotic expansion for $\operatorname{erfc}(x; y; \lambda)$, that is valid when y is large while x and λ remain bounded.

Theorem B.2. *Let x and λ be bounded such that $\operatorname{Re}(\lambda^2) > -1$. Then,*

$$\operatorname{erfc}(x; y; \lambda) \sim \operatorname{erfc}(\lambda x) \operatorname{erfc}(x - y) - e^{-\lambda^2 x^2 - (x-y)^2} \sum_{n=2}^\infty \frac{c_n}{y^n}, \quad (\text{B12})$$

as $y \rightarrow \infty$ in the sector $|\arg(-y)| \leq \frac{\pi}{2} - \delta (< \frac{\pi}{2})$. The coefficients $c_n = c_n(x, \lambda)$ are polynomials in x and λ and are defined in the proof below.

Proof. From (B1) and (B2), we derive an alternative integral representation:

$$\begin{aligned} \operatorname{erfc}(x; y; \lambda) &= \operatorname{erfc}(\lambda x) \operatorname{erfc}(x - y) - \frac{2\lambda}{\sqrt{\pi} \sqrt{\lambda^2 + 1}} \int_{-y}^\infty e^{-\frac{\lambda^2 t^2}{\lambda^2 + 1}} \\ &\quad \times \operatorname{erfc}\left(x \sqrt{\lambda^2 + 1} + \frac{t}{\sqrt{\lambda^2 + 1}}\right) dt \\ &= \operatorname{erfc}(\lambda x) \operatorname{erfc}(x - y) - e^{-\lambda^2 x^2} \int_{-y}^\infty e^{-(x+t)^2} w(t) dt, \end{aligned}$$

where

$$w(t) = \frac{2\lambda e^{(\lambda^2+1)x^2+2xt+\frac{t^2}{\lambda^2+1}}}{\sqrt{\pi} \sqrt{\lambda^2+1}} \operatorname{erfc}\left(x \sqrt{\lambda^2+1} + \frac{t}{\sqrt{\lambda^2+1}}\right).$$

Utilizing the standard asymptotic expansion of erfc , we ascertain that the function $w(t)$ remains uniformly bounded for large t within the sector $|\arg t| \leq \frac{\pi}{2} - \delta (< \frac{\pi}{2})$, and it exhibits the asymptotic expansion

$$w(t) \sim \sum_{n=1}^\infty \frac{e_n}{t^n},$$

as $t \rightarrow \infty$ in the sector $|\arg t| \leq \frac{\pi}{2} - \delta (< \frac{\pi}{2})$, uniformly for bounded values of x and λ , $\operatorname{Re}(\lambda^2) > -1$. The differential equation

$$w'(t) - 2\left(x + \frac{t}{\lambda^2 + 1}\right)w(t) = \frac{-4\lambda}{\pi(\lambda^2 + 1)}$$

yields the following recurrence for the coefficients $e_n = e_n(x, \lambda)$:

$$e_0 = 0, \quad e_1 = \frac{2\lambda}{\pi}, \quad e_{n+1} = -(\lambda^2 + 1) \left(x e_n + \frac{1}{2}(n-1)e_{n-1}\right), \quad n = 1, 2, 3, \dots$$

For any $N \geq 1$, and when $|\arg t| < \frac{\pi}{2}$ and $|\arg(-y)| < \frac{\pi}{2}$, we define the remainder terms $M_N(t; x; \lambda)$ and $R_N(y; x; \lambda)$ as follows:

$$w(t) = \sum_{n=1}^N \frac{e_n}{t^n} + M_N(t; x; \lambda) \quad (\text{B13})$$

and

$$e^{-\lambda^2 x^2} \int_{-y}^\infty e^{-(x+t)^2} w(t) dt = e^{-\lambda^2 x^2 - (x-y)^2} \sum_{n=2}^N \frac{c_n}{y^n} + R_N(y; x; \lambda), \quad (\text{B14})$$

respectively. Here, the coefficients $c_n = c_n(x, \lambda)$ follow the recurrence relation

$$2c_{n+1} = 2xc_n + (1-n)c_{n-1} - (-1)^n e_n, \quad n = 1, 2, 3, \dots,$$

where $c_0 = c_1 = 0$. Consequently, $c_2 = \frac{1}{2}e_1 = \frac{\lambda}{\pi}$. By differentiating both sides of (B14) with respect to y , and utilizing (B13) along with the recurrence relation for the coefficients c_n , we obtain a differential equation for $R_N(y; x; \lambda)$:

$$e^{\lambda^2 x^2 + (x-y)^2} \frac{\partial R_N(y; x; \lambda)}{\partial y} = \frac{Nc_N}{y^{N+1}} - \frac{2c_{N+1}}{y^N} + M_N(-y; x; \lambda).$$

Since $\lim_{y \rightarrow -\infty} R_N(y; x; \lambda) = 0$, we arrive at the integral representation

$$R_N(y; x; \lambda) = e^{-\lambda^2 x^2} \int_{-\infty}^y e^{-(x-t)^2} \left(\frac{Nc_N}{t^{N+1}} - \frac{2c_{N+1}}{t^N} + M_N(-t; x; \lambda)\right) dt.$$

By substituting $t = y - s$ and deforming the contour of integration, we obtain

$$\begin{aligned} e^{\lambda^2 x^2 + (x-y)^2} y^N R_N(y; x; \lambda) &= \int_0^{+\infty} e^{-s^2 - 2(x-y)s} \\ &\quad \times \left(\frac{Nc_N}{y\left(1 - \frac{s}{y}\right)^{N+1}} + \frac{2c_{N+1}}{\left(1 - \frac{s}{y}\right)^N} + y^N M_N(s - y; x; \lambda)\right) ds. \end{aligned}$$

Consequently,

$$R_N(y; x; \lambda) = e^{-\lambda^2 x^2 - (x-y)^2} \mathcal{O}(y^{-N})$$

as $y \rightarrow \infty$ in the sector $|\arg(-y)| \leq \frac{\pi}{2} - \delta (< \frac{\pi}{2})$. This estimation can be refined by a factor of y^{-1} by considering

$$R_N(y; x; \lambda) = e^{-\lambda^2 x^2 - (x-y)^2} \frac{C_{N+1}}{y^{N+1}} + R_{N+1}(y; x; \lambda). \quad \square$$

When considering the case that $y \rightarrow \infty$ within the sector $|\arg y| \leq \frac{\pi}{2} - \delta (< \frac{\pi}{2})$, we can combine (B12) with the reflection formula (B4). In particular, when we are concerned with the case that $y \rightarrow +\infty$, we find

$$\operatorname{erfc}(x; y; \lambda) \sim 2 \operatorname{erfc}\left(\frac{\lambda y}{\sqrt{\lambda^2 + 1}}\right) \quad (\text{B15})$$

provided x and λ are bounded and $\operatorname{Re}(\lambda^2) > -1$.

In the following theorem, we present our final result in this appendix: an asymptotic expansion for $\operatorname{erfc}(x; y; \lambda)$ with a fixed λ , as $x \rightarrow \infty$, uniformly in y .

Theorem B.3. *Let μ and λ be bounded such that $\operatorname{Re}(\lambda^2) \geq 0$, $\operatorname{Re}\left(\frac{\lambda^2 + 1 - \mu}{\lambda^2 + 1}\right) \geq 0$, $\operatorname{Re}(\lambda^2 + (1 - \mu)^2) > 0$, $\lambda \neq 0$, and $\lambda^2 + 1 \neq \mu$. Then*

$$\operatorname{erfc}(x; \mu x; \lambda) \sim e^{-(\lambda^2 + (1 - \mu)^2)x^2} \sum_{n=1}^{\infty} \frac{d_n}{x^{2n}},$$

as $x \rightarrow \infty$ in the sector $|\arg x| \leq \frac{\pi}{2} - \delta (< \frac{\pi}{2})$. The coefficients $d_n = d_n(\mu, \lambda)$ satisfy the recurrence relation

$$(\lambda^2 + (1 - \mu)^2)d_{n+1} + nd_n = \frac{(-1)^n}{\pi} \left(\frac{1}{2}\right)_n \left(\frac{\mu\lambda(\lambda^2 + 1)^n}{(\lambda^2 + 1 - \mu)^{2n+1}} + \frac{1 - \mu}{\lambda^{2n+1}}\right)$$

for $n = 1, 2, 3, \dots$, with initial condition

$$d_1 = \frac{1}{\pi\lambda(\lambda^2 + 1 - \mu)}.$$

Proof. We can use the partial derivatives (B6) and (B7) to calculate

$$\begin{aligned} \frac{d}{dx} \operatorname{erfc}(x; \mu x; \lambda) &= \left(\frac{\partial}{\partial x} + \mu \frac{\partial}{\partial y}\right) \operatorname{erfc}(x; \mu x; \lambda) \\ &= \frac{2(\mu - 1)}{\sqrt{\pi}} e^{-(1 - \mu)^2 x^2} \operatorname{erfc}(\lambda x) \\ &\quad - \frac{2\mu\lambda}{\sqrt{\pi}\sqrt{\lambda^2 + 1}} e^{-\frac{\mu^2 \lambda^2 x^2}{\lambda^2 + 1}} \operatorname{erfc}\left(\frac{(\lambda^2 + 1 - \mu)x}{\sqrt{\lambda^2 + 1}}\right). \end{aligned}$$

Therefore,

$$\begin{aligned} \operatorname{erfc}(x; \mu x; \lambda) &= \frac{2(1 - \mu)}{\sqrt{\pi}} \int_x^\infty e^{-(1 - \mu)^2 t^2} \operatorname{erfc}(\lambda t) dt \\ &\quad + \frac{2\mu\lambda}{\sqrt{\pi}\sqrt{\lambda^2 + 1}} \int_x^\infty e^{-\frac{\mu^2 \lambda^2 t^2}{\lambda^2 + 1}} \operatorname{erfc}\left(\frac{(\lambda^2 + 1 - \mu)t}{\sqrt{\lambda^2 + 1}}\right) dt, \end{aligned} \quad (\text{B16})$$

where μ and λ satisfy the conditions stated in the theorem, and the paths of integration are chosen so that $\arg t = 0$ for all sufficiently large values of t . By employing the standard asymptotic expansion of erfc , we derive the following asymptotic expansion:

$$e^{-\alpha^2 t^2} \operatorname{erfc}(\beta t) \sim \frac{e^{-(\alpha^2 + \beta^2)t^2}}{\sqrt{\pi}} \sum_{n=0}^{\infty} (-1)^n \frac{\left(\frac{1}{2}\right)_n}{(\beta t)^{2n+1}}, \quad (\text{B17})$$

as $t \rightarrow \infty$ in the sector $|\arg t| \leq \frac{\pi}{2} - \delta (< \frac{\pi}{2})$, where $\alpha \in \mathbb{C}$ and $\operatorname{Re}(\beta^2) \geq 0$, with $\beta \neq 0$. We aim to establish that

$$\int_x^\infty e^{-\alpha^2 t^2} \operatorname{erfc}(\beta t) dt \sim e^{-(\alpha^2 + \beta^2)x^2} \sum_{n=1}^{\infty} \frac{f_n}{x^{2n}}, \quad (\text{B18})$$

as $x \rightarrow \infty$ within the sector $|\arg x| \leq \frac{\pi}{2} - \delta (< \frac{\pi}{2})$, with $\operatorname{Re}(\beta^2) \geq 0$, $\beta \neq 0$, and $\operatorname{Re}(\alpha^2 + \beta^2) > 0$. By differentiating (B18) with respect to x and equating the resulting expression with (B17), we obtain the following recurrence relation for the coefficients f_n :

$$f_1 = \frac{1}{2\sqrt{\pi}\beta(\alpha^2 + \beta^2)}, \quad (\alpha^2 + \beta^2)f_{n+1} + nf_n = (-1)^n \frac{1}{2\sqrt{\pi}} \frac{\left(\frac{1}{2}\right)_n}{\beta^{2n+1}}, \quad n = 1, 2, 3, \dots \quad (\text{B19})$$

Applying (B18) and (B19) to (B16) yields the desired result. For any $N \geq 1$, and under the conditions $|\arg t| < \frac{\pi}{2}$ and $|\arg x| < \frac{\pi}{2}$, we define the remainder terms $M_N(t; \alpha; \beta)$ and $R_N(x; \alpha; \beta)$ as follows:

$$e^{-\alpha^2 t^2} \operatorname{erfc}(\beta t) = \frac{e^{-(\alpha^2 + \beta^2)t^2}}{\sqrt{\pi}} \sum_{n=0}^N (-1)^n \frac{\left(\frac{1}{2}\right)_n}{(\beta t)^{2n+1}} + M_N(t; \alpha; \beta) \quad (\text{B20})$$

and

$$\int_x^\infty e^{-\alpha^2 t^2} \operatorname{erfc}(\beta t) dt = e^{-(\alpha^2 + \beta^2)x^2} \sum_{n=1}^N \frac{f_n}{x^{2n}} + R_N(x; \alpha; \beta), \quad (\text{B21})$$

respectively. By differentiating both sides of (B21) with respect to y , and using (B20) along with the recurrence relation for the coefficients f_n , we obtain a differential equation for $R_N(x; \alpha; \beta)$:

$$\frac{\partial R_N(x; \alpha; \beta)}{\partial x} = -e^{-(\alpha^2 + \beta^2)x^2} \frac{2(\alpha^2 + \beta^2)f_{N+1}}{x^{2N+1}} - M_N(x; \alpha; \beta).$$

Given that $\lim_{x \rightarrow +\infty} R_N(x; \alpha; \beta) = 0$, we establish the integral representation

$$R_N(x; \alpha; \beta) = \int_x^\infty e^{-(\alpha^2 + \beta^2)t^2} \left(\frac{2(\alpha^2 + \beta^2)f_{N+1}}{t^{2N+1}} + e^{(\alpha^2 + \beta^2)t^2} M_N(t; \alpha; \beta)\right) dt,$$

where the integration path ensures $\arg t = 0$ for sufficiently large t . By substituting $t = x + s$ and deforming the contour of integration, we derive

$$\begin{aligned} e^{(\alpha^2 + \beta^2)x^2} x^{2N+1} R_N(x; \alpha; \beta) &= \int_0^{+\infty} e^{-(\alpha^2 + \beta^2)s^2 - 2(\alpha^2 + \beta^2)xs} \\ &\quad \times \left(\frac{2(\alpha^2 + \beta^2)f_{N+1}}{\left(1 + \frac{s}{x}\right)^{2N+1}} + e^{(\alpha^2 + \beta^2)(x+s)^2} x^{2N+1} M_N(x + s; \alpha; \beta)\right) ds. \end{aligned}$$

Consequently,

$$R_N(x; \alpha; \beta) = e^{-(\alpha^2 + \beta^2)x^2} \mathcal{O}(x^{-2N-1})$$

as $x \rightarrow \infty$ in the sector $|\arg x| \leq \frac{\pi}{2} - \delta (< \frac{\pi}{2})$, with $\operatorname{Re}(\beta^2) \geq 0$, $\beta \neq 0$, and $\operatorname{Re}(\alpha^2 + \beta^2) > 0$. We can improve this estimate by a factor of x^{-1} by considering the identity

$$R_N(x; \alpha; \beta) = e^{-(\alpha^2 + \beta^2)x^2} \frac{f_{N+1}}{x^{2N+2}} + R_{N+1}(x; \alpha; \beta). \quad \square$$

If we assume, for instance, that $0 < \mu < 1$, then we can express (B16) as the following identity:

$$\operatorname{erfc}(x; \mu x; \lambda) = \operatorname{erfc}\left((1 - \mu)x; 0; \frac{\lambda}{1 - \mu}\right) + \operatorname{erfc}\left(\frac{\mu\lambda x}{\sqrt{\lambda^2 + 1}}; 0; \frac{\lambda^2 + 1 - \mu}{\mu\lambda}\right).$$

Through analytic continuation, this identity remains valid provided that all third entries lie within the domain $\mathbb{C} \setminus \{it : t \in \mathbb{R}, |t| \geq 1\}$.

Appendix C: Application to a Pseudo-Parabolic PDE

Our motivation for the example in Section 7 comes from the well-known question of how the speed of wave propagation in nonlinear dissipative PDEs depends on the far-field behavior of the initial data. Perhaps the best studied example is Fisher's equation

$$\frac{\partial u}{\partial t} = \frac{\partial^2 u}{\partial x^2} + u(1 - u), \quad u(x, 0) = u_0(x), \quad -\infty < x < \infty, \quad (\text{C1})$$

here taken with the initial data

$$u_0(x) \sim e^{-\lambda x} \quad \text{as } x \rightarrow +\infty, \quad \lambda > 0. \quad (\text{C2})$$

Introducing a wavefront location $s(t)$, with $x = s(t) + z$, it is well-established that

$$u \sim U(z), \quad s(t) \sim 2t - \frac{3}{2} \ln t \quad \text{as } t \rightarrow +\infty, \quad \text{with } z = \mathcal{O}(1) \quad (\text{C3})$$

for $\lambda > 1$, but (see, [55] and references therein)

$$u \sim U(z), \quad s(t) \sim (\lambda + \lambda^{-1})t \quad \text{as } t \rightarrow +\infty, \quad \text{with } z = \mathcal{O}(1) \quad (\text{C4})$$

for $0 < \lambda < 1$.

To provide context for what follows, we first briefly sketch the relevant arguments in terms of exponentially small quantities whereby

$$\frac{\partial u}{\partial t} \sim \frac{\partial^2 u}{\partial x^2} + u, \quad u \sim A(x, t)e^{-f(x, t)} \quad (\text{C5})$$

holds ahead of the wavefront with

$$\frac{\partial f}{\partial t} + \left(\frac{\partial f}{\partial x}\right)^2 + 1 = 0, \quad \frac{\partial A}{\partial t} + 2\frac{\partial f}{\partial x}\frac{\partial A}{\partial x} = -\frac{\partial^2 f}{\partial x^2}A. \quad (\text{C6})$$

The relevant solutions to the first of (C6) as $t \rightarrow +\infty$, $x = \mathcal{O}(t)$ take the form $f = tF(\xi)$, $\xi = x/t$ so that

$$F = \frac{1}{4}\xi^2 - 1, \quad A = a(\xi)/\sqrt{t}$$

(the singular solution) for some $a(\xi)$ and

$$F = \lambda\xi - (\lambda^2 + 1), \quad A = \alpha$$

(the general solution) for some constants λ and α . These combine for (C5) to give

$$f = \lambda x - (\lambda^2 + 1)t, \quad \text{rays } x = 2\lambda t + X, \quad x/t > 2\lambda, \quad (\text{C7})$$

$$f = \frac{x^2}{4t} - t, \quad \text{rays } x = Xt, \quad x/t < 2\lambda,$$

where X parameterizes the rays in each case (and an interior layer with $x = 2\lambda t + \mathcal{O}(\sqrt{t})$ provides the transition between these two regimes). For

the results to be applicable to the nonlinear problem (C1), the constraint $f > 0$ (u exponentially small) must hold, with $f = 0$ identifying the location at which the nonlinearity becomes nonnegligible. In consequence, (C7) implies $s(t) \sim 2t$ for $\lambda > 1$ but $s(t) \sim (\lambda + \lambda^{-1})t$ for $\lambda < 1$, as in (C3)–(C4).

We now indicate how the corresponding analysis proceeds for the pseudo-parabolic generalization

$$\frac{\partial u}{\partial t} = \frac{\partial^2 u}{\partial x^2} + \mu^2 \frac{\partial^3 u}{\partial x^2 \partial t} + u(1 - u) \quad (\text{C8})$$

of (C1) (with μ constant) before setting up the problem that we analyze in Section 7. The Hamilton–Jacobi (eikonal) equation in this case reads

$$\frac{\partial f}{\partial t} + \left(\frac{\partial f}{\partial x}\right)^2 - \mu^2 \left(\frac{\partial f}{\partial x}\right)^2 \frac{\partial f}{\partial t} + 1 = 0,$$

so the general solution for F is given by

$$F = \lambda\xi - \frac{\lambda^2 + 1}{1 - \mu^2\lambda^2}, \quad (\text{C9})$$

while the singular solution to the associated Clairaut equation is given parametrically in terms of $P \equiv \frac{dF}{d\xi}$ by

$$\xi = \frac{2(1 + \mu^2)P}{(1 - \mu^2 P^2)^2}, \quad F = \frac{\mu^2 P^4 + (1 + 3\mu^2)P^2 - 1}{(1 - \mu^2 P^2)^2}. \quad (\text{C10})$$

The two acceptable roots to the quartic for $P(\xi)$ lead to the asymptotic behaviors

$$\begin{aligned} \text{(I)} \quad F &\sim -1 + \frac{\xi^2}{4(1 + \mu^2)} \quad \text{as } \xi \rightarrow 0^+, \\ F &\sim \frac{\xi}{\mu} - \sqrt{\frac{2(1 + \mu^2)\xi}{\mu^3}} \quad \text{as } \xi \rightarrow +\infty, \\ \text{(II)} \quad F &\sim \frac{1}{\mu^2} + 3(1 + \mu^2)^{\frac{1}{3}} \left(\frac{\xi}{2\mu^2}\right)^{\frac{2}{3}} \quad \text{as } \xi \rightarrow 0^+, \\ F &\sim \frac{\xi}{\mu} + \sqrt{\frac{2(1 + \mu^2)\xi}{\mu^3}} \quad \text{as } \xi \rightarrow +\infty, \end{aligned} \quad (\text{C11})$$

the latter giving a contribution exponentially subdominant to the former throughout $\xi \in \mathbb{R}^+$. For fast-enough decaying initial data (see below), if the propagation speed in linearly selected (i.e., a so-called “pulled front” arises, cf. [56]) then its wavespeed is given by

$$c^* = \frac{2(1 + \mu^2)P^*}{(1 - \mu^2 P^{*2})^2}, \quad P^* = \sqrt{\frac{\sqrt{(1 + \mu^2)(1 + 9\mu^2)} - 1 - 3\mu^2}{2\mu^2}}, \quad (\text{C12})$$

because $F = 0$ at $P = P^*$ in (C10).

It follows from (C12) that $P^* < \mu^{-1}$ and the condition for “fast-enough” above is that $\lambda > P^*$ in (C2), though more must be established in order to confirm this result. The situation for $\lambda < \mu^{-1}$ is straightforward and corresponds closely to the $\mu = 0$ results: the rays associated with (C9) have

$$x = \frac{2(1 + \mu^2)\lambda}{(1 - \mu^2\lambda^2)^2}t + X$$

and it is instructive now to analyze the transition between these and the expansion fan associated with (C10). This proceeds by setting

$$u = \exp\left(-\lambda x + \frac{\lambda^2 + 1}{1 - \mu^2\lambda^2}t\right)W, \quad x = \frac{2(1 + \mu^2)\lambda}{(1 - \mu^2\lambda^2)^2}t + z$$

in the linearized version of (C8) to give

$$(1 - \mu^2 \lambda^2) \frac{\partial W}{\partial t} = \frac{(1 + \mu^2)(1 + 3\mu^2 \lambda^2)}{(1 - \mu^2 \lambda^2)^2} \frac{\partial^2 W}{\partial z^2} - \mu^2 \left(2\lambda \frac{\partial^2 W}{\partial z \partial t} + \frac{2(1 + \mu^2)\lambda}{(1 - \mu^2 \lambda^2)^2} \frac{\partial^3 W}{\partial z^3} - \frac{\partial^3 W}{\partial z^2 \partial t} \right).$$

As $t \rightarrow +\infty$ with $z = \mathcal{O}(\sqrt{t})$ only the first of the terms on the right-hand side enters the leading-order balance, which thus comprises the heat equation (the relevant solution being a complementary error function) for $\lambda < \mu^{-1}$, but is a backward heat equation for $\lambda > \mu^{-1}$, indicating that there is more to be said.

For $\lambda < \mu^{-1}$, the above transition is with the dominant exponentials, (I) in (C11), whereas for $\lambda > \mu^{-1}$ it would be associated with (II), leading to an exponentially subdominant turning-point problem. We now isolate perhaps the simplest problem that captures such a phenomenon and proceed with its analysis in Section 7. Guided by the $\xi \rightarrow +\infty$ behavior in (C11), we consider $\lambda = (1 \pm \varepsilon)/\mu$ with $0 < \varepsilon \ll 1$ and set

$$u = e^{-x/\mu} v, \quad x = X/\varepsilon, \quad t = \varepsilon T$$

to give

$$2\mu \frac{\partial^2 v}{\partial X \partial T} - \frac{1 + \mu^2}{\mu^2} v = \varepsilon \left(\mu^2 \frac{\partial^3 v}{\partial X^2 \partial T} - \frac{2}{\mu} \frac{\partial v}{\partial X} \right) + \varepsilon^2 \frac{\partial^2 v}{\partial X^2}. \quad (\text{C13})$$

In Section 7, we investigate the leading-order balance in (C13) as $\varepsilon \rightarrow 0^+$, scaling out the μ dependence and implementing the simplest relevant boundary and initial conditions, which suffice for our purposes.

Thus, we consider

$$2 \frac{\partial^2 v}{\partial x \partial t} = v,$$

for which we have

$$2 \frac{\partial f}{\partial t} \frac{\partial f}{\partial x} = 1,$$

so that the singular and general solutions are

$$F = \pm \sqrt{2\xi}, \quad F = \nu \xi + \frac{1}{2\nu},$$

respectively, where ν is an arbitrary constant. This simplification suffices to demonstrate the subtleties that apply in the more general case for $\lambda < \mu^{-1}$, corresponding to $\nu = -1$ here.

For $\nu = 1$, the behavior is familiar, in terms of both real and complex analysis: the $F = \xi + \frac{1}{2}$ contribution dominates both of the other two throughout \mathbb{R}^+ and is present only to the right of the Stokes line

$$(\text{Im}(\xi))^2 = 1 - 2 \text{Re}(\xi),$$

across which it is turned off by the $F = \sqrt{2\xi}$ exponential. Thus, on \mathbb{R}^+ it is present only in $\xi > \frac{1}{2}$, corresponding to its being transported to the right at the characteristic velocity

$$\dot{x} = \frac{1}{2} \left(\frac{\partial f}{\partial x} \right)^2 = \frac{1}{2}. \quad (\text{C14})$$

For $\nu = -1$, (C14) again applies, but the situation is entirely different: the Stokes lines on which $F = \pm \sqrt{2\xi}$ can turn the $F = -(\xi + \frac{1}{2})$ contribution on or off are now both \mathbb{R}^+ and, while (C14) identifies the location of the (subdominant) turning point, it cannot be used to determine the regimes in which the latter contribution is present or absent, even on \mathbb{R}^+ : this

necessitates the detailed analysis of the higher-order Stokes phenomenon that we pursue above—it would be hard to view its consequences (notably in terms of the amplitude of the $F = \xi + \frac{1}{2}$ contribution) as intuitive.